The characteristics, origins, and geodynamic settings of supergiant gold metallogenic provinces

Robert Kerrich[1], Richard Goldfarb[2], David Groves[3], Steven Garwin[3, 4] & Yiefei Jia[1]

1. Department of Geological Sciences, University of Saskatchewan, Saskatoon SK S7N 5E2, Canada;
2. United States Geological Survey, Box 25046, MS 964, Denver Federal Center, Denver, CO 80225-0046, USA;
3. Centre for Strategic Mineral Resources, Department of Geology and Geophysics, University of Western Australia, Nedlands 6907, Western Australia;
4. Newmont Mining Corporation, 1700 Lincoln Street, Denver, Colorado 80203, USA

Correspondence should be addressed to Kerrich (email: Robert. kerrich@usa.sk.cn) or Jia (email: yij449@mail.usask.ca)

Received August 31, 2000

Abstract There are six distinct classes of gold deposits, each represented by metallogenic provinces, having 100's to ＞ 1 000 tonne gold production. The deposit classes are: (1) orogenic gold; (2) Carlin and Carlin-like gold deposits; (3) epithermal gold-silver deposits; (4) copper-gold porphyry deposits; (5) iron-oxide copper-gold deposits; and (6) gold-rich volcanic hosted massive sulfide (VMS) to sedimentary exhalative (SEDEX) deposits. This classification is based on ore and alteration mineral assemblages; ore and alteration metal budgets; ore fluid pressure(s) and compositions; crustal depth or depth ranges of formation; relationship to structures and/or magmatic intrusions at a variety of scales; and relationship to the P-T-t evolution of the host terrane. These classes reflect distinct geodynamic settings. Orogenic gold deposits are generated at mid-crustal (4—16 km) levels proximal to terrane boundaries, in transpressional subduction-accretion complexes of Cordilleran style orogenic belts; other orogenic gold provinces form inboard by delamination of mantle lithosphere, or plume impingement. Carlin and Carlin-like gold deposits develop at shallow crustal levels (< 4 km) in extensional convergent margin continental arcs or back arcs; some provinces may involve asthenosphere plume impingement on the base of the lithosphere. Epithermal gold and copper-gold porphyry deposits are sited at shallow crustal levels in continental margin or intraoceanic arcs. Iron oxide copper-gold deposits form at mid to shallow crustal levels; they are associated with extensional intracratonic anorogenic magmatism. Proterozoic examples are sited at the transition from thick refractory Archean mantle lithosphere to thinner Proterozoic mantle lithosphere. Gold-rich VMS deposits are hydrothermal accumulations on or near the seafloor in continental or intraoceanic back arcs.

The compressional tectonics of orogenic gold deposits is generated by terrane accretion; high heat flow stems from crustal thickening, delamination of overthickened mantle lithosphere inducing advection of hot asthenosphere, or asthenosphere plume impingement. Ore fluids advect at lithostatic pressures. The extensional settings of Carlin, epithermal, and copper-gold porphyry deposits result from slab rollback driven by negative buoyancy of the subducting plate, and associated induced convection in asthenosphere below the over-riding lithospheric plate. Extension thins the lithosphere, advecting asthenosphere heat, promotes advection of mantle lithosphere and crustal magmas to shallow crustal levels, and enhances hydraulic conductivity. Siting of some copper-gold porphyry deposits is controlled by arc parallel or orthogonal structures that in turn reflect deflections or windows in the slab. Ore fluids in Carlin and epithermal deposits were at near

hydrostatic pressures, with unconstrained magmatic fluid input, whereas ore fluids generating porphyry copper-gold deposits were initially magmatic and lithostatic, evolving to hydrostatic pressures. Fertilization of previously depleted sub-arc mantle lithosphere by fluids or melts from the subducting plate, or incompatible element enriched asthenosphere plumes, is likely a factor in generation of these gold deposits. Iron oxide copper-gold deposits involve prior fertilization of Archean mantle lithosphere by incompatible element enriched asthenospheric plume liquids, and subsequent intracontinental anorogenic magmatism driven by decompressional extension from far-field plate forces. Halogen rich mantle lithosphere and crustal magmas likely are the causative intrusions for the deposits, with a deep crustal proximal to shallow crustal distal association. Gold-rich VMS deposits develop in extensional geodynamic settings, where thinned lithosphere extension drives high heat flow and enhanced hydraulic conductivity, as for epithermal deposits. Ore fluids induced hydrostatic convection of modified seawater, with unconstrained magmatic input. Some gold-rich VMS deposits with an epithermal metal budget may be submarine counterparts of terrestrial epithermal gold deposits. Real time analogs for all of these gold deposit classes are known in the geodynamic settings described, excepting iron oxide copper-gold deposits.

Keywords: gold deposit, orogenic gold deposit, geodynamics, tectonic setting, supercontinent.

Numerous schemes have been proposed for the classification of gold deposits, based on a variety of precepts or criteria. The scheme of Boyle[1] was founded in morphology of the orebody, mineral paragenesis, host rock and age. Hodgson and MacGeehan[2] used the precept of syngenetic versus epigenetic, among other characteristics. According to Bache[3], gold deposits can be classified as (1) pre-orogenic volcano-sedimentary, (2) post-orogenic plutono-volcanic, or (3) detrital deposits. Gold deposits were classed by Poulson[4] on the basis of crustal setting, from deep hypothermal to near-surface epithermal. Robert et al.[5] proposed sixteen classes of gold deposits based on geological setting, form of mineralization, alteration, metal association, etc. They subdivide structurally controlled gold-silver vein deposits into batholith-associated (Korean type), greenstone hosted, turbidite hosted, and iron formation hosted veins.

The authors reach consensus on a classification for world-class gold deposits based on multiple lines of observational evidence and quantitative data, at a variety of scales. This classification draws on recently developed concepts in geodynamics, advances in analytical technology that have permitted large databases to be generated and analyzed, and in particular the application of precise geochronology that allows the timing of mineralization to be constrained to magmatic or tectonic events in a P-T-t framework. These classes are: (1) convergent margin orogenic gold deposits, that include all of the four subdivisions of gold-silver vein deposits of Robert et al.[5]; (2) continental margin to intracratonic Carlin and Carlin-like gold deposits; (3) arc-related epithermal gold-silver deposits; (4) oceanic arc to continental arc copper-gold porphyry deposits; (5) anorogenic to late orogenic iron-oxide copper-gold deposits; and (6) gold-rich submarine volcanic hosted massive sulfide (VMS) to sedimentary exhalative (SEDEX) deposits. Inasmuch as the world's main placer gold deposits develop in foreland basins to orogenic belts, placer deposits can be linked geodynamically to orogenic gold deposits.

Section one sets out plate tectonic concepts, the supercontinent cycle, and lithosphere char-

acteristics for the geodynamic underpinnings of this review. In the following sections, each of the six classes of gold deposits is systematically described, in terms of characteristics, classic deposits, world-class metallogenic provinces, structural style, host rocks, metal ratios, hydrothermal fluids, origins, and geodynamic setting(s).

1 Mineral deposits, geodynamic settings, and the supercontinent cycle

1.1 Plate tectonics

The theory of plate tectonics is a kinematic theory according to which the lithosphere, the upper mechanical boundary layer of the Earth, including crust and lithospheric mantle, is divided into a finite number of torsionally, but not flexurally, rigid lithospheric plates. These plates interact at divergent spreading centres, convergent subduction zones, and transform fault boundaries as they move across the surface of the Earth. The oceanic and continental lithospheric plates constitute the translationally mobile upper mechanical boundary layer of the three dimensional convection cells in the asthenospheric mantle. The upper and lower mantles convect independently. Heat is removed from the core and mantle to the surface lithosphere by this convection, and by plumes that likely form at the core-mantle boundary and advect through the convecting lower and upper mantles to the surface[6].

Subducting oceanic lithospheric plates have been imaged by seismic tomography penetrating the 670 km D′ boundary, and probably are stored in lithospheric ‘graveyards’ at the 3 000 km deep core-mantle boundary (D″), where they are sporadically reactivated as mantle plumes[7]. Accordingly, there is mass as well as heat exchange between the upper and lower mantles.

In the 1980s, Mitchell and Garson[8], and Sawkins[9], provided the first attempts to synthesize the relationship between different classes of mineral deposits and plate-tectonic geodynamic settings, an approach pioneered by Stanton. They convincingly demonstrated how deposits of diamonds and Sn-U formed in anorogenic continental hot spots; deposits of salt and limestone-hosted Pb-Zn formed on passive margins; granitoid-related ores of Cu and Mo, and base metal massive sulfides developed in magmatic arcs; and sandstone-hosted U and Cu developed within intracontinental basins, to give a few examples. This elegant synthesis worked convincingly for some deposit types in the Phanerozoic. However, at that time there were diverse views on the syngenetic versus epigenetic timing, and tectonic setting, of what are now termed convergent margin orogenic gold deposits; some deposits such as iron-oxide copper-gold had not been fully recognized as a distinct class of gold deposit; and extrapolations to the Precambrian met with conceptual problems stemming from uncertainties in the nature of plate tectonics during that era. Moreover, this initial approach of relating mineral deposits to geodynamic setting did not explain the episodic secular distribution of orogenic gold and some other deposits referred to below.

1.2 Supercontinent cycle

The supercontinent cycle is an extension of plate tectonic theory. The concept emerged in the

late 1980s from recognition that the continental masses assemble and disaggregate in a cyclic pattern on a timescale of 200—500 Ma[10—12]. All of the present continents formed a single landmass termed Pangea that broke up at 180 Ma, and this led to speculation that there may have been former supercontinents that broke up and reassembled in cycles going back to at least 2700 Ma (fig. 1).

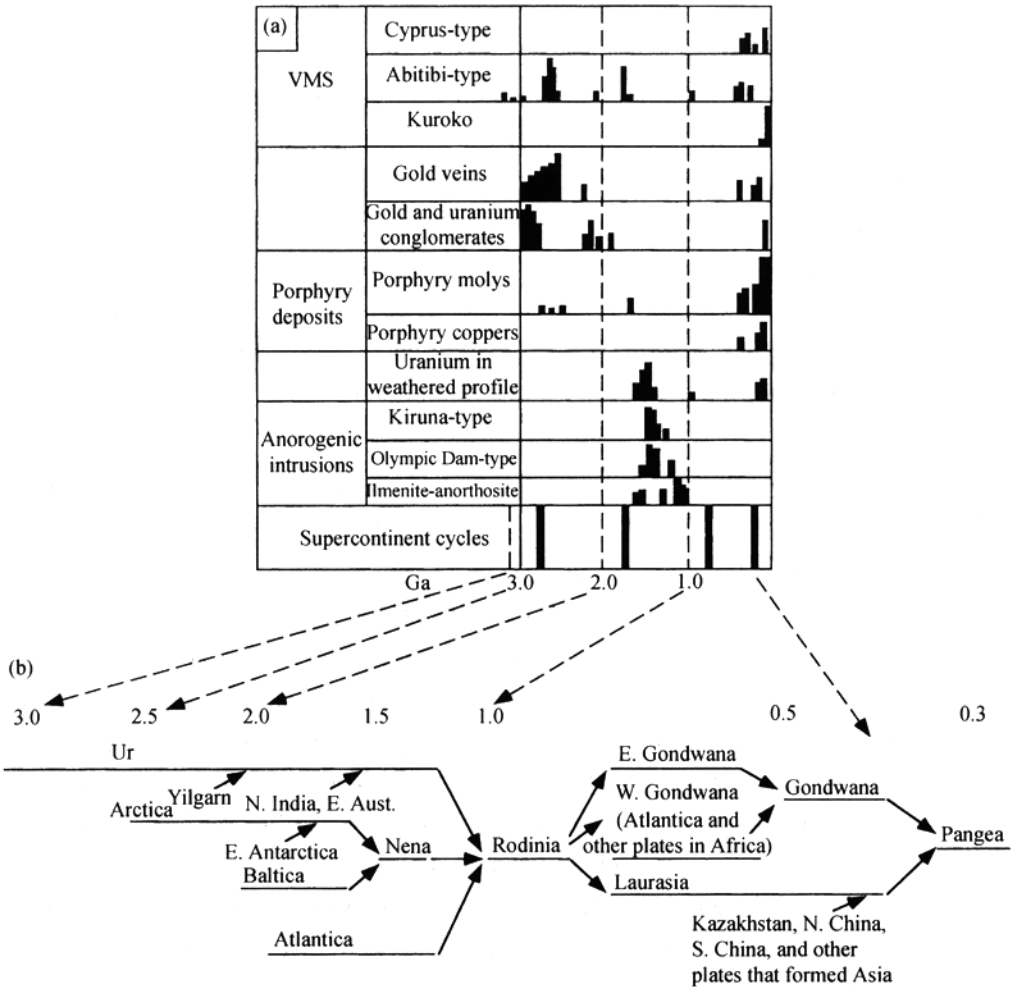

Fig. 1. (a) The secular distribution of select classes of mineral deposits in relation to the breakup and aggregation of continents as part of the supercontinent cycle (modified from Barley and Groves[13]). (b) Diagrammatic history of the major continents, in the supercontinent cycle framework (modified from Rogers[12]).

The mechanisms driving this cycle are not well understood. Murphy and Nance[11] recognized two principal styles of supercontinent aggregation, which they termed internal and external. Internal aggregation corresponds to continent-continent collision with a single well defined suture; examples include the 1800 Ma Trans Hudson Orogen (THO), Appalachian, and middle to late Tertiary Alpine-Himalayan orogenic belts. External aggregation corresponds to Cordilleran style tec-

tonics, where several allochthonous terranes are progressively accreted to a continental margin along numerous transpressional terrane boundary 'docking' faults, also termed the Turkic-style of orogenic belt[14].

Kerrich and Wyman[15] suggested that late Archean magmatic-accretionary events in the Superior and Slave Provinces of Canada, Finland, Southern Africa, India and Western Australia, all with associated orogenic gold deposits, likely corresponded to an early external supercontinent aggregation, and that the secular distribution of all orogenic gold deposits globally was linked to episodes of accretionary tectonics. Accordingly, Archean and post-Archean orogenic gold deposits formed in a common convergent margin geodynamic setting, and lithologies characteristic of the Archean, such as komatiites, tonalites or banded iron formation, are unlikely to have been the principal factors in the genesis of the Archean deposits [16,17].

In an important synthesis for understanding mineral deposits[13], it is shown that the geodynamic settings and temporal distribution of several major classes of metallic mineral deposits can be related to the cyclic aggregation and breakup of the continents, in the supercontinent cycle. Metal deposits related to anorogenic magmatism, such as Olympic Dam type iron-oxide copper-gold, and sandstone-hosted copper-lead, would form during initiation of supercontinent fragmentation, whereas deposits related to convergent tectonics, e.g. orogenic gold, and epithermal gold, predominate during periods of subduction and supercontinent aggregation.

Superimposed on this ~ 500 Ma supercontinent cycle are variations arising from: (1) the nature of the mantle lithosphere; (2) thermal decay of the mantle; (3) preservation; (4) external versus internal cycles; and (5) thermal structure of subduction zones. Diamonds are preserved beneath Archean cratons given the depth and characteristics of cratonic mantle lithosphere, and Proterozoic Olympic Dam type deposits are located at Archean craton margins where mantle lithosphere thins and has been metasomatically enriched (fig. 2). Kambalda-type nickel deposits are restricted to the late-Archean when the mantle was still hot enough to generate superplumes with sufficiently high thermal buoyancy flux to erupt abundant komatiites through oceanic and continental lithosphere. The scarcity of high crustal level porphyry copper ± gold and epithermal gold ores in terranes older than 200 Ma is considered to be the consequence of their low preservation potential in rapidly eroded magmatic arcs and collisional mountain belts. Preservation potential is higher in external Cordilleran style than in internal Himalayan style mountain belts. This feature, together with stable Archean lithosphere may explain the prodigiously rich VMS deposits in back-arc settings and orogenic gold in belts of transpressional accretion of the Superior Province. The secular change in host lithologies of orogenic gold deposits, and in the style of VMS deposits from Archean Abitibi type, through Proterozoic type, to the Phanerozoic Kuroko and Cyprus types, may reflect both thermal decay of the mantle, and differences in the angle of subduction, nature of the mantle wedge and arc magmas, that in turn stem from secular trends in the thermal structure of convergent margins (fig. 2).

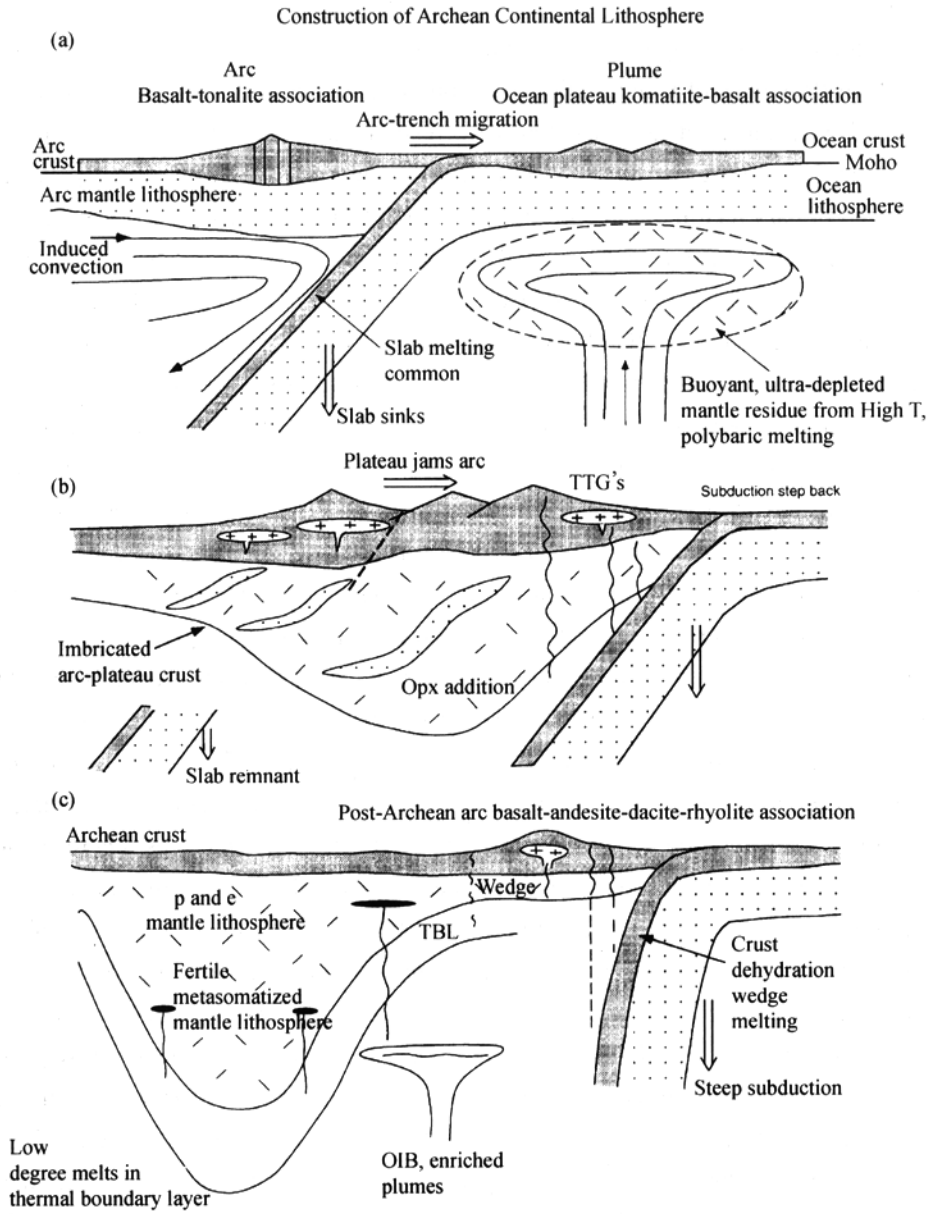

Fig. 2. Cartoon illustrating possible scheme for the development of Archean cratonic lithosphere by plume-arc interaction. (a) Slab pull under the arc causes arc migration towards oceanic plateau and its mantle residue——the product of a plume. (b) Buoyant plateau and mantle residue jam in subduction zone; arc and plateau crust imbricate; arc mantle and plume mantle residue imbricate to form a cratonic mantle lithosphere keel. (c) Enriched melts from thermal boundary layer (TBL) and mantle plumes fertilize continental mantle lithosphere. Subduction at craton margins is prevalently steep in the post-Archean eras (a) modified from Kelemen et al.[18]; see table 1).

Table 1 Formation of continental lithosphere

	Archean	Post-Archean
Crust features	Tectonic imbrication of arc magmas, trench turbidites, and ocean plateaus at convergent margins. 40—60 km thick. Blueschists, eclogites, melange present but rare.	Tectonic imbrication of arc magmas, trench turbidites, and ocean plateaus at convergent margins. 40—60 km thick. Blueschist, eclogites, melange.
Crust composition	High Na_2O, Al, $(La/Yb)_n$	High K, low Al, $(La/Yb)_n$
Process	Arc basalts + tonalites from shallow subduction of hot young ocean lithosphere. Tonalites (TTG) slab (basalt) melting. Garnet residual in eclogite.	Arc basalts and granitoids from steep subduction of cool old ocean lithosphere. Granodiorites (BADR) slab dehydration-wedge (peridotite) melting. Garnet absent.
Mantle lithosphere features	Refractory peridotite. Low Fe, high SiO_2. Low K, U, Th, Rb, Cs. 200—300 km thick. Diamonds.	Refractory peridotite. Low Fe, high SiO_2. Low K, U, Th, Rb, Cs. 200—300 km thick. Diamonds.
Process	Residues of polybaric melting in hot mantle plume, residue of ocean plateau komatiite-basalt sequence. Same slab eclogite captured by advancing arc; Plateau obducted, residue subcreted; TTG liquids hybridize with peridotite = high SiO_2.	Residue of basalt melt extraction in arc mantle, lithosphere peridotite. Some slab eclogite.

References in text.

The abundance of VMS deposits in the Superior Province, and the contrasting sparseness or absence of similar deposits in late Paleoarchean terranes of India, Southern Africa and Western Australia, might be considered at odds with such a unified supercontinent cycle framework for mineral deposits. Trace element and isotopic studies have shown, however, that Western Australian volcanic rocks of similar age to those of the Superior Province were generally erupted through continental lithosphere, and therefore do not correspond with the more primitive oceanic arc and back arc-plume settings represented by 2.7 Ga VMS-hosting volcanic terranes in Canada[19—22].

1.3 Archean versus post-Archean lithosphere

Cartoons depicting the tectonic setting of ore deposits generally do not extend beyond the base of the crust, the petrological MOHO. However, geodynamic settings, mantle magma reservoirs, and mineral deposits should be considered in the larger scale lithosphere-asthenosphere framework.

There is now near universal consensus that plate tectonics and the supercontinent, or supere-vent, cycle were operating in the Archean[23]. However, there is a fundamental difference in the processes by which lithospheric plates formed in the Archean and post-Archean; this bears directly on metallogeny. Modern oceanic lithosphere has a thin basaltic crust and depleted lherzolitic mantle lithosphere, collectively 5 to 70 km thick, depending on distance from the oceanic spreading axis. Compared to the underlying asthenosphere, oceanic lithosphere is relatively cool, mechanically rigid, and buoyant, except at convergent margins where negative buoyancy drives subduction. Consequently, plates move themselves via age-related density differences relative to convecting asthenosphere; they are not viscously coupled to upper mantle convection cells[24]. Archean ocean

crust was thicker because the higher mantle potential temperature generated larger melt fractions at ocean spreading centres[25].

Continental lithosphere has a crustal sector 20 to 80 km thick and a subcontinental mantle lithosphere sector 100 to 250 km thick. Continental mantle lithosphere under Archean cratons is thicker, more buoyant and refractory than under younger continental regions; its thickness, buoyancy, and thermal structure control the stability of Archean cratons, lead to the preservation of diamonds in the mantle lithosphere, and preservation of orogenic gold, komatiite hosted nickel, VMS and other deposits in the crust (fig. 2).

The asthenosphere is relatively hot and fluid, and convects. Between the non-convecting lithosphere and convecting asthenosphere is a thermal boundary layer, corresponding to the seismic low velocity zone. Heat is transferred through the asthenosphere, which is adiabatic, by convection, but through the lithosphere by conduction. Magmas passing through the lithosphere advect heat.

During the Archean, hot young oceanic lithosphere subducted at shallow angles. Consequently, oceanic arcs had a bimodal basalt-TTG (high Al-tonalite, trondjemite, granodiorite suite) association; the former from melting of peridotitic subarc wedge, the latter from slab crust melting[26]. Mantle plumes underwent deep, high degree polybaric melting (~30%) to generate ocean plateaus with a basalt-komatiite association, and a complementary buoyant, refractory residue (~70%[18]). As arcs retreated, ocean plateaus on ocean lithosphere jammed into the arcs generating imbricated arc-plateau crust, and imbricated subarc mantle and plume residue mantle lithosphere (fig. 2(a), (b)). Thicker ocean lithosphere may have inhibited development of slab windows and associated asthenospheric alkaline magmas. For shallow subduction, blueschists, eclogites, and mélanges are not readily obducted.

In the post-Archean era, cool older ocean lithosphere subducted steeply. Accordingly, arcs formed by slab dehydration-wedge melting, to give a basalt, andesite, dacite, rhyolite (BADR) association. Few plumes were hot enough to yield komatiites, such that the residue was thinner, less refractory and buoyant. Arc-plume assembly generated a compositionally different crust, and thinner mantle lithosphere. Proterozoic and Phanerozoic oceanic and continental arc granitoids formed at different sites in arc crust, as opposed to Archean slab-derived tonalites that are typically devoid of mineral deposits[26] (fig. 2(c)). Thinner ocean lithosphere promoted development of slab windows.

Low degree partial melts in the thermal boundary layer, and low degree melts in plumes, may stall in mantle lithosphere; such liquids are highly enriched in incompatible elements such as K, Th, Nb, Ta, Au, and LREE. They form domains of metasomatized mantle that may remelt later during decompression, extension, or impingement of a plume on the base of the lithosphere. Similarly, in deep Archean mantle lithosphere, carbonatitic liquids from an asthenosphere plume may react with P type (peridotite), and E type (eclogite) mantle to form diamonds (fig. 2(c); table 1).

In summary, the supercontinent cycle and knowledge of lithosphere development collectively provide an elegant unifying framework for understanding the origin, secular distribution, and cyclicity of the different classes of mineral deposits.

2 Orogenic gold deposits

2.1 Introduction

Structurally hosted lode gold systems in metamorphic terranes constitute a distinctive class of epigenetic precious-metal deposit; they are associated in space and time with accretionary tectonics, and are here termed orogenic gold deposits[13,15,27]. Their origin, however, has been contentious for over a century, and there remain polarized views on both the timing and mode of their formation. This class of gold-silver deposit has variously been named lode or reef type, terms that include veins in shear zones, through stockworks to mineralized wall rocks. The term mesothermal or mesozonal has also been used in view of their predominance in mid-crustal, greenschist facies environments. However, the deposits are now known to have formed over a large range of crustal depths from ＞25 km to the near surface environment, with a commensurately large range of PT conditions, the crustal continuum scheme of Groves and coworkers[27,28]; hence those terms are not appropriate. Gold-only[2] is a misnomer inasmuch as the deposits contain significant Ag, with Au/Ag ratios averaging 5, and sporadically have enrichments of W, Mo, or Te. Here, “turbidite”, or “slate belt” hosted lode gold deposits are included with their greenstone volcanic-hosted counterparts, as they all share common metal budgets, ore-fluid characteristics, and geodynamic setting. Similarly, the granitoid hosted Mesozoic gold-bearing quartz vein systems of Korea and eastern China are included, as these also share those specified characteristics with greenstone and turbidite-hosted deposit counterparts. Nor is the arbitrary and reductionist distinction between Archean, Proterozoic, and Phanerozoic orogenic gold deposits useful for the same reasons.

This class of precious metal deposit differs in terms of paragenesis, alteration style, metal budget, ore fluid chemistry, structural style, and geodynamic setting from Carlin-type, or epithermal gold deposits, that collectively are either in terranes that have not been metamorphosed or did not form coevally with metamorphism of the host terrane, and are associated with intracontinental extension or magmatic arcs[29—32]. Specifically, the relatively high Au/Ag ratios contrast with much lower ratios in Carlin and epithermal counterparts.

2.2 Characteristics

Studies[5,33—55] of orogenic gold deposits of all ages have revealed a number of common characteristics (table 2): (1) Rich gold metallogenic provinces are associated with accretionary orogenic events, principally in external supercontinent cycles, or external sectors of internal supercontinent aggregation cycles. (2) Many gold metallogenic provinces are sited proximal to translithospheric structures, or the tectonic boundaries of composite metamorphosed volcanic-plutonic or sedimentary terranes. (3) Mineralization is typically syn- to post-peak metamorphism,

Table 2 Principal characteristics of orogenic lode gold deposits

Classic provinces (classic deposit camps)	Mesoarchean	Barberton (Sheba, Fairview).
	Neoarchean	Abitibi (Timmins), Dhawar (Kolar), Quadrilatero, Brazil (Morro Velho), Slave (Con), Tanzania (Buluyanhulu), Yilgarn (Kalgoorlie), and Zimbabwe (Cam, Motor).
	Proterozoic	West Afria (Ashanti), Trans-Hudson (Homestake), Tapaios, Guyana (Las Christina), and NT, Australia (Granites).
	Paleozoic	Lachlan Fold Belt (Bendigo, Ballarat), Baikal Fold Belt (Sukhoi Log), Southern Tian Shan (Muruntau, Kumtor), Bohemian Massif (Kasperske Hory).
	Mesozoic-Tertiary	Otago (Macraes), Tombstone Belt (Fort Knox, Pogo, Scheelite Dome), Juneau Gold Belt (AJ, Treadwell), Sierra Foothills (Jamestown), Yana-Kolyma (Natalka), and Jiaodong Peninsula (Jiaojia, Linglong).
Structural style		Ductile to brittle-ductile, reverse, strike-slip faults or oblique-slip; anticlinal domes.
Mineralization style		Veins, breccias, disseminated.
Host rocks		Mafic and ultramafic volcanic rocks, intrusive rocks, BIF-chert, greywacke.
Metal associations		Au, Ag, ± As, Sb, Te, W, Bi; Au/Ag averages 5.
Gold fineness		800—950
Proximal alteration		Muscovite, Ca-Fe-Mg carbonates, chlorite, albite, pyrite, tourmaline.
P-T conditions		220—500℃, 0.5—4 kb
Ore fluids		Low salinity, aqueous-carbonic ± H_2S, CH_4, CO_2, ± N_2.
Isotopes (Water)		$\delta D = -20‰ — -80‰$; $\delta^{18}O = 6‰ — 10‰$.
Heat sources		Asthenosphere, crust.
Other features		Increasing salinity related to mixed fluid from sedimentary basins. Radiogenic isotopes indicate old and juvenile crust interaction with fluids, sporadically high boron. Reactivation of older deposits generates some secondary isotopic and fluid inclusion signatures.

and late-tectonic, within the larger time frame of orogenic belts involving accretion of one or multiple allochthonous terranes. (4) Orogenic gold deposits are distributed in belts of great geological complexity, with gradients of lithology, strain, and metamorphic grade, reflecting an orogenic environment. (5) Most supergiant metallogenic provinces are in greenschist facies metamorphic terranes. (6) Deposits are structurally controlled, and associated with second or higher order splays of translithospheric faults. The structures have high-angle oblique displacement, commonly with reverse slip, but with some examples in transcurrent fault regimes. (7) Deposits are generally restricted to the brittle-ductile transition, with syn-kinematic gold precipitation. (8) The alteration mineral paragenesis in greenschist facies domains is dominated by quartz, carbonate, mica, (± albite), chlorite, and pyrite (± scheelite and tourmaline). (9) There is a distinctive element association characterized by enrichment in Au, Ag (± As, Sb, Te, W, Mo, Bi, B), with low enrichments of Cu, Pb, Zn, Hg, and Tl relative to background abundances. Arsenic, Sb, and Hg are more abundant in the low temperature sector of the continuum of these deposits. (10) Ore forming hydrothermal fluids are dilute aqueous carbonic fluids, with uniformly low fluid salinities (typically <6wt%NaCl equivalent), and CO_2+CH_4 contents of 5—30 mole%, with sporadic H_2O-CO_2 un-

mixing. (11) Fluid pressures fluctuate from supralithostatic to sublithostatic within the brittle-ductile shear zones. (12) Within a given deposit, vein systems may have vertical extent of more than 2 km, with a lack of zoning or weak zoning, albeit with some zoning of metal content at the scale of an entire mining district.

Most of these deposits occur in terranes that experienced greenschist facies metamorphism, and the deposits feature greenschist-facies alteration assemblages. Recently, it has been recognized that Archean orogenic gold deposits in sub-greenschist, amphibolite, and even granulite facies terranes share numerous characteristics, such as structural setting, metal inventory, element association, and ore fluid properties and likely source, in common with greenschist hosted counterparts[28,35,36,38,43—45,56]. Accordingly, this class of structurally hosted orogenic gold deposit may be viewed as forming over a crustal depth range, or 'crustal continuum', extending from granulite to sub-greenschist facies environments[28,56]. All gold deposits of this orogenic class are hosted in metamorphosed terranes, and this feature is arguably one of the most significant unifying characteristics.

This section is concerned with orogenic gold deposits that formed close in space and time with tectonism and metamorphism of the host terranes[57—59]. Smaller deposits may form later in the same terranes; these tend to have distinct mineral parageneses[52]. Gold concentrations may also occur much later from secondary remobilization of primary ore by saline basement brines, as in some Proterozoic gold orebodies at Chibougamau, Quebec, that formed by leaching of Archean Au-rich porphyry systems[60,61].

2.3 Structural architecture, Coseismic mineralization

Orogenic gold deposits are associated with, or proximal to, first-order transcrustal generally terrane-bounding, or 'docking', structures that demark the boundaries of distinct, tectonically juxtaposed metamorphosed supracrustal sequences, or tectonostratigraphic terranes[15,37,41,48,62] (table 2). These first-order structures are typically characterized by megaboudinage; doubly plunging folds; complex anastomosing brittle-ductile shear zones; well defined L-S tectonic fabrics with steeply plunging to subhorizontal lineations; and gradients of lithological type, metamorphic grade, and intensity of hydrothermal alteration[38,63,64]. The geometry and displacement vectors in these complex structures indicate protracted histories of episodic movement and reactivation. Many are high angle reverse faults with later transcurrent motion[63,64]. The geometry of these regional structures at depth is poorly constrained. There is some seismic evidence from the Abitibi greenstone belt and Kalgoorlie Terrane that the high angle structures hosting the deposits become listric at depth. Local connection to depths of ~80 km in the mantle lithosphere is indicated by the syn-kinematic emplacement of lamprophyres along the structures, and the geochemistry of the lamprophyre dykes that signify residual minerals stable at $\geqslant$80 km[62]. Major mining camps are located on regional structures where there are large scale discontinuities, such as dilational or antidilational jogs as at Kirkland Lake and Malartic; deflections with strike-slip

thrust duplexes, for example, Timmins; or fault bifurcations or sharp changes in attitude exemplified by the Angel Camp and Jackson-Plymouth gold districts of the Foothills Metamorphic belt, California[65].

Although spatially and temporally associated with structures of regional extent, orogenic gold deposits are rarely located within these first-order structures, but instead are hosted in second- or higher-order splays off the regional structures. This geometrical relationship is particularly well developed in the Abitibi subprovince, where the majority of the deposits are located to the north or south of the two major east-west trending structures; the Destor-Porcupine and Kirkland Lake-Cadillac Faults. At Timmins, the giant Hollinger-McIntyre-Coniaunium and Dome vein systems are respectively on the Hollinger and Dome Faults, second order splays of the first order Destor-Porcupine Fault. Similarly, the Kirkland Lake and Val d'Or camps are north of the regional Kirkland Lake-Cadillac Fault. The giant lode gold deposits of the Kalgoorlie-Kambalda trend, Western Australia, are distributed east and west of the Boulder-Lefroy fault on subsidiary splays[66]. The reasons why the deposits typically flank the first-order structures have been discussed by McCuaig and Kerrich[67] and Cox[68].

On the scale of individual deposits, the morphology of fracture and shear zone systems in these second- and higher-order splays, which typically show displacements of tens to a few hundred meters, may be grouped into four general structural styles: (1) breccias; (2) stockworks and vein sets; (3) laminated veins in shear zones; and (4) predominantly ductile shear zones hosting thin, discontinuous, highly attenuated and deformed veins[56,69]. These four structural morphologies represent a gradation from dominantly brittle to dominantly ductile conditions that likely reflect increasing crustal depths and temperature.

Gold may be contained dominantly within quartz veins, as “replacement” within altered wall rocks bounding veins and shear zones, or as some combination of these two styles. Notable replacement dominated gold deposits are iron-formation hosted deposits, the Kalgoorlie deposit of the Yilgarn block, and vein selvage-related gold mineralization of the Hollinger-MacIntyre deposit, Timmins, Ontario[33,70,71].

These orogenic gold deposits formed synkinematically, and at syn- to post-peak metamorphic conditions, in gross rheological and thermal equilibrium with the host terranes. Accordingly, deposits in higher grade terranes are not metamorphosed lower temperature counterparts. For example, at Red Lake, Ontario, there is a transition from deposits in greenschist facies rocks with greenschist grade alteration assemblages to counterparts in amphibolite facies rocks with amphibolite grade alteration assemblages[72]. Similar transitions of metamorphic grade between deposits have been identified in Coolgardie Domain[73], Norseman Terrane[53] and Yellowknife gold camp[1].

Over the crustal range from subgreenschist to amphibolite and granulite facies, mineralization was syn- to post-peak metamorphism and synkinematic, with cyclic fluid pressure fluctuations driving a cycle of brittle hydraulic fracturing and vein emplacement, with intervening peri-

ods of slow ductile deformation, all in the framework of the coseismic-interseismic cycle of active faults. Hence the cyclicity of deformation style, fluid pulses, vein formation, and gold deposition are dynamically and genetically linked[58,65,74—77] (for a review see ref. [53]).

2.4 Metal inventory

Orogenic gold deposits are characterized by a distinct metal and trace element inventory consisting of high enrichments relative to background abundances of rare elements Au, Ag, As, Sb ± Te± Se ± W ± Mo ± Bi ± B, but generally low level or no enrichment of the abundant base metals Cu, Zn, Pb, and Au/Ag ratios averaging 5. Gold fineness in orogenic deposits of all ages, including slate belt examples, is high averaging 900, with low variability, whereas gold fineness in porphyry, volcanogenic, and epithermal deposits is lower and more variable[33,38,51,78,79]. Sporadic enrichments of galena, sphalerite, or molybdenite occur, but do not reach economic grades. The enrichment of rare elements, yet absence of enrichment of relatively abundant base metals, is likely due to differences in transport of the elements by the hydrothermal fluid. According to Loucks and Mavrogenes[80], gold is transported as the $AuHS(H_2S)^0_3$ complex, whereas transport as chloride complexes is more important in other environments.

2.5 Ore fluids

The hydrothermal ore-forming fluids were dilute, aqueous, carbonic fluids, with salinities generally $\leqslant$3 wt % NaCl equivalent, and $CO_2 \pm CH_4 \pm N_2 \pm H_2S$. They possess low Cl but relatively high S, possibly reflecting the fact that metamorphic fluids are generated in crust with ~60 $\times 10^{-6}$ Cl, but ~1 000$\times 10^{-6}$ S. Primary fluid inclusions are: (1) H_2O—CO_2, (2) CO_2-rich with variable CH_4 and small amounts of H_2O, and (3) 2-phase H_2O (liquid-vapor) inclusions. Inclusion types 2 and 3 are interpreted to represent immiscibility of the type 1 original ore fluid. Immiscibility was triggered by fluid pressure drop during coseismic events, and possibly by shock nucleation, leading to highly variable homogenization temperatures in an isothermal system[43—45,81—83]. Gold solute concentrations in the ore fluids have been estimated at ~20 μg/g (ppb), requiring commensurately large quantities of hydrothermal fluids, or about 6000 km^3 for the Abitibi terrane deposits.

Regardless of the actual concentration of Au in the hydrothermal ore-forming fluids, in order to form an economic orebody it is necessary to induce a change in the fluid chemistry that will efficiently remove gold from solution by destabilizing aqueous Au-S complexes. Based on available data, destabilization could be accomplished by a number of processes: (1) cooling the fluid; (2) oxidation of the fluid; (3) reduction of the fluid; (4) decreasing pH of the fluid, or; (5) lowering ΣS in the fluid. This modification of fluid chemistry can be achieved by: (1) large-scale pressure and temperature gradients along the fluid plumbing system; (2) reaction of the fluid with the wallrocks surrounding the fluid conduit; (3) transient pressure fluctuations inducing phase immiscibility in the fluid; (4) fluid mixing; or (5) chemisorption.

2.6 New constraints from nitrogen isotopes

After more than a century of research on orogenic lode gold deposits, their origin remains contentious. The principal hypotheses for their origin are: (1) deposition from granitoid-related magmatic hydrothermal fluids[84]; (2) precipitation from deeply convecting meteoric surface waters[85]; (3) the product of mantle derived fluid interaction with the lower granulite crust[38]; or (4) the product of fluids generated by metamorphism of ocean crust and sediments in a subduction-accretion complex[15,86]. These proposed genetic models are based on various lines of geological and geochemical evidence (mainly H, O, C, and S isotope studies) from different deposits. However, much of the isotope data cannot be interpreted uniquely: many of the $\delta^{13}C$ carbonate data have values consistent with mantle fluids, crustal magmas, or crustal dehydration, and the same is true of the majority of S-isotope data on sulfides. Similarly, many of the calculated $\delta^{18}O$ and δD values of fluids plot where metamorphic and magmatic fields overlap. Collectively, Sr and Pb isotope data permit mixing of fluids derived from crustal and mantle resources[87]. Clearly, a new, less ambiguous, approach is required to distinguish between these hypotheses.

Nitrogen, primarily as structurally bound NH_4^+, may substitute for K in potassium-bearing silicates such as micas and K-feldspars because of its similar ionic radius and charge[88,89]. The isotopic composition of nitrogen has large variations in geological samples (e.g. Clayton[90]), which makes this isotope system a potentially important tracer for the origin of terrestrial silicates and volatiles such as mantle-derived mid-oceanic ridge basalt (MORB, $\delta^{15}N = -8.7‰$ to $-1.7‰$) and diamonds ($\delta^{15}N = -10‰$ to $0‰$) which have a mean $\delta^{15}N$ value about $-5‰$[91—95]. Sedimentary and crystalline rocks show relative enrichments in ^{15}N, with $\delta^{15}N$ values between 0‰ and 10‰ for organic N in marine sediments[96]; between +5‰ and 10‰ for S-type granites, with low N contents, averaging 21×10^{-6}[97—99]; and between +2.5‰ and 18‰ for metamorphic rocks[100].

The results show that N content of micas from Archean gold deposits in Canada and Western Australia is between 20 and 200×10^{-6} (average 76×10^{-6}), and $\delta^{15}N$ spans 10‰ to 24‰ (fig.3). In contrast, biotite and K-feldspar from a peraluminous granite in the Archean Abitibi belt are characterized by systematically lower $\delta^{15}N$ of –5‰ to 5 ‰, and generally lower N contents of 10 to 50×10^{-6} [87]. Based on these results, Jia and Kerrich[87] conclude that N in the micas is unlikely to have been derived either from orthomagmatic fluids expelled from crystallizing granitiods, or from mantle derived fluids given the low N content and $\delta^{15}N$-depleted character of mantle nitrogen. It is also unlikely that N in the hydrothermal micas of gold deposits is meteoric surface water, given that global mean nitrogen isotopic values of meteoric water are $4.4 \pm 2.3‰$ ($n = 263$)[101]. Furthermore, meteoric water convection occurs at hydrostatic fluid pressures whereas structural analysis of the veins indicates their precipitation during hydraulic fracturing by fluids at lithostatic fluid pressure. Accordingly deeply convecting meteoric water can be ruled out[87]. Collectively, the dilute, aqueous carbonic and N-bearing composition of the ore fluids is consistent with the metamorphic fluid hypothesis, where fluids are derived from a $\delta^{15}N$-enriched source of volcanic and

siliciclastic sedimentary rocks at the greenschist to amphibolite transition. The setting is within a subduction-accretion complex, where fluids advect on regional scale structures into the supercrustal sequences where the deposits form.

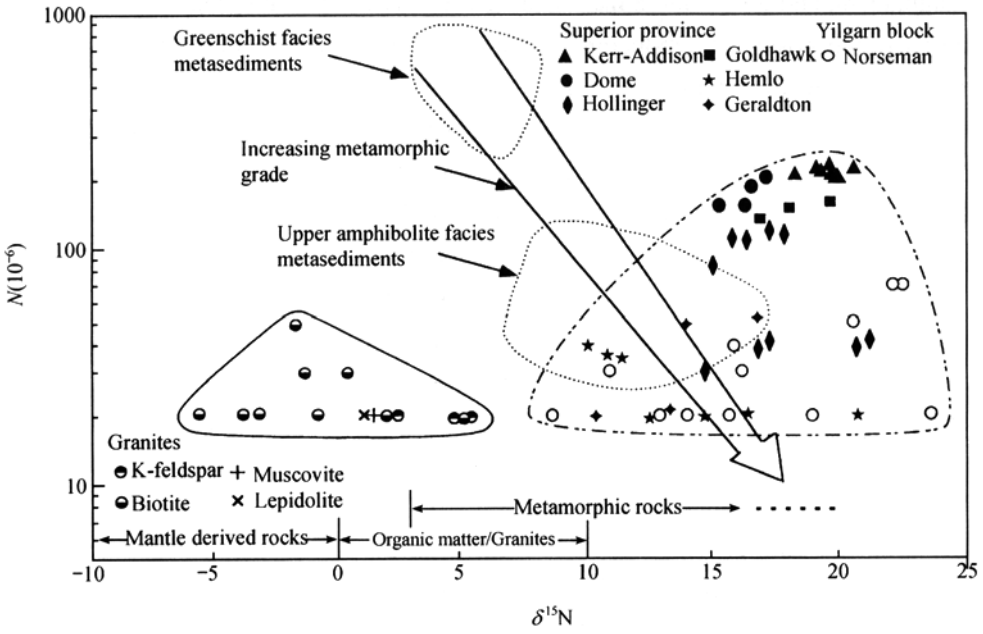

Fig. 3. N content and $\delta^{15}N$ values of hydrothermal mica separates from Archean orogenic gold deposits in Canada and Western Australia compared to results for K-silicates from granites, Abitibi greenstone belt of Superior Province. Modified from Jia and Kerrich[87].

2.7 Geodynamic settings of orogenic gold deposits

Globally, giant orogenic gold metallogenic provinces appear at four distinct times in Earth history: the Neoarchean (~2.7 Ga); the Neoproterozoic, with the Birimian goldfields and Homestake; the lower Palaeozoic, with Muruntau and Kumtor in central Asia and the Victorian goldfields of Australia; and in Mesozoic rocks of the North American Cordillera, exemplified by the Mother Lode, and eastern Asia. Each of these times corresponds to major accretionary orogenic processes. The specific geodynamic setting is of transpressive accretion of allochthonous terranes to one another, or a pre-existing continental margin, typified by Cordilleran tectonics. This tectonic regime is distinct from continent-continent collision, such as the Alpine-Himalayan Orogen, an internal orogen[13].

In the Superior Province and Yilgarn craton, gold mineralization post-dates termination of the main pulse of granitoid emplacement. Syn-tectonic granitoids in the Superior Province are dominantly slab melting TTG's, whereas the Yilgarn granitoids are intracrustal melts. Gold mineralization predates post-orogenic peraluminous 'S-type' granites in the Superior Province[57]. Gold deposits in these superterranes are located proximal to regional scale accretionary fault zones that tend to 'skirt' the large batholithic intrusions. Few deposits are located within granitoids. Based on

structural style in the southern Superior Province, and the ubiquitous metamorphosed nature of terranes hosting orogenic-gold deposits, Polat and Kerrich[102] suggested that the terranes are high-T, low-P type subduction accretion complexes, where subduction-accretion, metamorphism, magmatism, and gold mineralization are closely associated in space and time, but in detail gold mineralization postdates syn-tectonic batholiths. This model accounts for the restriction of orogenic gold deposits to metamorphic terranes (fig. 4).

Internal orogens, such as the Trans Hudson, Appalachian, and Alpine orogenic belts do not feature large lode gold provinces. Rather, they generally host small deposits, albeit with structural, mineralogical, and geochemical similarities to giant Archean, Palaeoproterozoic, and Phanerozoic counterparts, and similar post-peak metamorphic temporal relations; shoshonitic lamprophyres are sparse. These relationships may stem from the presence of deep plumbing systems that develop in the terrane boundaries of transpressive external orogens, in contrast to smaller, shallower, and less connected structural networks in internal orogens such as the 1.9 Ga Trans Hudson orogen (THO). An exception is the Homestake Mine, South Dakota (1100 t Au produced), where the local geology of this sector of the THO has features common to external orogenic belts, including a rift-drift-accretional geodynamic evolution[104,105].

Other orogenic gold provinces are not located on translithospheric accretionary structures. Examples are the Lupin deposit in the Northwest Territories (now termed Nunavut) of Canada, and the Victorian slate belt orogenic gold province, Southeast Australia[51]. In such cases outboard accretion may lead to lithosphere thickening, delamination of mantle lithosphere with upwelling of hot asthenosphere, collectively generating high crustal heat flow. Mesozoic orogenic gold deposits of China and Korea are distinctive in being located at the margins of Archean cratons, and located in or proximal to granitoids[106]. Notwithstanding the spatial association, the ore fluids are neither consistent with a magmatic origin, nor with meteoric water convecting in and proximal to a granitoid heat source. Rather, the deposit characteristics and ore fluid properties are similar to those of all other orogenic gold deposits[67]. Given the areal extent of these Mesozoic orogenic gold provinces, high crustal heat flow may stem from impingement of a mantle plume on the base of the lithosphere. Thinner cratonic margin lithosphere would then melt and dehydrate the overlying crust.

3 Carlin and Carlin-like gold deposits

3.1 Introduction

The tectonic controls on the genesis of Carlin-like gold deposits continue to remain an enigma some thirty years after discovery of the Carlin deposit itself in northern Nevada. It is still even highly debatable as to whether this is a totally distinct class of gold system, or alternatively whether some relationship exists between these gold systems and epithermal gold[107], granitoid-related gold[108], or orogenic gold deposits[109]. In fact, Phillips et al.[110] have recently sug-

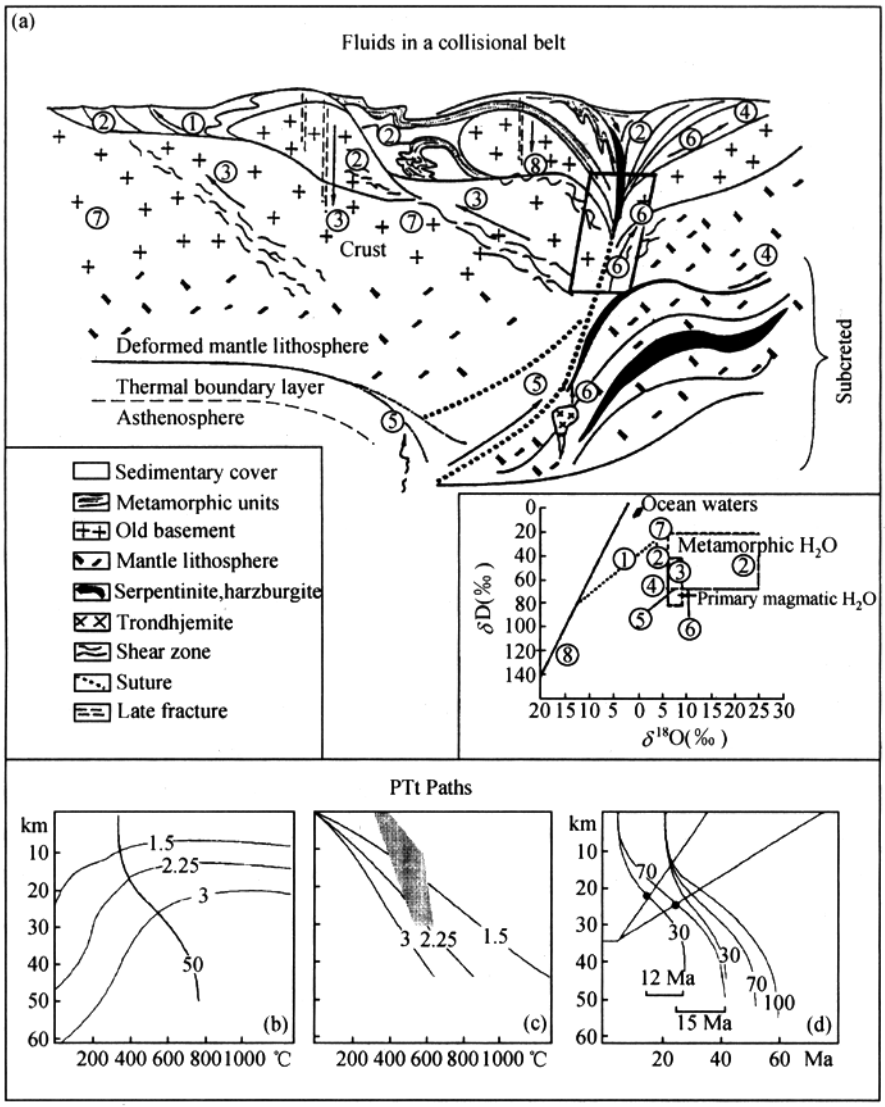

Fig. 4. (a) Schematic diagram illustrating possible fluid reservoirs involved in a collisional and/or transpressive geodynamic regime. ① Formation waters tectonically expelled from cover thrust units, advect along thrust faults. ② Syntectonic veins buffered by low-, or high-$\delta^{18}O$ lithologies. ③ Metamorphic fluids from old basement. ④ Metamorphic fluids from dehydration of subcreted oceanic lithosphere: these are the principal hydrothermal ore fluid for lode gold deposits. ⑤ Mantle volatiles from late decompression advect up suture. ⑥ Magmatic fluids from trondhjemites generated by melting base of subcreted lithosphere. ⑦ Formation brines that penetrated basement during extensional phase. ⑧ Low-$\delta^{18}O$ meteoric water from high-altitude mountain range. (b)—(d) Timing relationships between metamorphism at shallow and deep crustal levels modeled for deep-later type metamorphic terranes. Piezothermal arrays calculated with the mode and method of England and Thompson[103]. (b) A piezothermal for an erosion rate of 35 km per 50 Ma. and onset of erosion at 20 Ma after initial thickening (thick line). Thin lines represent the 400°C isotherm for heat source distribution II [103] and contoured for different thermal conductivities. (c) The changes of metamorphic peak temperature with depth. Contours are for differing conductivities of (a). The shaded field indicates the area in which crustal melting and fluid production are likely to occur. (d) Piezothermal arrays for two different times of erosion onset at 5 and 20 Ma after initial homogeneous crustal thickening to double thickness crust and for characteristic erosion times of 30, 70, and 100 Ma Superimposed straight lines are trajectories of rocks now preserved at the surface. Times and depth of metamorphic peak for these rocks is shown by the dots (modified from ref. [57]).

gested that deep weathering of Late Archean orogenic gold systems in the Yilgarn Craton produces gold systems that resemble those in Nevada. The basic geological characteristics of Carlin-like deposits are well described from northern Nevada and northwestern Utah[30, 111,112], but application of many of these features to other parts of the world is often questionable. Understanding of the global distribution of Carlin-like gold ores remains poor because many reported occurrences of anomalous gold disseminated in sedimentary rocks, which might be amenable to bulk-mining methods, are classified as Carlin-like with little additional justification.

The Carlin-like deposits in Nevada and Utah are mainly restricted to three important trends: the Carlin, Battle Mountain-Eureka, and Getchell trends. These trends are indicative of the spatial association between hydrothermal activity and pre-existing major faults within the Basin and Range physiographic province, an association first recognized by Roberts[113]. More modern geophysical studies have shown these faults to be Neoproterozoic basement structures, which may have originated during episodic rifting along a passive margin of ancestral North America [114,115]. The gold deposits are hosted by Cambrian through Triassic miogeoclinal clastic and carbonate rocks along the trends, with carbonaceous and calcareous siltstones being the most preferred host. Many ore zones are localized where high-angle normal faults intersect favorable lithological units.

3.2 Characteristics

More than one hundred Carlin-like gold deposits and occurrences are now recognized in the northern Basin and Range province of the western USA. They have a pre-mining resource of slightly more than 4 800 t Au that mainly grade 1—2 g/t, with about 60 percent of this resource within the Carlin trend itself. About 20 percent of this total recognized resource has been recovered through the end of the 20th century. Gold is both disseminated within given strata and in irregular, discordant breccia zones. It is submicron and consistently sited in arsenian pyrite rims around very fine pyrite grains[116, 117]. The Ag-As-Au-Hg-Sb geochemical signature, related to the common occurrence of realgar, orpiment, cinnabar, and stibnite, suggests a predominance of sulfur-complex within the hydrothermal systems. Au/Ag ratios are variable, but commonly >1.

A consistent and characteristic alteration pattern has been described[112,118]. Carbonate dissolution, mainly decalcification, but in places also including dissolution of dolomite, is the most widespread diagnostic alteration process. This process increases rock porosity and permeability, thus enhancing subsequent migration of hydrothermal fluids[119,120]. The carbonate dissolution is more efficient in calcareous siltstones, than in the pure carbonates, because these clastic sedimentary rocks have a higher initial permeability. Conversely, silicification is best developed adjacent to structures in carbonates where greater fluid/rock ratios exist. Argillic alteration is defined by the presence of kaolinite, illite, montmorillonite, and lesser sericite that have replaced detrital silicates in the clastic rocks. Sulfidization of iron-rich host rocks, as well as fluid mixing, is most commonly called upon for destabilizing gold-bisulfide complexes[121]. Ore deposition for the Carlin-like deposits in northern Nevada was at temperatures of about 180—250℃ and at depths

of about 2.5—6.5 km from a low-salinity (＜8wt%$_{NaCl.equiv}$), CO_2- (＜10mole%) and H_2S-bearing fluid[119,121,122]. There is a general lack of consensus as to whether ore fluids may be totally meteoric in origin[123] or may also have a deep crustal metamorphic or magmatic component[124].

3.3 Geodynamic setting

The absolute timing for gold deposition in the Nevada Carlin-like gold deposits has been controversial since initial discovery. However, isotopic dating studies now clearly indicate that these gold deposits formed between 42—30 Ma[124] (table 3). In a broad framework, this period represents a part of the time span of transition from convergence to extension in the Cordilleran foreland thrust belt, as the associated continental margin simultaneously shifted from a zone of orthogonal/transpressional collision to a transform margin. This Middle Eocene to Early Miocene transition included a slowing of convergence with the eventual sinking of a subducting slab into the mantle, the onset of extensive extension, unroofing of metamorphic core complexes, and

Table 3 Summary of selected large Carlin-like deposits

Region	Tectonics	Host rocks	Deposits	Gold/t (prod+res)	Grade/g • t^{-1}	Ore age/Ma	Reference
Nevada (Basin and Range), USA	back-arc extension; calc-alkaline magmatism	Pz_1-Tr miogeoclinal clastics and carbonates	Goldstrike-Post-Miekle	1800	5.0—24	42—30	[124]
			Twin Creeks	665	2.3		
			Gold Quarry - Maggie Creek	641	1.0—2		
			Jerritt Canyon	378	3.7		
			Cortez-Pipeline	300	8		
Tintina Gold Belt, Yukon (Canada) and Alaska (USA)	post-extensional subduction and calc-alkaline magmatism	Pz schist in pericratonic terrane and Pt-E. Cambrian miogeoclinal clastics	Brewery Creek	28	0.5—2.0	ca. 90	[125]
			True North	37	2.5		[126]
Dian-Gui-Qian area, SW Yangtze craton China)	shift from compressional to extensional regime	middle Pz -Tr miogeoclinal clastics and carbonates	Zimudan	＞32	5	K (?)	[127], a)
			Lannigou	＞60	7		
			Gaolong	＞20	4		
			Getang	22	6.2		
Chuan-Shaan-Gan area, NW Yangzte craton (China)	collisional tectonics and calc-alkaline magmatism	late Pz -Tr turbidites	Dashui	46	5.0—60	T_1-J_2	[127], b)
			La'erma	6	1.5—5.6		
			Dongbeizhai	52	5.5		
			Jiancha-ling	52	5		
Zarshuran, NW Iran	post-collisional felsic to intermediate volcanism	precambrian shales and carbonates	Zarshuran	22	10	ca. 14	[128,129]

a) Hu, R. Z., Su, W. C., Bi, X. W. et al., Geology and geochemistry of Carlin-type gold deposits in China, Mineralium Deposita, 2001, in press. b) Mao, J., Qiu, Y., Goldfarb, R. et al., Geology and distribution of gold deposits in the western Qinling belt, central China, Mineralium Deposita, 2001, in press.

widespread calc-alkaline magmatism landward of the Mesozoic Sierra magmatic arc (Seedorff, 1991; Burchfiel et al., 1992; Hofstra et al., 1999). These tectonothermal activities were associated with formation of the Carlin-like gold deposits, as well as many important epithermal gold deposits and large porphyry systems such as Bingham Canyon and Battle Mountain.

The restriction of Carlin-like deposits to a 12-Ma-long time window within an approximately 35-Ma-long episode of back-arc tectonism is puzzling. As shown[124], the deformational and magmatic events migrated from north (Washington-Idaho-Montana) to south (southern Nevada) over this broader Middle Eocene to Early Miocene time. Resulting metamorphic core complexes and magmatic bodies characterize this entire north-south transect across the western USA and, where they occur in northern Nevada and northwestern Utah, they show no consistent spatial association with the Carlin-like gold deposits[124,130].

A critical question that must be resolved is, therefore, what was so special about this specific area in the central Basin and Range at this one time. Although the miogeoclinal rocks and crustal structures are more widespread than simply the area of the Carlin gold deposits, Ilchik and Barton[123] suggest that the relatively reduced nature of these rocks in northern Nevada was critical for required high sulfur and gold solubilities within fluids produced during broad-scale extension. Another possibility for the restriction of the ores to this part of the Palaeo passive margin sedimentary sequence is a Paleozoic syngenetic gold enrichment within some of the sedimentary units, which is then remobilized by hydrothermal events initiated during the subsequent extension and increased geothermal gradient. Emsbo et al.[131] have noted disseminated and relatively coarse-grained gold within a number of the units in northern Nevada that are correlative with bedded barite and sea-floor base metal mineral occurrences. Finally, a plume beneath the central Basin and Range at ca. 42—30 Ma, the ancestral Yellowstone hot spot, may also have been significant for initiating voluminous fluid circulation[132,133].

3.4 Carlin-like deposits

The above, possibly critical, features noted from the central Basin and Range, are not consistently recognized in association with hypothesized Carlin-like gold deposits described elsewhere in the world. This uncertainty hinders establishment of any reasonable tectonic model that can be used for global exploration for Carlin-like deposits. Elsewhere in North America, deposits such as Brewery Creek[125], in the ca. 90 Ma Tombstone gold belt of east-central Alaska/central Yukon, are sometimes referred to as Carlin-like[126]. These include zones of auriferous brecciation and disseminated gold in carbonaceous, calcareous clastic rocks with an associated As-Sb-Hg signature, similarities with the Carlin-like deposits of Nevada. However, the temporal association with nearby granitoid magmatism, the occurrence of gold bearing veins in these granitoids, and the lack of documented pre-ore decalcification suggest these are not Carlin-like deposits, but rather may somehow be related to the other orogenic gold deposits of the Tombstone belt. Also in the North American Cordillera, Paleozoic strata near shale-hosted barite and base metal deposits in the Sel-

wyn and Red Dog basins might be favorable sites for discovery of Carlin-like gold deposits, assuming the model of Emsbo et al.[131] to be significant. The lack of later plutonism in either of the miogeoclinal basin sequences subsequent to Paleozoic metal deposition, however, may make these parts of the passive margin less prospective for generation of epigenetic Carlin-like gold systems.

Outside of northern Nevada and northwestern Utah, southern China is most commonly recognized for gold resources within Carlin-like deposits. Resources of about 15 Moz Au occur in the Dian-Gui-Qian and Chuan-Shaan-Gan areas, respectively along the southwestern and northwestern margins to the Yangtze craton. These may be, in part, significantly less productive systems than those in Nevada because of the more-limited, free-milling oxide zones. English language summaries of the auriferous areas include refs. [127,134, 135]. Early Paleozoic to Triassic calcareous and carbonaceous clastic rocks host ores; silicification, kaolinitization and decalcification have been noted, ore zones are characterized by a Au-Ag-Ag-Hg-Sb geochemical signature, and associated granitoids are uncommon.

The Dian-Gui-Qian area is economically the more important of the two, located along the boundary of Yunnan, Guangxi, and Guizhou. A variety of isotopic dates on the Carlin-like deposits from the area, all of somewhat questionable validity, are spread over Cretaceous time (Hu et al., 2001, listed at the foot of table 3). The deposits occur in sedimentary rocks of the Youjiang basin, a rift filled with middle Paleozoic to Triassic sediments within the Yangtze craton miogeocline. Folding and thin-skinned thrusting of these now gold-bearing, carbonate platform and foreland basin strata occurred a few hundred kilometers inland of the continental margin during the middle Mesozoic. This was a consequence of accretion/subduction of the Qiangtang-Indochina superterrane along this part of the Yangtze craton margin, with the suture marked by the Jinshajiang-Ailaoshan fault system[136]. Terrane accretion continued until about 50 Ma, when final continent-continent collision was marked by the docking of the Indian continental mass. Resulting Himalayan orogenesis included transform escape tectonics within the earlier accreted superterrane block[137]. However, there is little published information regarding the effects of the final collision on the Dian-Gui-Qian area and other parts of the interior Yangtzte block. Surprisingly, there is very little reported magmatism associated with the Mesozoic-Tertiary collisions along the edge of the craton. In a broad sense, the overall probable Cretaceous age for Carlin-like gold deposition occurs within a lengthy period where the older passive margin (miogeocline) was undergoing a transition from a compressional to a more extensional stress regime, which is somewhat similar to the western North America scenario. Until more reliable and detailed information is available regarding the regional tectonics of the southwestern Yangtze Craton, meaningful comparisons between China and North America are difficult to draw.

Carlin-like gold deposits are recognized from two localities in the Chuan-Shaan Gan area. Both of these, the western Qinling orogenic belt and the northeastern corner of the Songpan-Ganzi basin, are dominated by basinal rocks of late Paleozoic and Triassic ages, respectively. In the former, however, many of the larger 64—96 t Au deposits classified[127] as Carlin-like, including Ba-

guamiao, Shuangwang, and Liba, are undoubtedly orogenic gold deposits within large brittle-ductile shear zones (Mao et al., 2001, listed at foot of table 3). Since the middle 1980s about fifteen new discoveries in the western Qinling belt show most features that are characteristic of Carlin-like gold systems such as the Dashui, La'erma, Manaoke, and Pingding deposits. The second group of Carlin-like deposits, about 100 km to the south and including the roughly 2 Moz Au Dongbeizhai deposit, are also very similar, and their host strata indicate a maximum age of no older than Middle Triassic. Important differences between most of these deposits in the Chuan-Shaan-Gan area and those in Nevada are that the former are mainly structurally-controlled and found within relatively unreactive siliciclastic and carbonate units. These features may partly explain the relative lower tonnages in the Chinese deposits.

There are no absolute dates on the Carlin-like deposits in the Songpan-Ganzi basin. The rocks were folded and thrusted, as well as intruded by anatectic plutons, in the middle Mesozoic during the same collisional events along the craton margin, as described above. There is no evidence for any later extension here in this part of the Chuan-Shaan Gan area. Therefore, it can only be speculated that gold genesis may have been a part of the middle Mesozoic deformational episode within the basin and adjacent northwestern Yangtze craton margin. In contrast, numerous absolute dates are available for the western Qinling belt Carlin-like deposits and these typically range between 240 and 170 Ma (Mao et al., 2001). These age constraints suggest that this group of Carlin-like ores formed coevally with the nearby orogenic gold deposits also in this part of the Qinling orogen, both within the belt of terranes defining the early Triassic collisional suture between the North China and Yangtze cratons. Most significantly, in both of these parts of Chuan-Shaan Gan area, and in contrast to the western USA and perhaps the Dian-Gui-Qian area, the defined Carlin-like deposits appear to be associated with collisional tectonism. In this case, the proposed genetic link between orogenic gold and Carlin-like gold deposits[109] seems relatively more attainable.

The ca. 14 Ma Carlin-like deposits of the Zarshuran district of northwestern Iran, historically a significant producer of arsenic ores, are now important targets for disseminated gold. The deposits have reserves of about 22.4 t Au, and are hosted in a Precambrian sedimentary rock sequence[128,129]. The majority of the gold is hosted in a calcareous and carbonaceous shale unit that is intercalated with a series of carbonate beds. Mehrabi et al.[128] suggest that coeval andesitic to rhyolitic Miocene volcanism is indicative of a magmatic origin for the hydrothermal fluids, and associated deformation to development of a regional anticlinal trap. They also make the important observation that the relatively deeper levels of formation for Carlin-like deposits, such as $\geqslant$4 km in the Zarshuran district, favor a greater preservation potential of these types of gold systems compared to epithermal gold vein deposits. In contrast, Daliran et al.[138] indicate a much shallower formation depth for these ores in northwestern Iran, a possibility supported by nearby active geothermal systems.

An association of the Iranian gold deposits with the major Zagros fault zone may be signifi-

cant, although, and as for the Nevada Carlin-like deposits, the fault is a basement structure that was first active hundreds of millions of years prior to ore formation[139]. As with Nevada in the middle to late Tertiary, the Miocene of northwestern Iran was probably in a post-collisional tectonic state. Seaward of the future gold district, the final closure of a branch of the Neo-Tethys Ocean, and docking of the Zagros shelf/Arabian Peninsula region on the leading edge of Africa, occurred sometime during the Oligocene[139].

4 Arc-related epithermal gold deposits

4.1 Introduction

Epithermal mineral deposits are the main source of gold resources that have been formed within the upper few kilometers of crust. Giant epithermal gold deposits, as defined in Sillitoe[140], contain anywhere from 200 t to 1 000 t Au. Minerable gold grades in these deposits vary over about two orders of magnitude, from the bulk-minable ores at Round Mountain of just over 1 g/t to the bonanza-type (i.e. ＞32 g/t) gold ores of about 60 g/t at Hishikari. Similar to the copper-gold porphyry and skarn deposits, the epithermal deposits occur in both continental and oceanic arc tectonic settings. The majority of these rim the Pacific margin, in arcs that were active in middle Cretaceous or younger times. Other significant deposits are associated with Alpine events in southern Europe (e.g. Greece, Romania), and in locally-preserved, shallow-level remnants of late Paleozoic Gondwanan (e.g. NE Queensland) and Paleo-Tethyn (e.g. Central Asia Tian Shan) arcs. Epithermal gold deposits are typically classified into low-sulfidation or high-sulfidation subgroups, with hot spring gold deposits best interpreted as an expression of the former at the paleosurface.

4.2 Characteristics

Epithermal gold deposits are most typically assumed to be the products of igneous-driven hydrothermal cells within the upper 1—2 km of crust[32,141]. Therefore, a spatial association with volcanic lithologies and underlying porphyry systems characterizes the majority of the deposits. Both fluids exsolved from the shallow magma chamber and convecting meteoric waters, in variable proportions, are likely to be involved in ore formation in these settings. Temperatures of mineral deposition range between about 100 and 300℃ and reported Au/Ag ratios are quite variable. A spatial association with major transcurrent structures has been observed in places[32], although this may not be important in the ore-forming process[140]. Active auriferous geothermal systems in volcanic terranes (e.g. Matsukawa, Broadlands, Salton Sea) are now well accepted as modern-day analogs to past epithermal gold deposits (table 4).

The characteristics of low sulfidation (or adularia-sericite) systems are significantly different from those of high sulfidation (or acid sulfate, alunite-kaolinite) systems[161—164]. Low sulfidation deposits are typically sited laterally to the sub-volcanic intrusive bodies and are dominated by low-salinity meteoric waters. Massive open-space veins and stockworks host the gold ores in

Table 4 Summary of selected large epithermal gold deposits

Region	Tectonics	Deposits	High or low sulfidation	Gold/t (prod+res)	Grade/g • t^{-1}	Age of ore/ Ma	Reference
Continental deposits							
Andes	continental arc perhaps during change in subduction angle	Yanacocha, Peru	high	870	1.03	⩽15	[142]
		Pierina, Peru	high	310	2.8		
		El Indio, Chile	high	300	6.6		
		Pascua, Chile	high	340	1		
		La Coipa	high	95	1.37		
		Cerro Vanguardia	low	95			
		Orcopampa, Peru	low	12			
		Kori Kollo	low	156	2.26		
Western USA	back-arc continental extension during slab sinking	Cripple Creek	low	780	23	⩽30	[142]
		Summitville	high	15	1.6		
		Round Mt.	low	310	1.2		
		Goldfield	high	160	10.5		
		Comstock	low	280	14.6		
		McLaughlin	low	110	4.7		
NE Russia	back-arc continental extension during slab sinking	Kubaka	low	80	25	105—70	[143]
		Karamken	low	34			
		Julietta	low	22	20		
SE China orogen	post-collisional extension	Zijinshan	high	9	5	ca 100	[144]
Peri-Mediterranean of southern Europe	complex micro-continent collisions, with local extension perhaps due to onset of lithospheric detachment	Sacaramb	low		2—100	Miocene?	[145]
		Chelopech, Bulgaria	high	193	＞4		[146]
		Bor, Serbia	high	44	0.4		[147]
		Lahoca, Hungary	high	50	2.1		
		Telkibanya	low				
		Rodalquilar, Spain	high	10	7		
Central Asia	back-arc region to continental collisions	Kochbulak	high	125	13.4	Pz_2	[148]
		Kairagach	high	63			[149]
		Shkol'noe	low	9	9.04		
		Xitan	high	15	7		a)
		Axi	low	112	5.8		
Thomson and Hodgkinson-Broken River fold belts, E-Australia	back-arc extension along continental margin	Cracow	low	30	0.5—4.3	C—P	[150]
		Kidston	low	130	1.25—1.58		[151]
		Pajingo	low	12	9.9		
Oceanic island arcs							
Southwest Pacific	oceanic arc	Ladolam	low	＞600	3.5	⩽10	[151]
		Porgera	low	＞550	4.7		[152]
		Lepanto	high	＞120	3.5		[153—155]
		Chinkuashih	high	92	4.6		
		Wafi	high	60	0.6		
		Hishikari	low	250	55		
		Emperor	low	＞150	10		
		Martha Hill	low	＞150	2.0—3		
Carribbean	Oceanic arc	Pueblo Viejo	high	＞700	3.0—4	130	[156]

(*To be continued on the next page*)

(*Continued*)

Region	Tectonics	Deposits	High or low sulfidation	Gold/t (prod+res)	Grade/g • t^{-1}	Age of ore/ Ma	Reference
Lachlan belt, Australia	accreted island arcs	Peak Hill	high	>9	0.5—2	O	[157]
Stikinia and western	accreted island arcs	Sulphurets (Snow-field)	low	22	2.8	T_3—J_1	[158]
Canada		Stewart	low	70	7	T_3—J_1	
Southern Ural Mountains, Russia	accreted island arcs	Berezniakovskoje gold belt	low	50-100	>3	D_3	[159]
Avalon terrane, eastern Canada	accreted island arc	Hope Brook	high	45	2.5	latest Pt	[160]

a) Rui, Z., Goldfarb, R. J., Qiu, Y. et al., Paleozoic-Early Mesozoic gold deposits of the Xinjiang Autonomous Region, northwestern China, Mineralium Deposita, 2001, 36, in press.

volcanic environments, with commonly associated pyrite, argentite, tennantite/tetrahedrite, arsenopyrite, tellurides, and base metal sulfides. Very distinctive ore textures include breccias, banded and crustiform veins, and druse-filled cavities. In more sedimentary rock-dominant terranes, realgar, orpiment, cinnabar and stibnite are the more common sulfide mineral phases. Adularia and calcite, along with widespread quartz±chalcedony, are notably abundant because of the near-neutral hydrothermal fluids that were buffered by the country rocks. Illite is common in adularia-rich assemblages nearest the causative intrusion, and gradually gives way to smectite at greater distances along the fluid cooling path and extending to the surface[164]. Where boiling occurs, the rising steam escaping toward the surface produces an alteration signature similar to that seen in the high-sulfidation deposits (see below).

The high sulfidation systems are, in contrast, dominated by magmatic fluids[164]. Rather than hosted in discrete veins, most of the gold in these deposits occurs within replacement zones in volcanic rocks or as disseminations in more permeable rocks. As discussed by Hedenquist[165], these metalliferous zones develop where a relatively channelized, escaping oxidized magmatic fluid discharges into the overlying groundwater table. The resulting extremely acidic water (pH≤2) leaches the country rock and leaves a massive vuggy silica residue, with associated kaolinite, alunite, pyrophyllite/diaspore and barite associated in the adjacent country rocks. Pyrite, enargite, and luzonite are the most consistent metal phases found with gold in the vuggy silica; base metal sulfides and tennantite/tetrahedrite are also present in many metal assemblages. The larger high-sulfidation deposits appear to be associated with relatively shallow crustal levels, localized in highly permeable ignimbrites and other types of tuffs and lacustrine sediments[142].

4.3 Tectonomagmatic setting of mineralization

Epithermal gold deposits are most consistently sited in the same general tectonic settings as those characteristic of gold-bearing porphyry deposits. This is especially true for the Circum-Pacific, where both oceanic and continental arcs are well recognized for their metalliferous magmatic systems. Depending on the thermal regime, epithermal ores may evolve temporally during the growth of an arc (e.g. southern Europe, Andes, Mariana Islands) or during post-

collisional thermal events (e.g. NE Iran, Cripple Creek). In both cases, the deposits may be concentrated in the back arc region of a convergent plate margin environment or in the shallow volcanic part of the arc itself. Associated crust varies in type and thickness, but associated magmatism is consistently potassic (i.e. K＞Na in the related igneous rocks).

The potassic igneous rocks are younger, emplaced at stratigraphically higher crustal levels, and are erupted further landward of an active trench than the non-potassic igneous rocks. The latter, typically close to the continental margin, include low potassium tholeiites and calc-alkaline igneous rocks. Collectively, these features indicate potassic magma formation at deeper levels along the Benioff zone[79]. The association between potassic igneous rocks and epithermal gold deposits was well documented in the Circum-Pacific region by Sillitoe[155]. He pointed out that approximately 20 percent of the large epithermal deposits in this region are clearly associated with shoshonitic and alkaline potassic igneous rocks, whereas these rocks make up no more than three percent of all igneous rocks in the Circum-Pacific. A tectonic setting in which post-collisional, partial melting of a no longer active, sunken slab could oxidize mantle sulfides and release gold into the evolving potassic magma[155] is perhaps critical.

As pointed out[79], there may be a great deal of ambiguity involved with the tectonic classification of epithermal gold deposits. The one main consistency is the presence of elevated geotherms at shallow crustal levels, bringing magmas and fluids into the near crustal environment. This contrasts with the earlier discussed orogenic gold deposits that evolve in deeper crustal levels under more typical thermal gradients. The high geothermal gradients typically develop in both arc and back-arc positions as supported by the presence of epithermal gold deposits in both settings.

4.4 Continental volcanic arcs

The Andes represent the best-documented example of volcanic arc-related epithermal gold deposits in a continental setting. An abundance of important epithermal gold ores have been formed and preserved mainly during the last 15 Ma throughout the arc. These include high-sulfidation systems such as Yanacocha (896 t), Pierina (320 t) and Pascua (352 t). Generally not as high in gold tonnage, low-sulfidation deposits are also widespread in the Andes and include Cerro Vanguardia (Argentina; 100 t) and Kori Kollo (Bolivia; 160 t Au). Kay et al.[166] indicate that many of the deposits formed in the waning stages of Andean magmatism, where a peak in compressional deformation correlated with a maxima for crustal thickening and regional uplift. In contrast to this model that relies on a shallowing of the subduction zone, other workers correlate the epithermal hydrothermal activity with a change from flat to a steeper, more normal subduction angle of the Nazca plate (e.g. James and Sacks[167]). This would allow for an influx of hot asthenospheric flow and crustal thickening via magmatic underplating, with a westward migration of arc magmatism, uplift, and probably hydrothermal activity. Whereas the exact temporal correlation between Nazca plate history and gold veining remains controversial, the epithermal gold ores of the Andes are undoubtedly the consequence of shallow-level syn-arc magmatism.

In contrast, high- and low-sulfidation epithermal mineralization in the western USA correlates with post-arc continental magmatism. There is an apparent younging of major epithermal systems oceanward from about 30 Ma in the Colorado Mineral Belt (e.g. Cripple Creek, 800 t), to ca. 25—20 Ma from western Colorado to central Nevada (e.g. Round Mountain, Goldfield), to 14 Ma in western Nevada (e.g. Comstock), and to the last few million years along the San Andreas fault system (e.g. McLaughlin). All of these gold systems developed subsequent to 120—80 Ma arc magmatism, and to Laramide (e.g. 80—50 Ma) basement uplifts and foreland basin formation in the related back arc[168]. They broadly correlate with the sinking of the Farallon slab after uplift of the present-day Rocky Mountains, extensional tectonism migrating back towards the continental margin, and the Early Miocene initiation of the San Andreas transform fault system. The deposits, therefore, formed at least 50 Ma after cessation of the main Cordilleran arc magmatism, and on both sides of the Mesozoic continental margin arc.

It is likely, but unknown, that significant Andean-style epithermal gold deposits developed in shallow levels of the southern and central North American Cordilleran arc earlier in the Mesozoic, as mainly deeper crustal levels are now exposed in the Sierra batholith and much of the Klamath Mountains. Farther to the north, a few tens of kilometers inland of an Eocene continental margin magmatic arc (Cascades to Coast batholith), ca. 50 Ma epithermal gold deposits formed during back-arc extension in the northern Cordillera, between northern Washington (e.g. Republic) and the southern Yukon (e.g. Mount Skukum/Wheaton River).

Other Circum-Pacific Mesozoic continental volcanic arcs that are spatially associated with an abundance of epithermal gold deposits occur in the Russian Far East and in southeastern China. In both regions, ore formation seems to show a close temporal association with preserved Pacific, shallow level arc-related magmatism. In northeastern Russia, high- and low-sulfidation gold deposits are widespread (e.g. Kubaka, Karamken) within the ca. 105—70 Ma Okhotsk-Chukotka volcanic arc[143,169,170]. The relatively-narrow, ＞3500-km-long, calc-alkaline arc may be related to slab rollback beneath, and associated extension within, the accreted Mesozoic oceanic terranes of easternmost Russia[171]. Therefore, the epithermal gold deposits are associated with a narrow arc, such as in the Andes, but they post-date the main period of collisional tectonism, such as in the North American Basin and Range province. This again re-emphasizes the association of continental epithermal gold with shallow, high-temperature crustal regimes, rather than with a single spatial/temporal tectonic setting.

A distinct late Yanshanian (e.g. mainly Early Cretaceous) metallogenic province extends in a NNE-trend for about 1 000 km along the coastal side of the southeastern China fold belt. Epithermal gold deposits are widespread along most of the coastal region, although, as with much of China, they are not widely developed; the high-sulfidation Zijinshan deposit with 9.6 t Au is the largest recognized resource. The deposits are immediately south of an area of economically important Cu-Fe-Au-Mo porphyry and skarn deposits along the lower Yangtze River[172], and it is likely that this area too is prospective for additional epithermal gold deposits. The epithermal de-

posits are associated with 146—87 Ma potassic, calc-alkaline igneous rocks that appear to be products of post-collisional crustal extension within Neoproterozoic and younger country rocks[173]. Metallogenic settings are comparable to those of the Oligocene-Miocene of the USA Basin and Range.

The peri-Mediterranean region of southern Europe, extending from southeastern Spain to Bulgaria, has been an important source of epithermal gold for 5000 years. On the eastern side of this belt, production from mainly the South Apuseni Mountains of Romania, the Drina-Rhodope arc of Bulgaria[145], and parts of northern Greece may have reached 2240 t Au[146]. Major high- and low-sulfidation deposits include Chelopech (Bulgaria, 201.6 t), Bor (268.8 t) and Lahoca. More recently, additional epithermal gold provinces have been delineated in Sardinia and Tuscany[174]. The gold deposits throughout this Carpathian-Balkan region formed at shallow crustal levels in Late-Oligocene to Miocene time, simultaneously with widespread potassic, calc-alkaline magmatism. The overall tectonic setting of the gold ores is complex[175] and difficult to generalize. The ores post-date the main stage of Alpine continent-continent collision that ended at about 40 Ma. The subsequent history is defined by a series of microcontinent collisions, arc-forming events, and extensional episodes in the sutured area that likely represents a diachronous post-Eocene tectonism of the region. Much of the tectonism may have been controlled by some type of lithospheric detachment and resulting shallow emplacement of asthenosphere[176].

Whereas most of the epithermal gold deposits in continental settings are Cretaceous through Cenozoic in age, locally preserved, shallow levels of older Paleozoic orogens also contain some important ore systems. Such gold deposits of Variscan (late Paleozoic) age are scattered throughout relatively low-grade metamorphosed parts of the Tian Shan in central Asia. These deposits, some spatially associated with important Cu-Au porphyry systems, include Kochbulak (128 t) and Kairagach in the Chatkal-Kurama district of Uzbekistan[148], Shkol'noe in the Kundjol district of northern Tadjikistan[149], and Xitan and Axi in Xinjiang, China (Rui et al., 2001, listed at the foot of table 4). Geochronological data indicate that the gold deposits and related magmatism developed late- to post-collisional, and thus are not accreted island arc gold systems (see below). The distribution of these deposits north of the main Variscan suture zone, and much of the related deformation and magmatism, again suggests a back-arc tectonic setting for the central Asian epithermal deposits. More reliable detailed studies are needed, however, before it can be determined whether the deposits formed as part of the main arc event or during post-collisional, back-arc extension.

On the opposite side of the Paleo-Tethys Ocean, Paleozoic epithermal gold deposits formed within various fold belts of the Tasman orogen. Although better known for its important orogenic gold deposits, preserved shallow levels of the orogen host some important epithermal gold ores of varied age. Older arc-related hydrothermal episodes included formation of the Ordovician high-sulfidation Peak Hill epithermal system during development of the Lachlan fold belt[151]. Unlike many typical high-sulfidation epithermal deposits, but similar to the giant Pueblo Viejo

epithermal gold deposit, Peak Hill is characterized by a pyrophyllite, rather than a vuggy quartz, core zone[157]. The epithermal veins are broadly spatially, distinctly temporally, and probably genetically, associated with the important Au-Cu porphyry deposits, such as Cadia Hill, throughout northern New South Wales. Some workers have proposed that the arc magmatism associated with the shallow gold systems formed in an oceanic setting and represents, therefore, accreted oceanic island arc epithermal/porphyry gold deposits (e.g. Cooke et al.[177]) such as is recognized in northwestern North America (see below discussion of Stikinia).

Younger epithermal deposits preserved within the Tasman orogen occur in a more definite continental setting within the Thomson and Hodgkinson-Broken River fold belts of Queensland[178]. These have many features in common with Tertiary Basin and Range low-sulfidation epithermal deposits (Nevada) discussed above. The Queensland deposits were also formed in continental basins, similarly associated with back arc extensional volcanism[179]. The Cracow deposit in the Bowen basin (about 32 t Au) is associated with Early Permian circular volcanic features, which evolved during Late Carboniferous-Early Permian felsic to intermediate volcanic episode. Nearby low-sulfidation, auriferous breccia pipes in Precambrian basement rocks (e.g. $>$ 128 t Au at Kidston) are also part of the same hydrothermal epoch, but may represent the part of a continuum of mineralization styles that is more closely tied to the causitive intrusions[151]. Within the Drummond basin, hydrothermal deposits of approximately the same age range from epithermal veins (e.g. Pajingo, Mt. Coolon) to hot springs style ores, and probably are contemporaneous with felsic to intermediate volcanism[150]. With the final seaward growth of the Tasman orogen in the Late Permian to Triassic, volcanism and low-sulfidation epithermal events (e.g. North Arm) migrated to the east into the evolving New England fold belt[178].

4.5 Oceanic island arcs

Epithermal gold deposits are notably associated with Cenozoic oceanic arcs in the southwest Pacific, with giant systems containing 320—960 t Au at Lihir, Porgera, and Lepanto. These deposits, generally grading 2—10 g/t Au, are consistently ca. $\leqslant$10 Ma. Many of the epithermal systems from this region are genetically associated with copper-gold porphyry deposits. As is pointed out below, the transition from orthogonal to oblique subduction may be critical for the localization of magmas and fluids[151]. High-sulfidation deposits are well recognized above many mineralizing plutons in the region (e.g. Lepanto, Philippines), whereas low-sulfidation deposits are sited in lateral environments. It is the latter group that is, however, most important economically, forming the majority of the high tonnage resources in the calc-alkaline subaerial volcanic sequences of the Southwest Pacific.

The distribution of epithermal deposits, from Taiwan of China to the North Island of New Zealand, is described in detail[152]. Most deposits are ultimately the products of subduction of one oceanic plate beneath another. However, in a number of locations, epithermal gold deposits overly a zone where an oceanic plate is subducting beneath continental crust. These include the subduc-

tion of the Pacific plate beneath Australia to form parts of New Guinea, parts of Sumatra and Java, and the North Island of New Zealand[152].

The Southwest Pacific epithermal deposits are relatively base metal-rich, are dominated by crystalline and not chalcedonic quartz, and typically lack adularia in low-sulfidation deposits[108]. Silver contents of the epithermal veins are also generally uncharacteristically low relative to those for gold. These are important differences from the epithermal deposits of the western USA. Many of the Southwest Pacific deposits have formed at greater depths than are typical of epithermal systems in other regions. Kelian, on the island of Java, for example, formed at depths of at least 900—1500 m at temperatures of 280—310℃, indicating P-T atypical of the epithermal gold deposit type[152]. Also, the earlier, alkalic intrusion-related ores at Porgera show many features characteristic of orogenic veins and not simply classic epithermal deposits[181].

Both the solely young ages and the commonly "deep" epithermal systems are consequences of high rainfall, rapid uplift, and extreme erosion rates that expose deeper parts of the still-remaining hydrothermal systems[152]. Surface discharge from hydrothermal systems is uncommon within the oceanic arcs perhaps due to the high hydrostatic head that must be overcome for vertical flow in these high relief environments[151]. Instead lateral flow along highly-permeable zones may exceed 5—10 km before vertical structures are reached that are favorable for development of vein systems from mixed magmatic-meteoric fluids. In contrast to this more common arc environment, within the back-arc continental rift setting of New Zealand, present-day hot springs are actively depositing gold from mainly heated meteoric waters near Taupo.

Subduction-related tectonics within Meso-Pacific oceanic island arcs in the Late Triassic and Early Jurassic, immediately prior to their collision with and docking along the Canadian Cordillera continental margin, were associated with a major interval of porphyry formation[158]. Resulting alkalic Cu-Au and calc-alkalic Cu-Mo ± Au porphyry deposits now cluster throughout present-day central British Columbia, occurring within the accreted island arcs developed upon what are termed the Stikinia and Quesnellia terranes. The alkalic stocks are both silica-saturated and silica-undersaturated, and have primitive mantle geochemical signatures[182]. Commonly the Canadian Cordillera porphyry deposits zone outwards to important gold-rich epithermal vein systems (Sulphurets, Red Mountain). Some of these low sulfidation epithermal systems show a more replacement style of mineralization (e.g. Snowfield). Other epithermal gold-silver vein districts in the Stikine terrane, such as Stewart and Toodoggone, are related to subvolcanic intrusions that are part of the same Early Jurassic magmatic episode.

A similar tectonic scenario appears to characterize a belt of epithermal gold deposits within the southern Ural Mountains. Epithermal gold deposits of the Bereznjakovskoje gold belt extend along the eastern edge of the mountain range and contain 64—128 t Au in a Late Devonian intermediate volcanic and subvolcanic rock sequence[159]. These arc-hosted gold lodes probably formed in an oceanic setting and, as with Stikinia above, were accreted to a continental margin during the Uralide orogeny.

Preserved epithermal gold deposits from the Precambrian are rare, but, given favorable conditions for preservation in a stable region, cannot be totally discounted. A high sulfidation epithermal gold deposit within a latest Proterozoic oceanic arc in the Avalon terrane of eastern Canada has been reported[183]. The arc would have formed somewhere within the Iapetus Ocean and, some 200 Ma later, was accreted to North America. Early tilting or burial of the volcano-plutonic sequence may be a critical factor for preservation of the shallow-level gold systems[183].

5 Copper-gold porphyry deposits

5.1 Introduction

Porphyry deposits are the leading source of copper and molybdenum, but some also contain abundant gold and silver. Several gold-rich deposits contain from 300 to more than 1 500 t of gold. Gold-rich porphyry deposits occur in both continental and island-arc orogenic settings. Classic provinces in continental settings include the central Andes, western USA, and Papua New Guinea-Irian Jaya, whereas volcanic island-arc deposits occur throughout the western Pacific (table 5). The largest gold-rich porphyry deposits are listed in table 6).

Table 5 Principal characteristics of copper-gold porphyry deposits

Age range	Mainly Cenozoic and Mesozoic, but can be any age; Tertiary most common
Classic provinces (Classic deposits)	Continental margin: Western USA (Bingham and Dos Pobers), Central Andes (Bajo de la Alumbrera and Marte), Papua New Guinea-Irian Jaya (Grasberg, Ok Tedi, Freida River). Island arc: Western Pacific (Panguna, Batu Hijau, Lepanto-Far South East)
Structural style	Mainly brittle, with early semi-ductile "A veinlets" related to magmatic intrusion; fracture patterns indicate regional and local stress fields
Mineralization style	Steeply dipping stockwork veins and fractures localized about causative intrusion (s); progression of "A", "B" and "D" veins through space and time
Host rocks	Intermediate to felsic calc-alkaline and K-alkaline porphyritic intrusions and adjacent volcanic, sedimentary and other rock type; coeval andesitic to dacitic volcanic rocks are common in island arc settings; K-alkaline rocks more common in continental settings
Metal associations and ratios	Central Cu-Au (Mo, Ag); outer Pb-Zn (Ba, Mn); Mo common in core of continental deposits and in periphery of island arc deposits. Common Au ($\times10^{-6}$): Cu(%) of 1:3 to 1:1 with $>1:1$ for deposits with Au$>0.6\times10^{-6}$
Gold fineness	Native gold and electrum
Proximal alteration	Variation in space and time with respect to causative intrusion(s) emplacement: central and early K-silicate alteration; peripheral and late intermediate argillic; sericitic and advanced argillic alteration associated with intrusive margins, faults and lithocaps(advanced argillic)
P-T conditions	Early-stage magmatic fluid, $\delta^{18}O=+6‰$ — $+10‰$ (K-silicate alteration); Late-stage external fluid, $\delta^{18}O=-10‰$ — $+5‰$ (phyllic and advanced argillic)
Heat sources	Causative intrusion (s)
Other features	Topology of subducting slab exerts a control on porphyry mineralization in the overlying arc; as do deformational settings that lead to crustal thickening, block uplift and arc-transverse fault/fracture zones

For details see refs. [140, 183—189].

5.2 Deposit characteristics

Porphyry deposits are characterized by disseminated, veinlet- and fracture-controlled cop-

Table 6 Summary of selected large gold-rich porphyry copper deposits

Deposit, Location	Au/t[a)]	Cu (%)[b)]	Au/g • t^{-1}	Tectonic setting[c)]	Chem. assoc.[d)]	Age/Ma	Reference
Grasberg, Indonesia	1599	1.3	1.42	Cont	KA	3	[190*, 191]
Bingham, Utah, USA	933	0.7	0.31	Cont	KA	~38	[192, 193*]
Panguna, Papua New Guinea	766	0.46	0.55	VIA	CA	3.4	[194]
Bajo de la Alumbrera, Argentina	516	0.53	0.64	Cont	KCA-SH	8	[195, 196*]
Lepanto-Far South East, Philippines	441	0.73	1.24	VIA	CA	1.5	[197, 198]
Batu Hijau, Indonesia	366	0.53	0.4	VIA	CA	3.7	[199, 200*]
Ok Tedi, Papua New Guinea	287	0.67	0.61	Cont	KCA	1.2	[201*]

a) Contained metric tonnes of gold determined from reported reserves and past production, with the exception of the resource figure quoted for Lepanto-FSE. b) Average grades are those reported, or calculated from reserve and production data, in the references indicated by star (*). c) Tectonic setting: Cont=continental; VIA=volcanic island arc. d) Chemical association of causative intrusions and related rocks: CA=calc-alkaline; KCA=high-K calc-alkaline; KA=K-alkaline; SH=shoshonite.

per-iron sulfide minerals distributed throughout a large volume of rock in association with potassium silicate, sericitic, propylitic and, less commonly, advanced argillic alteration in porphyritic plutons and the immediate wall rocks[186,202,203]. In porphyry systems, there exists a close spatial and temporal link between volumetrically-small causative intrusions and broadly dispersed magmatic-hydrothermal alteration and mineralization. Porphyry copper deposits are large, typically hundreds to thousands of million tons, and low to medium in grade with 0.3%—1.5% copper. The majority of gold-rich porphyry deposits occur in the circum-Pacific and contain 0.3—1.6 g/t gold[140,204].

The general characteristics of porphyry systems are summarized in table 5. The most important characteristics are: (1) Presence of causative intrusions of intermediate to felsic composition, and small diameter (<2 km). (2) Shallow levels of emplacement, typically 1—4 km. (3) Porphyritic texture of causative intrusions, where feldspar, quartz and mafic phenocrysts are contained in a fine-grained to aplitic groundmass. (4) Multiple phases of intrusion, which may be pre-, syn- or post-ore; late-stage diatremes are typical in western Pacific volcanic arc settings. (5) Multiple stages of hydrothermal alteration associated with each mineralizing intrusion. (6) Extensive development of fracture-controlled alteration and mineralization in both porphyritic intrusions and adjacent wallrock. (7) A progression from early, discontinuous and irregular veins and veinlets (“A veinlets”), through transitional planar veins (“B veins”), to late through-going veins (“D veins”) and breccia bodies. (8) Hydrothermal alteration that progresses from early, central potassium silicate and distal propylitic styles, to late sericitic, advanced and intermediate argillic alteration types. (9) Sulfide and oxide minerals which vary from early bornite-magnetite, through transitional chalcopyrite-pyrite, to late pyrite-hematite, pyrite-enargite or pyrite-bornite. (10) Early alteration and copper mineralization generated by magmatic fluids with 30 to 60 wt% NaCl equivalent salinities over a temperature range of 400 to ＞600℃. Fluids related to late alteration and mineralization commonly include a meteoric component and are more dilute (<15 wt% NaCl equivalent) and lower in temperature at 200 to 400℃.

5.3 Tectonic controls on mineralization

The majority of published papers concerning the controls on the localization of intrusion-related copper and gold porphyry deposits have focussed on the general tectonic framework of volcano-plutonic arcs, structural setting, magma composition, lithological association, and crustal-scale faults. According to Sillitoe[140], porphyry deposits occur either in compressional or extensional regimes of both continental and oceanic island-arcs. Corbett and Leach[151] discuss the effects of orthogonal- versus oblique-convergence on the styles of crustal deformation and deposit types in arc settings; they observe that intrusion-related mineralization typically develops in arcs having orthogonal convergence during localized changes to oblique convergence.

Solomon[205] suggests that many gold-rich porphyry deposits in the western Pacific arcs formed as a consequence of a reversal in subduction polarity, as exemplified by north Luzon, Philippines and Bougainville, Papua New Guinea. The development of calc-alkaline and K-rich alkaline magmas in this setting likely reflects deep second-stage melting of the previously melted mantle wedge above the subducting slab and upwelling in a dynamic tectonic environment. There is a direct genetic link between high-K igneous rocks and the formation of gold-rich porphyry copper and epithermal deposits[155,206,207], as discussed in the previous section. In addition, many workers believe that it is the high oxidation state of porphyry magmas that leads to metal enrichment, through the vapor saturation of the crystallizing melt[208—210].

Some studies stress the importance of compressive deformation, crustal thickening and rapid uplift in the localization of intrusion-related deposits at high-levels in continental margin settings[166,211]. The focussing of ascending magma and hydrothermal fluids along major transcurrent faults and regional lineaments, defined by satellite imagery and geophysical data, is a regularly cited theme. Porphyry and intrusion-related epithermal deposits are localized along strike-slip faults and lineaments that extend sub-parallel to, or are oblique to perpendicular to magmatic arcs. Examples of arc-parallel fault zones that control the distribution of mineral deposits include the Philippine fault in the Philippines, and the West Fissure-Domeyko fault system in Chile[212]. Examples of arc-transverse structural controls are the Lakekamu transfer structure——Bulolo graben system in Papua New Guinea[151], and cross-arc segmentation of magmatism and mineral deposits in the Andes[29]. In the central Andes the potential relationship between the topology of the subducting slab, magma genesis and mineralization in the overlying arc has been highlighted[166,213,214].

The relationships between tectonic elements and the localization of both porphyry copper-gold and intrusion-related epithermal deposits are documented below. Particular emphasis is placed on the relationship of the topology of the subducting slab to the style of deformation and its control on magmatism and associated mineralization in the overlying arc crust (fig. 5). Examples are drawn from the Neogene and Pleistocene mineral districts in Papua New Guinea, Indonesia, and the Philippines, and the Miocene districts of the central Andes, where the effects of subsequent tectonic events are relatively minor. These regions have been studied extensively and abun-

dant data are available. The potential to apply these relationships to the early Tertiary deposits of the western USA is also discussed.

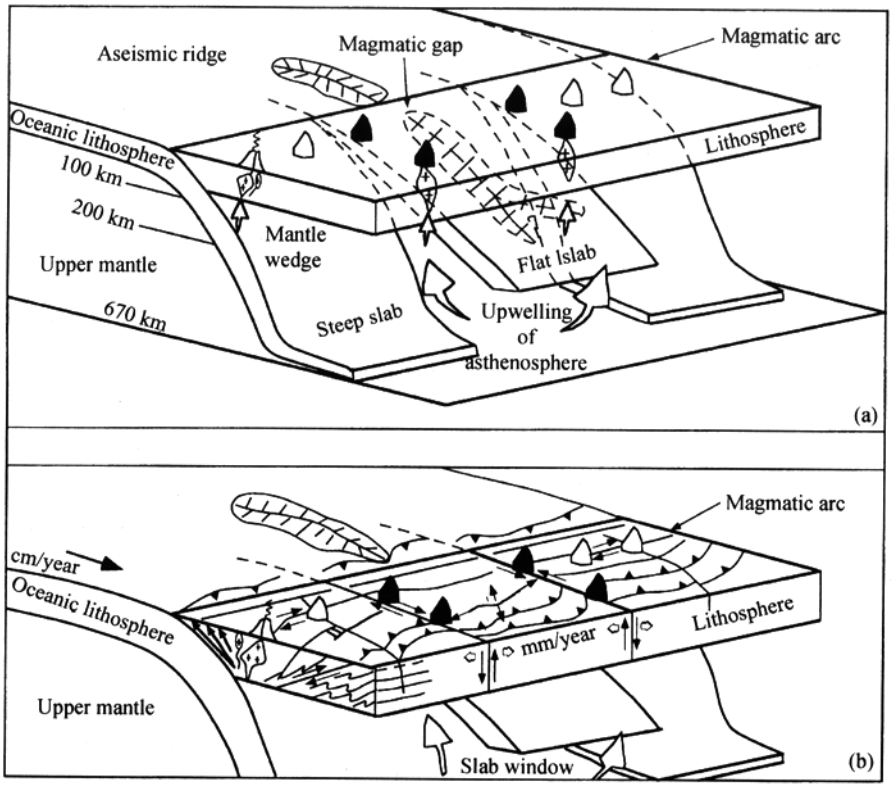

Fig. 5. Schematic block diagrams illustrating both the subduction of a buoyant aseismic ridge and the relationship of the topology of the down-going slab to the style of deformation and localization of magmatism in the overlying continental or oceanic plate. (a) Generalized geometry: upwelling of asthenosphere and arc-transverse magmatic trends (symbolized by darker volcanoes) are localized by tears in the slab; note magmatic gap above flat-slab region. (b) Deformation styles in overlying plate: note arc-parallel and arc-transverse fault and fracture systems. Diagrams adapted from refs. [151, 215, 216].

5.4 Crustal thickening, block uplift and topology of the subducting slab

5.4.1 Continental settings. Compressional tectonics led to localized deformation and crustal thickening immediately prior to, or during, the emplacement of mineralized intrusions in the Cordilleran margin of the central Andes and the Papuan fold and thrust belt in continental New Guinea. This crustal thickening caused the uplift of the Cordillera, Altiplano and Puna Plateau in the central Andes[166], and the Central Ranges in New Guinea[217]. Both regions lie above 3000 m and have experienced significant erosion.

In the central Andes, crustal thickening was accompanied by a decrease in dip of the subducting Nazca Plate during the waning stages of arc volcanism as the arc migrated towards the east[166,214]. A general southward younging in the age of intrusion-related deposits exists, from

early Miocene in the Maricunga Belt in the north, to latest Miocene at El Teniente in the south. This distribution coincides with the southward progression of crustal thickening and decrease in slab-dip. Kay et al.[166] document this parallel relationship on the basis of REE and other chemical signatures of calc-alkaline and K-rich alkaline lavas erupted coevally with mineralization. The cause of this reduction in slab-dip is not certain, but may represent the southward progression of the subducted trace of the buoyant aseismic Juan Fernandez Ridge beneath the central Andes[211,214,218].

In contrast, the geochemical data[213] presented for the late Miocene Farallon district, about 250 km east of the Maricunga Belt, show no indication of substantial crustal thickening during, or prior to, mineralization. The emplacement of the Bajo de la Alumbrera and other porphyry deposits in this district may require another mechanism than that proposed by Kay et al.[166], as is discussed below.

The mineralized Plio-Pleistocene K-rich alkaline intrusions, such as Ok Tedi and Grasberg in the Central Ranges of New Guinea, do not overlie a well defined Wadati-Benioff zone and lack coeval subaerial volcanic rocks. However, this paucity of volcanic rocks may in part reflect the extensive uplift and erosion of the region. The source of the K-rich alkaline magmas is unconstrained. Favored possibilities include delayed partial melting of the mantle modified by Cretaceous (?) subduction beneath the continental margin, prior to the accretion of allochthonous arc terranes[219], or alternatively asthenospheric upwelling arising from the docking of arc terranes transported from the east[220].

The emplacement of many of the western USA porphyry deposits occurred during the latest Cretaceous to early Tertiary Laramide orogeny, a period of folding, thrusting and crustal thickening[186,221]. A shallow angle of subduction for the Farallon plate is inferred to have developed due to an increase in the rate of convergence during this time[221]. Alternatively, Murphy et al.[132] proposed that the Farallon Plate was buoyed by the migration of the subduction zone over a mantle plume, beginning at about 70 Ma. Many of the western USA deposits, with ages that range from about 54 to 72 Ma, lie proximal to the inferred hinge of the Farallon plate at 60 Ma[222], as modified by Kirkham[215].

5.4.2 Island-arc settings. The Plio-Pleistocene gold and copper deposits in the Baguio and Mankayan districts of the Luzon Central Cordillera of the northern Philippines occur in an uplifted portion of oceanic basement that lies more than 1 500 m above sea level. The presence of mid Miocene coralline limestone (Kennon Formation) and convex geomorphologic valleys attest to the Pliocene to Recent uplift of this region. The Central Cordillera contains folded and thickened crust that lies above the trace of the subducted aseismic Scarborough seamount chain. The eastward-directed subduction of this chain beneath the Manila trench in Pliocene to Recent times is inferred to have led to the formation of a broad structural arch termed the Stewart bank, slab flattening, and resultant uplift[223]. According to Yang et al.[223] there was a 2 to 3 Ma hiatus in arc

magmatism during the interruption of subduction by initial ridge-arc collision, followed by renewed magmatism at about 2 Ma related to upwelling asthenosphere localized by a tear in the down-going slab. The timing of this second magmatic pulse correlates well with the 1.5 to 1.2 Ma timing of porphyry and epithermal mineralization at Lepanto in the Mankayan district[198].

Crustal thickening and regional uplift are relatively under-developed in the volcanic island arcs underlain by oceanic crust in Indonesia. However, Pliocene porphyry copper-gold deposits and related high-sulfidation systems, including Batu Hijau in Sumbawa and the Tombulilato district in North Sulawesi, occur in arc crust that lies above kinks in the subducting slabs, which are inferred from the distribution of earthquake hypocenters (Wadati-Benioff zone; Garwin, in preparation). These kinks define arc-parallel segments of varying slab-dip that locally coincide with the margins of subducted oceanic plateaus, for example the Roo rise on the Indian plate south of Batu Hijau. Hence, even in regions where large-scale crustal thickening is lacking, the topology of the subducting slab is inferred to exert a control on the localization of intrusion-related deposits in the overlying arc.

5.5 Crustal basement, collisional events and regional-scale faults

The majority of the largest and richest porphyry copper-gold deposits lie along arcs constructed on continental margins, where causative intrusions are inferred to be emplaced at high structural levels due to crustal thickening and rapid uplift[211]. However, in the magmatic arcs of Indonesia, exclusive of Irian Jaya, intrusion-related porphyry and high-sulfidation epithermal gold systems are preferentially developed in arcs built on oceanic lithosphere. The continental sectors of the western Indonesian arcs, the Sunda and Central Kalimantan arcs, lack large porphyry deposits and evidence of Neogene crustal thickening, such as the regional fold and thrust belts that characterize the central Andes and the Central Ranges of New Guinea. Hence, in orogenic arc settings that lack the localization of compressional deformation and block uplift, thick continental crust may impede rapid magma ascent and high-level emplacement of mineralizing intrusions. Structurally prepared sectors of arcs built on thin oceanic lithosphere may prove to be ideal hosts for intrusion-related deposits, as discussed below.

The moderately- to steeply-dipping Indian plate slab is subducting obliquely beneath the Sunda arc in Sumatra, with the Sumatra dextral strike-slip fault accommodating a large portion of the arc-parallel component of subduction. This segment of the Sunda arc lacks any significant intrusion-related copper-gold deposits, with the singular exceptions of the Tangse porphyry copper-molybdenum and Miwah high-sulfidation epithermal systems in the northern tip of Sumatra[224], where the dip of the slab flattens to about 30^{o}. Hence, gentle slab dips appear to be a common denominator for intrusion-related mineralization in continental arc settings.

In contrast, the development of intrusion-related deposits in the volcanic island-arcs of eastern Indonesia is generally controlled by arc-transverse normal- and oblique-slip fault zones in oceanic lithosphere that overlies kinks in the subducting slab, as discussed above. The Batu Hijau

porphyry deposit, on Sumbawa in the Banda arc, lies within 30 km of a major left-lateral oblique-slip fault zone that controls the distribution of Miocene volcano-sedimentary units and the present coastline of the island. Northerly directed subduction is nearly orthogonal to the trend of the arc in the vicinity of Sumbawa[225]. This geometric relationship is inferred to have been relatively stable since the middle Tertiary[226]. The age of the causative intrusions and mineralization in Batu Hijau (~3.7 Ma)[227] corresponds to the approximate timing of the collision of the Australian continent with the Banda arc at ~4 to 2.5 Ma, in the vicinity of Timor towards the east[226,228]. This collision is inferred to have caused arc-parallel extension, as the arc expanded westwards away from the site of collision. Fault plane solutions from recent earthquake hypocenters indicate about 3 mm/a of east-west extension along arc-transverse strike-slip faults in the vicinity of Sumbawa-Timor[229,230].

Hence, major tectonic events, such as continent-arc, arc-arc and ridge-arc collisions, may cause a deviation in the regional stress field of an arc undergoing near-orthogonal convergence, leading to episodic dilation along arc-transverse strike-slip fault arrays. In turn, such events act to localize the rapid ascent of magma and associated efficient release of mineralizing fluids at high structural levels. Similarly, the formation of intrusion-related Plio-Pleistocene deposits in the Luzon Central Cordillera of the northern Philippines, and at Chinkuashih in northern Taiwan, may also be related to fault reactivation due to variations in regional stress fields. In this case, the variations in stress fields were caused by the collision of the Philippine Sea plate with the Eurasian continent in of China, which commenced at about 5 Ma[216]. Another example of the causative relationship between collisional tectonic processes and intrusion-related mineralization occurs in the Bougainville-Solomon island arc of the southwest Pacific. There, the Pliocene development of the Panguna (Bougainville) and Koloula (Guadalcanal) porphyry deposits correlates with a reversal in the polarity of subduction[205]. These deposits are related to northeasterly directed subduction, which was initiated following the termination of southwesterly directed subduction in the middle to late Miocene, due to the collision of the arc with the Ontong Java plateau[205].

Regional-scale arc-transverse faults are not well documented from ground mapping in the central Andes and the Central Ranges of New Guinea. However, the cross-arc distribution of mineral deposits, district-scale faults, age-equivalent volcano-plutonic units and remotely-sensed lineaments, have led workers to postulate the existence of deep-seated fault zones in the overlying lithospheric plate or in the down-going slab. Examples include arc-transfer structures that extend through several of the large deposits in mainland Papua New Guinea[151] and the trace of the "Easter Hot Line" beneath the Miocene Maricunga belt and Farallon district of Chile-Argentina[213,231].

The Easter hot line marks a linear zone of upwelling asthenosphere localized by an easterly trending kink or tear in the subducting Nazca plate as the slab-dip flattens from north to south. It lies adjacent to the northern boundary of the Chilean flat-slab and is inferred to overlie the rifted margin of the Arequipa-Antofalla Craton[213]. Hence, the localization of early- to late-Miocene

mineral deposits along this belt may reflect the reactivation of deep-seated crustal faults. The arc-transverse distribution of deposits, which extends eastwards from the El Teniente deposit through Paramillos Sur to the San Luis belt in Chile-Argentina, follows the southern margin of the Chilean flat-slab, adjacent to the edge of the subducted Juan Fernandez Ridge. This axis also coincides with a kink in the down-going slab, and may reflect decompression melting and upwelling of asthenosphere through a tear in the subducting plate, referred to by some as a slab window[215].

The distribution of early Tertiary porphyry deposits in the western USA defines local cross-arc axes, as typified by the northeast-trending Idaho-Montana porphyry belt[232], which locally coincides with the trans-Challis–Great Falls lineament. The Butte mining district, Montana occurs adjacent to this lineament[233], which is inferred to mark an intra-plate discontinuity that dates back to the Precambrian. According to Kirkham[215], the northeast-trending porphyry belt may have developed in a similar setting to arc-transverse mineral trends in the central Andes, adjacent to the margins of flat-slab segments in the subducted Farallon plate at about 60 Ma.

5.6 Conclusions

The largest and most significant intrusion-related copper-gold and gold deposits in the western Pacific and the central Andes are associated with a common set of tectonic-related geological features. Many of the deposits occur in continental orogenic settings, which are characterized by crustal thickening, block uplift and a flattening or variation in the dip of the subducting slab. However, volcanic island-arcs underlain by oceanic crust also host large deposits. In both continental and oceanic settings, kinks or tears in the subducting slab, or instabilities in the mantle, localize asthenospheric upwelling, which leads to the rapid ascent of magma to high-levels in the overlying crust, where vapor saturation, exsolution of volatiles and copper-gold deposition may occur. The spatial coincidence of kinks in the down-going slab with deformation zones in the overlying arc lithosphere facilitates magma emplacement by establishing a link between the asthenosphere and the upper levels of the arc crust (fig. 5). The episodic reactivation of crustal-scale fault- and fracture-systems in transpressional to transtensional settings further enhances crustal permeability in orogenic arcs, where changes in plate convergence direction, collisional events and the subduction of buoyant aseismic ridges serve to vary the orientation of predominantly arc-orthogonal compressive stress fields.

In contrast, the largely extensional tectonic settings that form in pull-apart basins, developed along arc-parallel strike-slip fault zones in oblique-convergence arc settings, and in back-arc rift basins, favor the decoupling of ore-bearing volatile phases from ascending magmas and cooling intrusions. Low-sulfidation epithermal gold and volcanic-hosted massive sulfide deposits, which typically indicate a less direct relationship to causative intrusions, would be more common in these tectonic settings.

6 Iron-oxide Cu-Au deposits

6.1 Introduction

Iron-oxide copper-gold deposits are a relatively recently-recognized class of structurally controlled, epigenetic deposits. They generally formed in extensional environments predominantly in the Palaeoproterozoic to Mesoproterozoic[234—237]. Large deposits of this class typically contain ＞100 Mt at 0.8%—1.6% Cu and 0.25—0.8g/t Au. According to Hitzman et al.[235], they may form part of an even more-extensive class of deposits, termed iron-oxide Cu-U-Au-REE deposits which include the giant P-bearing iron ores of Kiruna, Sweden and the iron-rich REE ores of Bayan Obo, Inner Mongolia, China.

The type example of this deposit class is Olympic Dam, with about 2 000 Mt of 1.6% Cu and 0.6g/t Au, which formed in the Stuart Shelf, South Australia[238]. Other world-class examples include Ernest Henry, with 167 Mt at 1.1% Cu and 0.5g/t Au in the Cloncurry district of Queensland[237]. Deposits that likely belong to this class, but which are as yet not well documented, include Salobo with about 1 000 Mt at 0.85% Cu and 0.4 g/t Au; Igarape Bahia/Alemao with 140 Mt at 1.5% Cu and 0.8g/t at Alemao; and other deposits at Carajas, Brazil[239], although other associations have been suggested for these deposits[240]. The Candelaria deposit (326 Mt at 1.06% Cu and 0.26g/t Au) in the Chilean Andes is possibly of this type; however it has some unusual features such as the presence of significant Fe-sulfides, lack of the characteristic minor-element concentrations, and a typical skarn paragenesis[241]. Smaller deposits (1—10 Mt) occur in southeast Missouri, USA, and the Wernecke Mountains, Yukon[235].

6.2 Characteristics

The principal characteristics of the deposit class are taken from Hitzman et al.[235], plus subsequent references on specific mineral provinces, with additional contributions on Carajas, Brazil, from the personal experience of one of us (table 7). They are characterized by: (1) High tonnage and low grade. (2) A dominance of iron-oxides, magnetite and/or hematite. (3) Low sulfide content of relatively low-sulfur copper minerals. (4) Low SiO_2 content. (5) Characteristic metal association of Fe-Cu-Au-REE, commonly with anomalous Ag, As, Co, F, Mo, Nb, Ni, P and/or U. (6) High Cu/(Cu + Zn + Pb) ratios.

At the regional scale, the deposits lie proximal to, or along, crustal-scale faults or shear-zones, or lineaments defined from remotely-sensed and/or geophysical data sets. At the deposit scale there is also structural control: they occur along, or between, lower-order faults or shear structures; along lithostratigraphic contacts; or at, or adjacent to, contacts between granitoids and supracrustal rocks. In terms of morphology they may have classic pipe-like shapes, for example Olympic Dam; resemble ring dikes, as at Igarape Bahia/Alemao, Sossego at Carajas; be somewhat irregular, e.g. Ernest Henry; or have the sheet-like form of Candelaria. Most large ore bodies consist, at least in part, of breccias, but there may also be replacement of reactive or porous rocks. In breccia-dominated ore bodies there is commonly replacement of fragments, and the margins of the

Table 7 Principal characteristics of iron-oxide Cu-Au deposits

Age range/Ga	1.8—0.1 (most 1.8—1.4)
Classic provinces (Classic deposits)	Stuart Shelf, South Australia (Olympic Dam); Cloncurry Region, Queensland (Ernest Henry); Carajas Region, Brazil (Salobo, Igarape Bahia); Atacama Province, Chile (Candelaria).
Structural style	Mostly brittle to brittle ductile structures, variable structural control.
Mineralization style	Variably oriented, commonly steep, breccias, discordant veins or concordant replacement-style bodies.
Host rocks	Extremely variable. Range from Archean gneisses and greenstones to broadly coeval granitoids or volcanic and sedimentary rocks.
Metal associations	Fe-Cu-Au (Ag, As, Co, Fe, Mo, Nb, Ni, P, REE, U)
Gold fineness	Not recorded, but electrum as well as gold.
Proximal alteration	Intense alteration. Variation with depth. May be Na-Ca feldspar to K-feldspar to sericite and fayalite to grunerite to actinolite to carbonate with decreasing depth. Quartz poor, particularly at depth.
P-T conditions	Variable. Probably 200—400℃ for Cu-Au, but up to 600℃ for Fe-silicates and magnetite.
Ore fluids	High salinity, acid, oxidized fluids.
Isotopes (water)	$\delta^{18}O$= +6‰ to +10‰
Heat sources	Probably magmatic (alkaline?) intrusions. Olympic Dam coeval with anorogenic magmatism.
Other features	May be transitional to giant P-bearing iron ores of Kiruna and to REE-rich iron ores of Bayan Obo. May be related to Au-Pd deposits such as Serra Pelada and Jacutinga-type.

pipes. In contrast to many other hydrothermal deposit classes, the ores are generally devoid of, or deficient in, quartz, and silicate minerals are replaced by magnetite, indicating SiO_2 dissolution rather than deposition.

The deposits are hosted in a wide variety of rocks, from coeval anorogenic granitoids exemplified by Olympic Dam; to older metamorphic terranes of volcanic or metasedimentary rocks such as Ernest Henry and Candelaria; to much older terranes of gneiss, granitoids or metavolcanic rocks such as the Archean host rocks at Carajas.

6.3 Vertical zonation

There appears to be significant variation of alteration mineralogy with depth. The depth of formation is estimated to extend from about l km to at least 6 km below surface although there are exceptions[235]. There is a general trend with increasing depth from dominantly hematite exemplified by Olympic Dam, to magnetite for the Ernest Henry and Carajas deposits, with a corresponding change in accompanying Fe-rich minerals from carbonate through actinolite to grunerite, and fayalite as at Salabo[240]. There is also a parallel trend from sericitic, through potassic, to Na-Ca feldspar alteration with depth[235]. Quartz may be more abundant at higher crustal levels. The depth variations correspond in a general sense with those recorded in orogenic gold deposits as in the continuum model of Groves[28], and in some porphyry-Cu systems such as Yerrington, Nevada[242]. Unlike porphyry systems, however, the deposits are not sited in or adjacent to a recognizable source intrusion. There are few data on variations in metal ratios, although Au/Cu ratios are reported to decrease with increasing depth at Candelaria[241], and locally at Olympic Dam[243]. The ca. 2.0 Ga Phalabowra Fe-P-Cu ores in South Africa have similarities to the Fe-oxide Cu-Au class in that they are magnetite-rich, contain S-poor Cu minerals such as chalcopy-

rite-bornite-chalcocite, and have high P and REE contents. They are, however, sited within an alkaline igneous complex. Consequently, these may represent the most proximal ores to the alkaline magmatic source in the class as a whole, with higher-level deposits distal expressions of these deep-seated, volatile-rich magmatic-hydrothermal systems tapped by fundamental lithospheric structures.

Typically these deposits formed in multiple stages, with a higher temperature stage characterized by Fe-oxides and associated calc-silicates and/or Fe-rich silicates, followed by a lower-temperature stage of Cu-sulfides, dominantly chalcopyrite, bornite, and chalcocite, and gold mineralization, with further Fe-oxides[238]. Other orebodies such as Candelaria show more complex overprinting relationships.

6.4 Source(s) of hydrothermal fluids and metals

Available fluid-inclusion, mineral-stability and other thermodynamic data from a number of these deposits indicate that the mineralization formed from variable, but generally high salinity, low pH and oxidizing hydrothermal fluids. Temperatures ranged from 600℃ for deposition of early magnetite and associated Fe-silicates at deeper crustal levels to 200—400℃ for the Cu-Au mineralization (summaries in refs. [235, 236]). The few published oxygen and carbon isotope data are consistent with involvement of a deep magmatic or metamorphic fluid, at least for the early stages of mineralization[235], with some meteoric water influx in the later stages[244]. The Au-Pd deposit at Serra Pelada in the Carajas Region is a sulfide-poor hematite-rich deposit, and is in the same lithotectonic and metallogenic province as several iron-oxide copper-gold deposits. It most likely formed from a similar saline acid, oxidizing hydrothermal fluid[245], and hence could be genetically related to the iron-oxide copper-gold deposit-class.

6.5 Genetic models

The ultimate source of the mineralizing fluids has been intensely debated. Most authors reject magmatic segregation models initially invoked to explain the Kiruna P-rich iron ores[246], but rather now invoke a hydrothermal origin. According to some workers the primary ore fluids have been exsolved from specific magmas. Within the proponents of a magmatic source, both alkaline magmas[234], and specific granitoid suites[247] have been proposed as fluid and metal sources. Alternatively, the ore fluids were connate basinal brines, derived perhaps from older evaporites, commonly in extensional settings[248].

There is no obvious close spatial relationship to specific igneous bodies, and hence if these deposits are magmatic-hydrothermal in origin they must form distal to the parental magmas, Phalabowra excepted. This is in contrast to deposit styles such as porphyry copper-gold, which are proximal to the magma source. However, numerous lines of evidence support a genetic relationship to magmas, and specifically to alkaline magmas: (1) The high temperature (600℃) and magmatic/metamorphic isotopic signature of at least the early hydrothermal fluid. (2) The saline ore fluid, which is characteristic of magmatic, rather than low salinity metamorphic fluids. (3) The

distinctive ore-metal association of both compatible and incompatible elements, which is similar to that of alkaline rocks, as first recognized by Meyer[234]. (4) The pipe to ring-dike forms of the breccia bodies, which resemble those of explosive alkaline intrusions. (5) The broad similarity of the carbonatite-hosted, magnetite-chalcopyrite-bornite±chalcocite-apatite ores at Phalabowra to the iron-oxide copper-gold ores. (6) The broadly coincident timing of the Olympic Dam ore body with anorogenic magmatism[249]. (7) The depleted mantle-like Nd isotope signature of the Phalabowra and Olympic Dam deposits, combined with the occurrence of hydrothermally-altered lamprophyric dykes containing high-Cr chromites in the Olympic Dam breccia ore body, and coincident magnetic and gravity anomalies consistent with an alkalic mafic body at depth[250]. (8) The common siting of at least the Proterozoic deposits near transition from thick Archean to thinner post-Archean mantle lithosphere (fig. 2(c)), where extension will develop preferentially at such lithosphere boundaries, leading to decompressional melting of metasomatized domains of mantle lithosphere, and in turn alkaline magmatism characterized by enrichment of incompatible and compatible elements.

As a corollary, the evaporite model fails to explain the origin of the Carajas deposits, which are hosted in Archaean terranes of gneisses and granitoid-greenstones rather than coeval rocks in extensional basins.

6.6 Geodynamic setting

The Proterozoic deposits on the Stuart Shelf and in the Carajas region appear to have formed in association with intracratonic magmatism, bimodal volcanism and associated anorogenic (A-type) granitoids, during major extensional tectonic events, as is the case for most other regions containing these deposits[235]. Craton margins appear to be important: the Olympic Dam deposit is sited within 50 km of the Torrens hinge zone, which effectively demarks the eastern margin of the Archean Gawler craton[243]; and Carajas is sited in the only remaining remnant of a once-extensive Archean craton, on the eastern margin of one of the most extensive anorogenic terranes on Earth (fig. 2(c)). The tectonic setting for the Cloncurry deposits, including Ernest Henry, is less clear. According to Williams[237], the deposits are broadly coeval with an intrusive suite of I-type tonalite, granodiorite, monzogranite and alkali feldspar bodies[247], associated with a transition from ductile to brittle deformation in the compressional Isan orogeny. They also appear to lie close to a boundary between thick Archean lithosphere and thinner lithosphere, although Archean rocks straddle both sides of the boundary.

The Phanerozoic examples, such as Candelaria, formed in continental arcs or areas of extension behind continental arcs. Thus, there are different tectonic settings for different deposits within the overall deposit class, with both extensional anorogenic provinces and extensional environments within compressional settings hosting Fe-oxide copper-gold deposits. Phanerozoic deposits such as Candelaria may not be exact equivalents of the Proterozoic iron-oxide copper-gold deposits; they possess characteristics that are intermediate between these and porphyry copper-gold de-

posits related to alkalic igneous rocks[206]. It is possible that differences between the characteristics of various deposits in the broader class of Fe-oxide copper-gold deposits, such as metal associations and sulfur-metal ratios, relate to source magmas: mafic alkaline to carbonatitic magmas for the Cu-Au-REE-P-F-U class; but alkalic granitoids for copper-gold deposits with relative lack of incompatible element enrichment. The former may be generated in anorogenic extensional settings, whereas the latter occur in local extensional settings, or related to late extensional deformation, in overall compressional orogenic belts. However, there are too few well-documented deposits with published metal associations to be certain.

7 Gold-rich VMS and SEDEX deposits

7.1 Introduction

Volcanogenic massive sulfide deposits form on or subjacent to seafloor, from the conjunction of magmatic, hydrothermal, and sedimentary processes. They occur in volcanic and volcanic-sedimentary sequences ranging in age from the 3.4 Ga Pilbara craton, Western Australia[251] to modern hydrothermal sulfide sediments presently accumulating at ocean ridge, seamount, propagating ridge, arc, and back arc settings. This section draws on major reviews[252—254].

The gold content of VMS deposits is variable from 10 g/t in the 2.7 Ga Horne deposit, Noranda, to <0.2 g/t [255,256]. Production from VMS deposits provided 33% of the Cu, 29% of the Pb, 56% of the Zn, 30% of the Ag, and 3.6% of the Au in Canada in 1988[242]. The Thompson-Bousquet deposit in the Abitibi greenstone belt may be an Au-rich VMS deposit[257]. Total production of gold from Canadian VMS deposits is 970 t, and 237.5 t has been produced from the Mount Morgan deposit alone[255,256]. Together with the abundant base metals in VMS deposits, are variable Au contents, and variable contents of Ag, Cd, Sn, Bi, Se, Co, and In recovered during smelting[252].

7.2 Characteristics

The base of VMS systems is a subvolcanic sill located several hundreds of meters below the seafloor. Sills, specifically the margins, are characterized by intense high temperature alteration that is an integral part of a laterally extensive tabular body of alteration composed of epidote, albite, and quartz. Compositionally, these altered zones are hydrothermally leached of metals, with intense modification of alkali and alkali earth metals, and silica addition.

Above the sill is a structurally controlled alteration pipe, or conduit, that widens vertically upwards towards the seafloor. The pipe has a more intensely altered core that grades into stockwork, or so-called stringer, ore subjacent to the seafloor, and a less altered annulus. Massive sulfide ore is sited above the pipe, or distally if allochthonous. Ore bodies are zoned from Cu-rich stockworks to Zn- and Pb-rich stratiform massive sulfide. Barium and Mn precipitated distally if ocean bottom water was oxidizing. Water depth may control metal ratios. Mineralogically, the majority of VMS deposits are simple, composed of ~90% pyrite, with chalcopyrite, sphalerite, and galena [252](fig. 6).

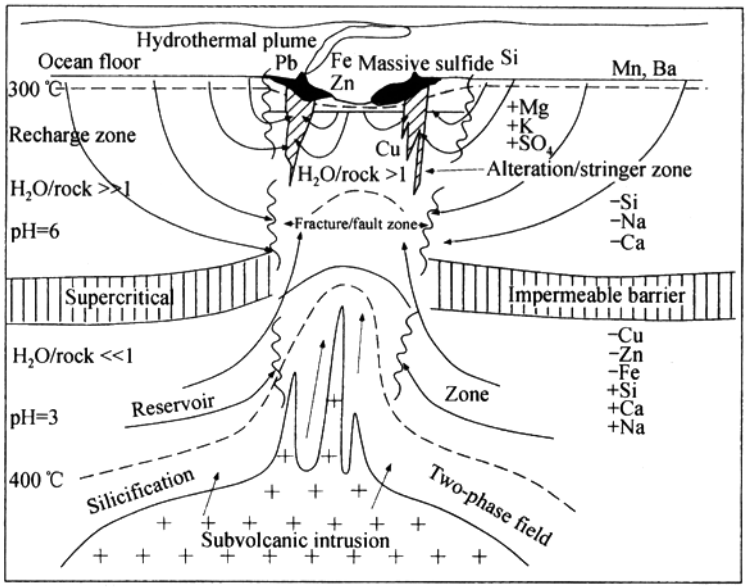

Fig. 6. Generalized model of VMS-producing hydrothermal system, incorporating elements of all subtypes of VMS deposits. Crosses are a subvolcanic intrusion, which may be contributing some metals and gases to the hydrothermal fluid. The heavy cross-hatched areas under the massive sulfide deposits are alteration pipes. This diagram is drawn perpendicular to the fracture system that controls hydrothermal discharge (modified from Franklin[252]).

There is a general consensus that VMS deposits can be classified into two groups based on metal budget; a Cu-Zn and a Zn-Pb-Cu group. Both groups include Au-rich examples. The former are generally characterized by prominent stockwork zones, and occur in mafic volcanic dominated sequences with minor proximal felsic units. The latter are dominantly tabular massive stratiform ore with subdued stockworks, and occur in felsic dominated volcanic sequences which may have significant proportions of sedimentary rocks in the footwall (table 8).

7.3 Processes

In terms of processes, subvolcanic sills are a focussed source of heat, and the high temperature alteration bodies represent reaction of convecting seawater with the footwall sequence to leach metals. Reaction of modified seawater with basalt at 350—400℃ lowers the pH to dissolve metals from rocks into the hydrothermal fluids[258]. Silicified domains of the laterally extensive tabular alteration zones act as an impermeable cap to lower the Rayleigh number, and hence prevent the rapid dissipation of energy from the sills that occurs in a permeable, high Rayleigh number convective system[259].

Intense alteration of the core of the pipe stems from reaction of the metal bearing hydrothermal ore fluids as they advect up the structural conduit. Volumetrically, ore fluids are dominated by heated seawater, but there may be unconstrained inputs of magmatic fluids and metals. Less intense alteration of the annulus results from mixing with entrained cooler and less modified sea-

water with high temperature fluids in the core of the pipe.

Table 8 Principal characteristics of VMS deposits

Age range	Mesoarchean to present day, but Neoarchean and Phanerozoic most common.
Classic provinces (classic deposits)	2.7 Ga volcanic terranes of the Superior Province (Mattagami, Horne, Quemont, Noranda); Paleoproterozoic Trans-Hudson (Flin Flon, Canada); Paleozoic volcanic belts of eastern Australia (Mount Morgan, Mount Leyll). High sulfidation: Paleoproterozoic, Skellefte, Sweden (Boliden).
Structural style	Sited above brittle faults, either caldera collapse faults. Cu-Zn: Pronounced stockwork feeder pipe; Zn-Pb-Cu: subdued stockwork.
Mineralization style	Stratabound tabular bodies of massive sulfide, underlain by variably developed stockwork feeder zone.
Host rocks	Cu-Zn class: mafic dominated volcanic sequences, with proximal felsic intrusions; Zn-Pb-Cu class: felsic dominated volcanic sequences, with variable proportions of sedimentary rocks in the footwall. High sulfidation: felsic to intermediate volcanic sequences, variable sediments.
Metal association and ratios	Cu-Zn class: variable Au (<0.2 to 10×10^{-6}), Ag; Zn-Pb-Cu class: variable Au (<0.2 to 10×10^{-6}) , Ag; Au/Ag 0.02 to 0.07, variable Cd, Sn, Bi, Se, Co, In contents. High sulfidation: base metals, Au, Ag, As, Sb, Hg.
Gold fineness	300—700
Alteration	Cu-Zn: Fe-rich chlorite, pyrite, chalcopyrite, quartz in subjacent footwall and stockwork core of pipe, annulus of muscovite. Deep tabular bodies of high temperature (350—400℃) epidote, albite, quartz at level of subvolcanic sill. Zn-Pb-Cu class: sericitic core, with annulus of Mg chlorite. High sulfidation: advanced argillic.
PT conditions	At or below seafloor, water depths 500 m to ＞2 km.
Ore fluids	Hot, chemically modified seawater at 350℃ to 200℃ with unconstrained quantities of magmatic fluids and metals, and progressive mixing of ambient seawater. Cu-Zn: higher T (＞300℃), low pH (<4.5), moderate to high fO_2. Zn-Pb-Cu: lower *T* (150—300℃), moderate pH (4.5—6), moderate fO_2. High sulfidation: oxidized, acidic, S-rich magmatic fluids.
Isotopes (water)	δD= +20‰— +50‰; $\delta^{18}O$= −3‰— +6‰. High sulfidation: magmatic ranges, mixing with sediments.
Heat sources	Subvolcanic sill.

Metal zoning reflects progressive cooling of the ore fluids by mixing in ambient seawater. Copper is precipitated first, such that the fluids evolve to more Zn and then Pb-rich compositions. Diachronous epiclastic units signify active growth faulting; either caldera collapse faults, or alternatively extensional faults in rift settings.

7.4 Gold-rich VMS deposits

A review of gold in VMS systems is given[260]. Large and coworkers have conducted extensive studies of VMS deposits, including Au-rich examples from eastern Australia. There are two principal VMS metallogenic provinces: the Rockhampton district in eastern Queensland that includes the Au-rich Mount Morgan deposit; and the Cambrian Mount Read volcanic sequence of western Tasmania, with the Rosebury, Hercules, Que River, Hellyer, and Mount Lyell VMS deposits[255]. Collectively, gold abundance in those deposits ranges from 0.2 to 4.75 g/t, with an average of 1.6 g/t.

Large et al.[255] recognize the same duality of VMS deposits as Franklin[252], based on metal

budget, spatial association, and type of volcanic terrane. The Cu-Zn±Au class is represented by the Mount Chalmers, Mount Morgan, and Mount Lyell deposits, whereas the Zn-Pb-Cu-Ag ± Au class is represented by the Rosebury, Que River, and Hellyer deposits. According to Large et al.[255], in the Cu-Zn VMS deposits, gold is transported as a $AuCl_2^-$ complex, in high temperature (＞300℃), low pH (＜4.5), high salinity, and moderate to high fO_2 ore fluid. For the Au-rich Zn-Pb-Cu deposits, they conclude that Au is present as an $Au(HS)_2^-$ complex, in an ore fluid characterized by lower T (150—300℃), moderate pH (4.5—6), and moderate fO_2. They propose a zone refining process to explain the Au-rich caps of Zn-Pb-Cu VMS deposits.

Active vents on the seafloor with high temperature hydrothermal discharge have aqueous gold contents of 0.1×10^{-12}—0.2×10^{-12}. Hence these systems transport a metric ton of gold per thousand years. High aqueous H_2S contents are required to stabilize $Au(HS)_2^-$ to low temperatures. Gold is precipitated in active vents as ambient water mixes in, and the oxidation state crosses the H_2S/SO_4 boundary[256]. Gold contents of hydrothermal precipitates from active vents are 0.07—4.9×10^{-6}. Gold-rich precipitates are high sulfidation assemblages, with Zn (＞10%), Pb (＞0.1%), Ag (＞100 g/t), As (＞200 g/t), Sb (≤500 g/t), and lower abundances of Hg and Tl[256].

A summary of gold contents of VMS deposits is given in Hannington et al.[260]. There is not consensus on all the data points: for example, the Proterozoic Homestake deposit, South Dakota, is generally considered to be an orogenic gold deposit but not a VMS (see earlier section), and Wyman et al.[261] have argued that much, if not all, of the gold at the Archean Agnico Eagle deposit, Quebec, is structurally controlled, postdating the barren massive sulfide.

7.5 High-sulfidation Au-rich VMS

Epithermal precious metal deposits have been subdivided into high- and low-sulfidation types. The division is based on sulfide mineralogy, alteration, and spatial association to intrusive bodies[165,262,263]. Classic Cu-Zn and Zn-Pb-Cu VMS deposits have low-sulfidation mineralogy. The Pb-Zn-Cu class of VMS deposit hosted in felsic dominated volcanic sequences, also has a high-sulfidation member[154]. The high-sulfidation member is characterized by a high-sulfidation sulfide assemblage, advanced argillic alteration, and an epithermal trace element suite of Au, Ag, As, Sb, Hg; they form from oxidized acidic, and S-rich fluids of magmatic origin.

Sillitoe et al.[154] describe modern arcs with shallow water hydrothermal systems generating high-sulfidation accumulations having an epithermal Au and trace element suite. These systems occur in environments transitional between terrestrial epithermal and deep water VMS systems, although samples with advanced argillic alteration have been dredged from the Lau back arc basin under water depths of ~2 km. High-sulfidation VMS deposits are known from Proterozoic terranes to active hydrothermal systems. The Cu-rich Paleoproterozoic Boliden deposit, Skellefte district, produced 118 000 t Cu, 128 t Au, 411 t Ag, with an As, Sb, Co, W, Bi, Se, Te, Hg suite[154].

7.6 Gold-rich SEDEX deposits

Classic sedimentary exhalative deposits (SEDEX) characterized by a Pb-Zn-Ag budget occur in rifted epicontinental to intracontinental sedimentary basins, generally with syn-mineralization volcanic activity[177,264]. Some recent discoveries, notably Eskay Creek in British Columbia, may warrant a subclass of Au-rich SEDEX deposits, or alternatively a new class of gold deposits. The Eskay Creek deposit is sited in the Cordilleran Stikine terrane, at the contact between a middle Jurassic bimodal volcanic sequence and an overlying mudstone-basalt sequence. Proximal lithological units are pyroclastic deposits, andesite, and shallow marine sandstone and shales. Syndepositional faulting signifies an extensional environment. According to Roth et al.[265], the characteristics are atypical of most VMS deposits, whereas Sherlock et al.[266] term Eskay Creek a VMS sulfide-sulfosalt deposit.

As of 1998, one of the zones had reserves of 1.9 Mt, grading 3.2% Pb, 5.2% Zn, 0.7% Cu, 60.2 g/t Au, and 2652 g/t Ag. Gold rich zones possess an As, Sb, Hg association. The deposit formed from relatively low-temperature ore fluids at ＜20℃, under water depths of 1.5 km. Ore fluids were gas-rich and underwent liquid-gas phase change, and mixed with a lower temperature (~100℃), more saline fluid, in which the high K/Na and Cl/Br ratios signify a magmatic origin. Sherlock et al.[266] consider that the high precious to base metal ratios are due to inefficient precipitation mechanisms for base metals at low temperatures.

7.7 Geodynamic settings

Based on mapped caldera structures, and the geochemistry of associated magmatic rocks, VMS deposits in the Archean Superior Province appear to form in rifting intraoceanic arcs, or in back arcs. All of the VMS deposits formed over the last 20 Ma of 300 Ma of magmatic activity, and that interval is interpreted as extension of oceanic lithosphere. At Matagami and Noranda there is an association of Fe-rich tholeiitic basalts with high-Si rhyolites, an association found in modern backarcs[267]. In the Noranda area and Wawa subprovince there is association of ‘anomalous’ andesites with fractionated LREE and HREE, interlayered with ‘normal’ arc tholeiitic basalts, and adakites (the volcanic equivalent of high Al, high La/Yb_n tonalites)[26]. Anomalous andesites are mixtures of arc tholeiitic basalt and adakite liquids. It is not clear how the two distinct magmatic processes operate coevally. Here we suggest that the locally high geothermal gradients in the subduction zone, required to generate slab melt derived adakites results from local plume impingement that flattens the subducting slab. Barley et al.[21] also propose a back arc setting for VMS deposits in 2.7 to 2.6 Ga greenstone belts. The supergiant Kidd Creek VMS deposit, Timmins, is hosted in a sequence of interlayered komatiites, low-Ti basalts, and primitive to evolved arc tholeiites. Wyman et al.[268] interpret the geodynamic setting as a plume impinging on an intraoceanic arc. High thermal flux advected by plume magmas may account for this unusually large deposit.

Proterozoic VMS deposits at Flin Flon, Manitoba, Canada also appear to form in an extensional environment. The Flin Flon district is a complex tectonic collage of MORB, OIB, primitive

to mature arc, and back arc fragments[269,270]. Some VMS deposits in Phanerozoic terranes are also interpreted to have formed in rifted oceanic arcs, or back arcs, including the Au-rich VMS deposits of eastern Australia[255]. VMS deposits also form in continental margin arcs, or back arcs: examples including the Boliden deposits, Skellefte, Sweden[271]; the Ordovician Bathurst district, New Brunswick, Canada[272]; and the Iberian pyrite belt. Alternatively, Boulter[273] compares the setting of Rio Tinto to a sill-sediment complex, such as is forming in the Guayanas basin, Sea of Cortez.

If high sulfidation VMS deposits are submarine counterparts of terrestrial epithermal precious and base metal deposits, then they form in similar geodynamic settings; oceanic and continental arcs[154]. The geodynamic setting of the Eskay Creek deposit is not yet resolved. According to Sherlock et al.[266], the flat REE patterns of basalts are unlike fractionated arc magmas, but rather are akin to rift related basalts.

The source and flux of volatiles from the subduction zone to the subaerial Kudryary volcano in the Kurile islands has been constrained from rare gas and stable isotope systematics. The $^3He/^4He$ ratio of 6.7 R_A corresponds to 84% mantle helium, and requires 1×10^6 t/a of mantle to be degassed to generate this flux, or about 300 km^3/Ma. The CO_2 budget of 50×10^6 mol/a is comprised of 12% mantle CO_2, 67% marine carbonate, and 21% subducted sedimentary organic. In sub-seafloor crust, which is characterized by high hydraulic conductivity, abundant convecting seawater dilutes the magmatic input.

8 Geodynamics of world class gold deposits: Synthesis

Continental lithosphere has grown at convergent margins throughout earth history[274]. However, as discussed above, the thermal structure of convergent margin subduction zones has decayed through time: progressively steeper subduction angles have led to different composition, thickness, and mechanical properties of continental lithosphere (fig. 2). Cooling of the mantle as a whole has resulted in decreasing intensity and temperature of plume, or 'hotspot', magmatism and the composition of primitive plume magmas has evolved from komatiite-basalt sequences to basalt-dominated sequences.

Mantle plumes are involved both in the growth and destruction of convergent margins. Thick ocean plateau crust is buoyant: hence ocean plateaus jam into subduction zones rather than subduct[275,276]. Examples are the Caribbean-Columbian and Ontong Java ocean plateaus that have jammed into the Pacific Rim subduction system, respectively in the Caribbean and near Papua New Guinea. This conceptual advance has given rise to a new appreciation of Archean greenstone belts as subduction-accretion complexes. Convergent margin tectonics generates bimodal arc magmas with trench turbidites. During subduction rollback plume related ocean plateau sequences are imbricated with the arc. As composite subduction-accretion complexes migrate oceanwards, tonalitic batholiths intrude the arc-trench-plateau complex[277—279]. Capture of ocean plateaus by subduction zones solves the paradox of the Mg, Ni deficit of the andesite model of Taylor and

McLennan[280] for crustal growth[281].

Another consequence of decreasing plume magmatism through time is greater continental freeboard. Isley and Abbott[282] have demonstrated a 98% correlation between the secular distribution of iron formations and oceanic plume magmatism. There are four superplume events between 3.8 Ga and 1.6 Ga, with the global 2.7 Ga greenstone belt event corresponding to the second. As a consequence, in Archean terranes with abundant Algoman BIF and komatiite-basalt plateau sequences, thick terrestrial siliciclastic deposits are sparse due to flooding of the continents.

There is compelling evidence that continental lithosphere grew early in earth history, with continued growth and recycling of both ocean and continental lithosphere generating near-steady state continental mass[283,284]. Models of progressive or episodic growth are based principally on Nd-isotope data, and are unconstrained. Destruction of continental lithosphere occurs at convergent margins by subduction-erosion and sediment subduction[285]. There are geochemical signatures in plume basalts of Archean and Phanerozoic age for prior subduction recycling of continental lithosphere to the core-mantle boundary, and its return to the surface in mantle plumes from which the basalts are erupted ~1 Ga later[286,287]. Impingement of anomalously hot mantle plumes on convergent margins also promotes destruction of oceanic and continental convergent margins via topographic uplift accompanied by erosion. Dalziel et al.[288] term this 'plume modified orogeny'.

Giant gold metallogenic provinces do not form in response to chemical evolution of the mantle as a whole. Core formation, with attendant sequestering of siderophile elements, including Au, W, Mo, and PGE from the silicate earth was complete within 10's Ma of earth accretion[289]. Consequently, the siderophile inventory of the silicate earth is believed to stem from a late veneer of accreted meteorites[290]. Sun et al.[22] have demonstrated a secular invariance in the Ti/Pd ratio of the mantle, a ratio of a lithophile to a siderophile and chalcophile element, such that the gold content of the mantle has also remained constant. However, localized low degree alkaline partial melts in the asthenosphere may be highly enriched in Au and incompatible elements such as Th, U, Rb, and REE (fig. 2(c)).

8.1 Accretionary orogenic belts proximal to continental margins

There is a distinctive secular distribution to orogenic gold deposits. They are abundant in 2.7 Ga and Paleoarchean greenstone belts; the Neoproterozoic; lower Paleozoic of central Asia and the Tasman orogenic belt; and Jurassic to Triassic accretionary events in the North American Cordillera and China.

The sparsity of orogenic gold deposits in the Neo- and Mesoarchean terranes reflects the fact that these are predominantly high-grade tonalite-gneiss belts that represent arc midcrust, with minor intensely deformed and metamorphosed greenstone remnants. Given the fact that the majority of orogenic gold deposits form and are preserved in greenschist facies terranes, these were either eroded from higher levels of the gneiss terranes, or some gold deposits formed at convergent oro-

genic margins but were destroyed by plume impingement on the orogens[288].

2.7 Ga corresponds to the conjunction of a Cordilleran style supercontinent accretion with a superplume event. Transpressive terrane accretion is a favorable tectonic setting for generating orogenic gold deposits. Cold, dense oceanic plates cool the base of the subduction-accretion complex until terrane-terrane collision terminates subduction, and granitoid magmatism also terminates. Isotherms then rise through thick subcreted volcanic-sedimentary melange inducing dehydration reactions, with transport of aqueous incompatible elements, including Au, Ag, As, Sb, Se, Te, Bi, B, Cs, Rb, and K up terrane boundary structural conduits to sites of precipitation in the brittle-ductile regime. Coupling of the plume residue to imbricated arc-plateau crust resulted in high preservation potential, given the thick, refractory and mechanically rigid mantle lithosphere 'keel' (fig. 1).

Wyman et al.[268] have pointed out that few of the 2.7 Ga greenstone belts have orogenic gold deposits, and that the prodigiously rich gold metallogenic provinces of this age are highly localized. For example, 5000 t of gold have been produced from the 2.4 million km^2 Archean Superior Province, yet 4000 t of this total has been mined from two narrow corridors in the southern volcanic zone of the Abitibi belt. In the model of Wyman et al.[268] this spatial concentration of gold deposits results from subduction step-back (fig. 7). Qiu and Groves[291] proposed that collision followed by delamination, that advects hot asthenosphere to the base of thinned lithosphere, was the driving force for the Yilgarn orogenic gold province.

During stability of the 2.7 Ga supercontinent and subsequent breakup, few orogenic gold deposits formed. The next major accretionary orogenic events were at 2 Ga in Northeast Brazil and West Africa, and the 1.9 Ga Trans Hudson orogen of North America. Major gold deposits formed in the Birimian and Trans Hudson; however, these orogenic events were dominated by internal continent-continent collisions where formation and preservation of orogenic gold deposits is less favorable than in external Cordilleran style orogenic belts. Stability, then breakup of the 2 Ga supercontinent accounts for the Meso- to Paleoproterozoic 'gap', when few gold deposits formed or were preserved.

Giant orogenic gold provinces formed at convergent margins in the Phanerozoic. They were either destroyed, or alternatively preserved where terrane accretion incorporated the mineralized belts into a continent, such as in Asia, the Tasman orogenic belt, and Cordillera. Proterozoic and Phanerozoic terranes hosting giant orogenic gold provinces are characterized by a higher proportion of metasedimentary rocks than Archean counterparts. Convergent margins acquired a progressively larger sedimentary budget as continental freeboard increased in response to decreased plume magmatism in ocean basins. Goldfarb et al.[86] have demonstrated that orogenic gold deposits in the Cordillera are specifically related to a change of plate vectors.

Black smokers in back arc basins provide a real-time analog for many of the processes thought to be involved in the formation of volcanogenic massive sulfide (VMS) deposits. Are there also real time analogs for orogenic gold deposits? A series of distinctive hot, or warm springs

aligned on major crustal structures occur in the circum-Pacific belt. When compared to

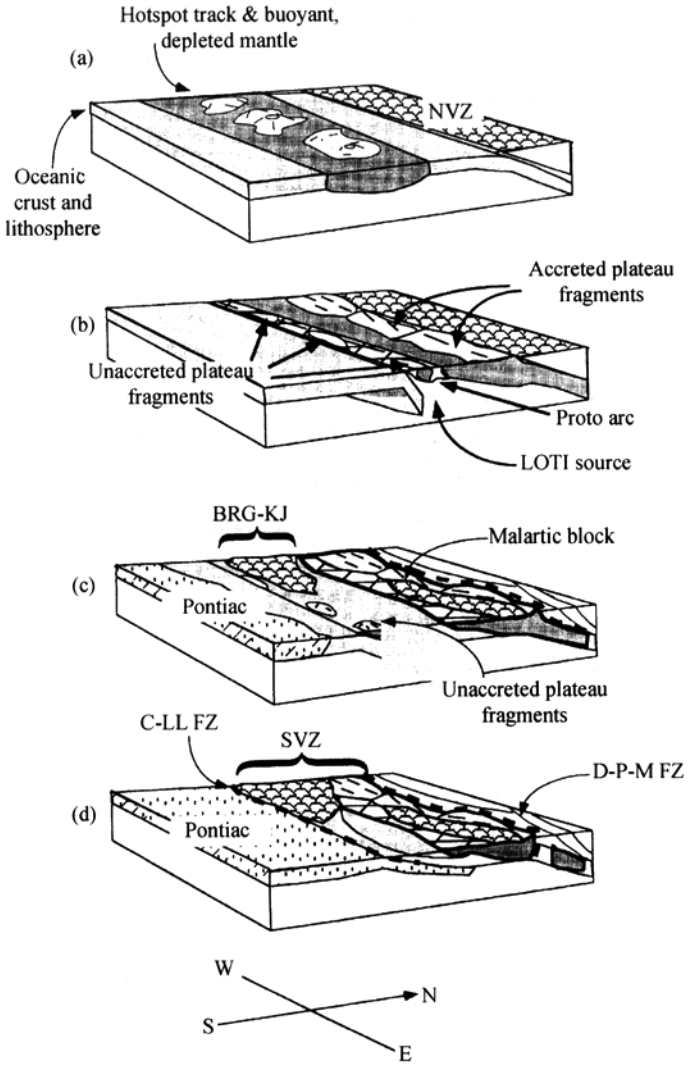

Fig. 7. Geodynamic history of the Southern Volcanic Zone (SVZ). (a) plume ascent under and near an Abitibi arc generates a topographic and thermal high outboard of the arc (indicated by pillow pattern). (b) Subduction zone jamming and suture of plateau fragments causes step back of subduction and formation of proto arc (a simplified representation). Low-Ti tholeiites and plateau fragments- komatiite flows nearer plume occur together. (c) Rifting of the juvenile arc along and near the Malartic Block (pillow pattern indicates Val d'Or domain) results in eruption of the Kinojevis Group (KJ) along a propagating ridge, followed by the Black River Group (BRG) arc succession. Some komatiitic sequences are isolated south of the BRG. (d) Underthrusting of the Pontiac subprovince is followed by strike-slip movement along the Destor-Porcupine-Manneville fault zone (D-P-M FZ)-the Cadillac-Larder Lake fault zone (C-LL Fz). Modified from Wyman et al.[268].

meteoric water dominated hot spring systems, the structurally controlled variety are distinctive in terms of: (1) discharge at topographic ridges rather than in depressions, signifying a geopressurized fluid; (2) abundant CO_2; (3) low salinity; (4) relatively enhanced solute concentrations of As, Sb, B, Li, Rb (etc.); (5) low abundances of base metals; and (6) an association with mercury and/or sulphur deposits. Isotopically, the CO_2 springs are consistent with fluids of metamorphic origin, with little or no involvement of local meteoric water. All of the hot or warm springs discussed above involve advective flow of thermal waters, likely of metamorphic origin, along major crustal structures. In California, the CO_2-hot springs have been interpreted as the surface expression of active metamorphism in the Franciscan complex[292].

In the Southern Alps, New Zealand, Craw and Koons[293] describe dilute aqueous, CO_2-bearing fluids generated by metamorphic dehydration being released up structures during rapid uplift; and gold is precipitated from these fluids either by cooling, or mixing with dilute low-salinity meteoric fluids. They suggest that these may be analogs of orogenic gold systems[293]. In terms of orogenic gold deposits that form inboard of collisional plate margins, such as the deposits of China and Korea[106,294], which may form in response to delamination of mantle lithosphere, there is seismic evidence for this phenomenon beneath Tibet.

8.2 Oceanic arcs, and oceanic and continental back arcs

Most arcs, and all active back arcs, are in a state of extension. As the oceanic slab sinks and rolls back beneath an arc, the arc and back arc pair migrate oceanward, coupled to the sinking slab by trench suction and induced convection[24] (figs. 2(a) and 8(b)). During back arc extension the asthenosphere rises to compensate for lithosphere thinning. Both elevation of isotherms in the rising asthenosphere, and decompressional melting, advect heat to the lithosphere, which is thinned by coupled listric and transfer fault systems. Accordingly, there is the conjunction of high heat flow, magmatism, enhanced hydraulic conductivity, and associated hydrothermal systems.

8.2.1 Submarine settings. The geodynamic setting in which VMS deposits are thought to form is oceanic arcs, and oceanic or continental back arcs. Modern accumulations of massive sulfide at hydrothermal vents, are known from ocean ridges, seamounts, propagating ridges (e.g. Red Sea), and arcs and back arcs[296]. However, the largest deposits which most closely resemble Au-rich VMS deposits in form, metal budget, and magmatic association are in oceanic or continental back arcs[297].

Back arc basins of the circum Pacific are active. Included are the Taupo-Havre-Lau system; the north Fuiji basin; the New Hebrides, Mariana, and Okinawa troughs; the East Scotia and Japan seas; and Shikoku and Kurile basins. Back arc basins are sited above mantle with pronounced seismic wave attenuation due to elevated isotherms in the asthenosphere and the presence of melts. As an arc under extension migrates oceanward a back arc opens and an independent spreading center develops. Initial stages of rifting are characterized by Fe-rich tholeiites and high silica rhy-

olites, caldera development, and explosive volcanism. Mafic magmatism is from variable sources:

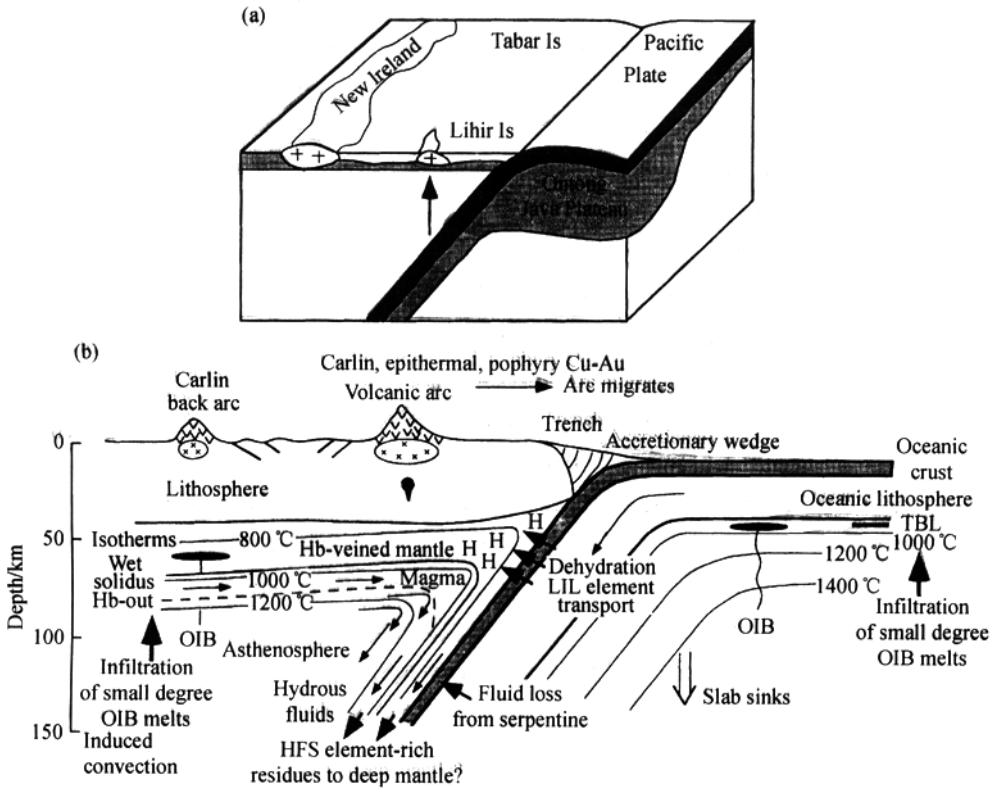

Fig. 8. Processes operating in a subduction zone and back arc (modified from Tarney et al.,[295]). K and incompatible element enriched domains of lithosphere from OIB melts may enter the arc either from slab rollback or from induced convection in subarc asthenosphere, or through a slab window.

initially, back arc basin basalts (BAB) from the subarc mantle wedge, and when a spreading center develops, MORB-like and enriched OIB-like basalts.

Compared to ocean ridge systems there are differences in the thermal and structural characteristics of ocean crust, magma compositions, hydrothermal fluids, and type of sediment. Modified seawater hydrothermal fluids discharging at vents are at 200—400℃, pH = 2—5, with higher concentrations of Zn, Ba, Pb, Cd, and As than ridge hydrothermal fluids. Accumulations of massive sulfide have been described from the Woodlark basin[298]; the Lau basin, including Au-rich sulfides[299,300]; the Eastern Manus basin[301]; and the Okinawa continental back arc[302]. The Okinawa back arc is a close analogue to the Kuroko VMS deposits which formed during mid-Miocene opening of the Japan sea back arc[303].

8.2.2 Subaerial settings. The geodynamic association between epithermal gold-silver and porphyry copper-gold deposits with subduction has been recognized since the early 1970s[29]. Both

deposit types occur in oceanic and continental margin arcs; accordingly it is possible that the ultimate source for the metals is modified mantle wedge (fig. 8).

Four types of oceanic arcs are recognized, based on the composition of arc basalts generated from enriched, undepleted, depleted or highly depleted mantle wedges[304]. Depleted refers to previous stages of melt extraction, which remove incompatible elements including Au, Ag, Pb, Th, U, As, Sb, Cs, Tl, and LREE from the mantle wedge in the melts. Given the association of some epithermal gold-silver and porphyry copper-gold deposits with K-rich magma derived from enriched mantle wedge, it is possible that the enrichment event is critical to generating magma with appropriate metal and volatile budgets.

There are two possible geodynamic scenarios for enrichment of arc mantle wedge lithosphere: subduction jamming or entrainment of OIB-enriched mantle into the subarc mantle. The giant Ladolam gold deposit on Lahir island, Papua New Guinea, is sited above a subduction zone into which the Ontong Java ocean plateau has jammed. McInnes et al.[305] have shown that veined peridotite xenoliths from mantle lithosphere beneath the deposit are 2 to 800 times more enriched in Cu, Au, Pt, and Pd than surrounding depleted arc mantle. Gold ores have osmium isotope compositions similar to the xenoliths, signifying that the mantle is likely the source of Cu and precious metals. Metasomatic enrichment of the mantle wedge is from fluids and/or melts streaming off the jammed plateau. Wedge peridotite then melts to produce volatile and K-rich basalts, which evolve to more felsic compositions in arc crust by assimilation-fractional crystallization. Mathur et al.[306] have determined a correspondence between the size of Chilean porphyry copper deposits and osmium isotope compositions, where the largest deposits have the most mantle like signatures. Arc mantle wedge depleted in previous melt extraction events requires a relatively larger volatile budget from the slab to remelt (fig. 8). Consequently, the conjunction of events required to generate volatile-rich magmas for porphyry copper-gold deposits may be: (1) stage one early wedge depletion and (2) later refertilization of the refractory residue from stage one depletion, by slab fluids and/or melts, all in the context of slab architecture controlling arc lithosphere structure as discussed above (fig. 5).

Alternatively, K-rich arc magmas may form where OIB melts impinge on an arc, or OIB-enriched magmas from the lithosphere or thermal boundary layer enter an arc (fig. 8), or where OIB melts enter the arc system through a slab window (figs. 5 and 8(b)). Carlin and Carlin-like deposits in continental margin arcs probably involve similar processes as for epithermal deposits. Carlin deposits from Nevada are in a continental back arc, where lithosphere extension advects heat to the crust, as well as mantle and crustal magmas. Plume impingement may have played a critical role.

8.3 Intracratonic extension with anorogenic magmatism

Iron oxide copper-gold deposits constitute the only major class of gold deposit not related to a convergent margin geodynamic setting at the time of mineralization. At 1.5 Ga a supercontinent

broke up. Anorogenic magmatism was associated in space and time both with assemblage and breakup of the supercontinent. Crustal thickening in collisional orogenic belts that developed during assembly led to post-tectonic crustal heating, and voluminous anorogenic rapakivi granites were emplaced over 1.76 to 1.55 Ga. During and following supercontinent rifting, a suite of mantle derived anorogenic anorthosites, granites and rhyolites were emplaced $<$1.5 Ga. Seventy percent of known Proterozoic anorogenic magmatism aged 1.5 to 1.27 Ga occurs in a belt 1000 km wide and 5000 km long extending from southern California to Labrador. The iron oxide copper-gold REE deposits of Missouri are part of this belt[307,308].

There are two possible sources of heat to drive anorogenic magmatism during intracontinental extension. Far field forces thin the continental lithosphere, deflecting asthenosphere isotherms upward, and decompressional melting advects heat into the lithosphere. Alternatively, impingement of a mantle plume on the base of continental lithosphere will induce intracontinental extension, as in the 1.1 Ga Midcontinent rift (Windley, 1995). It is not known if one of these two mechanisms or both were involved in the 1.5 Ga supercontinent rifting.

The siting of Meso- to Paleoproterozoic iron oxide copper-gold deposits near boundaries between thick Archean and thinner and younger lithosphere provides clues to their origin. The following sequence of geodynamic events may be envisioned: (1) In the Archean, arcs capture ocean plateaus, and thick, refractory continental mantle lithosphere keels develop (fig. 2). (2) Over time, low-degree OIB melts of the asthenosphere infiltrate mantle lithosphere to produce domains metasomatically altered and enriched in incompatible elements[309] (fig. 2). (3) Following assembly of the Paleoproterozoic to Neoproterozoic supercontinent crustal melting generates rapakivi granites, leaving a water-deficient but halogen-rich lower crustal residue. (4) During supercontinent rifting, extension is focused at margins of Archean cratons where there is a transition from thick refractory to thinner less refractory mantle lithosphere (fig. 2). (5) Low degree mafic, but incompatible element enriched, melts formed by decompression of the thermal boundary layer and metasomatically altered domains of mantle lithosphere (fig. 2). (6) High degree melts of asthenosphere pond at the base of the crust, generating second stage crustal melts of halogen-rich A-type granites. (7) Magmatic and crustal fluids are involved in mineralization.

The east African rift may be a modern analogue for the environment in which iron oxide copper-gold deposits form. Intracontinental extension involves Proterozoic lithosphere, with metasomatically altered domains from which alkaline magmas are produced[309]. There are extensive tholeiitic to alkali basalts from asthenosphere melting. Lakes fed by alkaline, oxidizing hydrothermal fluids are precipitating cherts enriched in REE and incompatible elements (R. Renaut, personal communication).

Acknowledgements The authors accept responsibility for any errors of fact or misrepresentation in this review. We thank Chen Yanjing for the invitation to write this review article. The second section was modified and expanded from Chapter 2 of the MITEC Report 93E06. We thank Derek Wyman for permission to use figure 2 of Wyman et al. (1999). We are grateful to Colin Steel for drafting. K. Ansdell, S. Ivanov, Y. Pan, and D. Wyman provided incisive critiques. This paper is modified and updated from a manuscript in the Society of Economic Geologists Review volume of gold deposits, GOLD 2000. R. Kerrich

acknowledges the George McLeod endowment to the Department of Geological Sciences, University of Saskatchewan.

References

1. Boyle, R. W., The geochemistry of gold and its deposits, Geological Survey of Canada Bulletin 280, 1979, 580.
2. Hodgson, C. J., MacGeehan, P. J., A review of the geological characteristics of "gold only" deposits in the Superior Province of the Canadian Shield, Geology of Canadian Gold Deposits, Canadian Institute of Mining and Metallogeny Special Paper 24, 1982, 211—229.
3. Bache, J. J., World Gold Deposits, A Geological Classification, New York: Academic, 1987, 18—26.
4. Poulson, K. H., Lode gold, Geology of Canadian Mineral Deposit Types (eds. Eckstrand, O.R., Sinclair, W.D., Thorpe, R.I.), Geological Survey of Canada (Geology of Canada 8), 1995, 323—392.
5. Robert, F., Poulsen, K. H., Dube, B., Gold deposits and their geological classification, Proceedings of Exploration 97, 4th December International Conference on Mineral Exploration (ed. Gubins, A.G.), 1997, 209—220.
6. Stein, M., Hofmann, A. W., Mantle plumes and episodic crustal growth, Nature, 1994, 372: 63.
7. Vander Hilst, R. D., Widiyantro, S., Creager, K. C. et al., Structure of the lowermost mantle and D", The Core-Mantle Boundary Region, (eds. Gurnis, M., Wysession, M.E., Knittle, E.), Geodynamics Series, 1998, 28: 5.
8. Mitchell, A. H. G., Garson, M. S., Mineral Deposits and Global Tectonic Settings, London: Academic, 1981, 405.
9. Sawkins, F. J., Metal Deposits in Relation to Plate Tectonics, Berlin: Springer-Verlag, 1984, 325.
10. Hoffman, P. E., United plates of America, the birth of a craton, Annual Review of Earth Planetary Science, 1988, 16: 543.
11. Murphy, J. B., Nance, R. D., Mountain belts and the supercontinent cycle, Scientific American, 1992, 266: 84.
12. Rogers, J. W., A history of continents in the past three billion years, Journal of Geology, 1996, 104: 91.
13. Barley, M. E., Groves, D. I., Supercontinental cycles and the distribution of metal deposits through time, Geology, 1992, 20: 291.
14. Sengor, A. M. C., Plate Tectonics and Orogenic Research After 25 Years: A Tethyan Perspective, Earth Science Reviews, 1990, 27: 1.
15. Kerrich, R., Wyman, D. A., Geodynamic setting of mesothermal gold deposits: An association with accretionary tectonic regimes, Geology, 1990,18: 882.
16. Kerrich, R., Feng, R., Archean geodynamics and the Abitibi-Pontiac collision: implications for advection of fluids at transpressive collisional boundaries and the origin of giant quartz vein systems, Earth Science Reviews, 1992, 32: 33.
17. Kerrich, R., Wyman, D. A., The mesothermal gold-lamprophyre association: significance on accretionary geodynamic setting, supercontinent cycles, and metallogenic processes, Mineralogy and Petrology, 1994, 51: 147.
18. Kelemen, P. B., Hart, S. R., Bernsrein, S., Silica enrichment in the continental upper mantle via melt/rock reaction, EPSL., 1998, 164: 387.
19. Kerrich, R., Wyman, D. A., The trace element systematics of igneous rocks in mineral exploration: an overview, Trace Element Geochemistry of Volcanic Rocks: Applications for Massive Sulfide Exploration (ed. Wyman, D.A.), Geological Association of Canada, Short Course Notes, 1996, 12: 1.
20. Wyman, D. A., Bleeker, W., Kerrich, R., A 2.7 Ga komatiite, low Ti tholeiite, arc tholeiite transition and inferred proto-arc geodynamic setting of the Kidd Creek deposit: evidence from precise trace element data, Economic Geology Monograph 10, 1999, 511.
21. Barley, M. E., Krapez, B., Groves, D. I. et al., The late Archean bonanza: metallogenic and environmental consequences of the interaction between mantle plumes, lithospheric tectonics and global cyclicity, Precambrian Research, 1998, 91: 65.
22. Sun, S. S., Nesbitt, R. W., McCulloch, M. T., Geochemistry and petrogenesis of Archaean and early Proterozoic siliceous high-magnesian basalts, Boninites (ed. Crawford, A.J.), Winchester: Unwin Hyman, 1989, 148.
23. Condie, K. C., Episodic continental growth and supercontinents: a mantle avalanche connection? EPSL, 1998, 163: 97—108.
24. Kearey, P., Vine F. J., Global Tectonics, Oxford: Blackwell, 1990, 302.
25. Bickle, M. J., Mantle evolution, Early Precambrian Basic Magmatism (eds. Hall, R.P., Hughes, D.J.), Glasgow: Blackie, 1990, 111—135.
26. Drummond, M. S., Defant, M. J., Kepezhinskas, P. K., Petrogenesis of slab-derived trondjemite-tonalite-dacite/adakite magmas, Earth Science, 1996, 87: 205.

27. Groves, D. I., Goldfarb, R. J., Gebre-Mariam, M. et al., Orogenic gold deposits: a proposed classification in the context of their crustal distribution and relationship to other gold deposit types, Ore Geology Reviews, 1998, 13: 7.
28. Groves, D. I., The crustal continuum model for late-Archaean lode-gold deposits of the Yilgarn Block, Western Australia, Mineralium Deposita, 1993, 28: 366.
29. Sillitoe, R. H., Tectonic segmentation of the Andes: implications for magmatism and metallogeny, Nature, 1974, 250: 542.
30. Berger, B. R., Bagby, W. C., The geology and origin of Carlin-type gold deposits, Gold Metallogeny and Exploration (ed. Foster, R.P.), Glasgow: Blackie, 1991, 210–248.
31. Bonham, H. F. Jr., Bulk mineable gold deposits of the Western United States, Economic Geology Monograph 6, 1989, 193—207.
32. Henley, R. W., Epithermal deposits in volcanic terranes, Gold Metallogeny and Exploration (ed. Foster, R.P.), Glasgow: Blackie, 1991, 133—164.
33. Groves, D. I. Phillips, G. N., The genesis and tectonic controls on Archean lode gold deposits of the Western Australian shield: a metamorphic-replacement model, Ore Geology Reviews, 1987, 2: 287.
34. Kerrich, R., The stable isotope geochemistry of Au-Ag vein deposits in metamorphic rocks, Mineralogical Association of Canada Short Course 13 (ed. Kyser T.K.), 1987, 287.
35. Kerrich, R., Geodynamic setting and hydraulic regimes: shear zone hosted mesothermal gold deposits, Mineralization and Shear Zones, Geological Association of Canada Short Course 6, 1989, 89—128.
36. Kerrich, R., Geochemical evidence on the sources of fluids and solutes for shear zone hosted mesothermal Au deposits, Mineralization and Shear Zones, Geological Association of Canada Short Course 6, 1989, 129—197.
37. Colvine, A. C., An empirical model for the formation of Archean gold deposits: products of final cratonization of the Superior Province, Canada, Economic Geology Monograph 6, 1989, 37—53.
38. Colvine, A. C., Fyon, J. A., Heather, K. B. et al., Archean lode gold deposits in Ontario, Ontario Geological Survey Misc. Paper 139, 1988, 136.
39. Goldfarb, R. J., Leach, D. L., Rose, S. C. et al., Fluid inclusion geochemistry of gold-bearing quartz veins of the Juneau Gold belt, southeastern Alaska: implications for ore genesis, Economic Geology Monograph 6, 1989, 363—375.
40. Goldfarb, R. J., Miller, L. D., Leach, D. L. et al., Gold deposits in metamorphic rocks of Alaska, Economic Geology Monograph 9, 1997, 151—190.
41. Goldfarb, R. J., Snee, L. W., Pickthorn, W. J. et al., Orogenesis, high-T thermal events, and gold vein formation within metamorphic rocks of the Alaskan Cordillera, Mineralogical Magazine, 1993, 57: 375.
42. Rock, N. M. S., Groves, D. I., Perring, C. S. et al., Gold, lamprophyres, and porphyries; what does their association mean?, Economic Geology Monograph 6, 1989, 609—625.
43. Ho, S. E., Bennett, J. M., Cassidy, K. F., Fluid inclusion studies, Gold Deposits of the Archaean Yilgarn Block, Western Australia: Nature, Genesis and Exploration Guides (eds. Ho, S.E., Groves, D.I., Bennett, J.M.), Perth: Vanguard Press, 1990, 198—211.
44. Ho, S. E., Groves, D. I., Bennett, J. M. et al., Gold deposits of the Archaean Yilgarn Block, Western Australia: Nature, Genesis and Exploration Guides, Perth: Vanguard Press, 1990, 407.
45. Ho, S. E., Groves, D. I., McNaughton, N. J. et al., The source of ore fluids and solutes in Archean lode gold deposits of Western Australia, Journal of Volcanology and Geothermical Resources, 1992, 50: 173.
46. Kontak, D. J., Smith, P. M., Kerrich, R. et al., An integrated model for Meguma Group lode gold deposits, Nova Scotia, Canada, Geology, 1990,18: 238.
47. Cox, S.F., Wall, V.l., Etheridge, M.A. et al., Deformational and metamorphic processes in the formation of mesothermal vein-hosted gold deposits - examples from the Lachlan Fold Belt in central Victoria, Ore Geology Reviews, 1991, 6: 391.
48. Groves, D. I., Foster, R. P., Archaean lode gold deposits, Gold Metallogeny and Exploration (ed. Foster, R. P.), Glasgow: Blackie and Son, 1991, 63—103.
49. Poulsen, K. H., Card, K. D., Franklin, J. M., Archean tectonic and metallogenic evolution of the Superior Province of the Canadian Shield, Precambrian Research, 1992, 58: 25.
50. Foster, R. P. Piper, D. P., Archaean lode gold deposits in Africa; crustal setting, metallogenesis and cratonization, Ore Geology Reviews, 1993, 8: 303.
51. Phillips, G. N., Hughes, M. J., The geology and gold deposits of the Victorian gold province, Ore Geology Reviews, 1996, 11: 255.

52. Robert, F., Diverse gold mineralization styles in Precambrian greenstone terranes in Canada, Precambrian '95, 1995, 126.
53. McCuaig, T. C., Kerrich, R., Groves, D. I. et al., The nature and dimensions of regional and local gold-related hydrothermal alteration in tholeiitic metabasalts in the Norseman Goldfields: the missing link in a crustal continuum of gold deposits, Mineralium Deposita, 1993, 28: 420.
54. Jia, Y., Li, X., Kerrich, R., A fluid inclusion study of Au-bearing quartz vein systems in the Central and North Deborah deposits of the Bendigo gold field, central Victoria, Australia, Economic Geology, 2000, 95: 467.
55. Böhlke, J. K., Comparison of metasomatic reactions between a common CO_2-rich vein fluid and diverse wallrocks: intensive variables, mass transfers, and Au mineralization at Alleghany, California, Economic Geology, 1989, 84: 291.
56. Groves, D. l., Barley, M. E., Barnicoat, A. C. et al., Sub-greenschist- to granulite-hosted Archaean lode gold deposits of the Yilgarn Craton: a depositional continuum from deep-sourced hydrothermal fluids in crustal-scale plumbing systems, The Archaean Terrains: Processes and Metallogeny (eds. Glover, J.E., Ho S.E.), Perth: Vanguard Press, 1992, 325—337.
57. Kerrich, R., Cassidy, K. F., Temporal relationships of lode gold mineralization to accretion, magmatism, metamorphism and deformation—— Archean to present: a review, Ore Geology Reviews, 1994, 9: 263.
58. Miller, L. D., Goldfarb, R. J., Gehrels, G. E. et al., Genetic links among fluid cycling, vein formation, regional deformation, and plutonism in the Juneau gold belt, southeastern Alaska, Geology, 1994, 22: 203.
59. Kent, A. J. R., Cassidy, K. F., Fanning, C. M., Archean gold mineralization synchronous with the final stages of cratonization, Yilgarn Craton, Western Australia, Geology, 1996, 24: 879.
60. Guha, J., Kanwar, R., Vug brines—— fluid inclusions: a key to understanding of secondary gold enrichment processes and the evolution of deep brines in the Canadian Shield, Saline Water and Gases in the Crystalline Rocks, Geological Association Canada Special Paper 33 (eds. Fritz, P., Frape, S.K.), 1987, 95—101.
61. Kerrich, R., Ludden, J., The role of fluids during formation and evolution of the Southern Superior province lithosphere: A review, Canadian Journal of Earth Sciences, 2000, 37: 1.
62. Wyman, D. A., Kerrich, R., Archean lamprophyres, gold deposits and transcrustal structures: implications for greenstone belt gold metallogeny, Economic Geology, 1988, 83: 454.
63. Hodgson, C. J., The structure of shear-related, vein type gold deposits: a review, Ore Geology Reviews, 1989, 4: 231.
64. Swager, C., Stratigraphy and structure in the Southeastern Goldfields Province, An International Conference on Crustal Evolution, Metallogeny and Exploration of the Eastern Goldfields (Extended Abstracts), AGSO Record 1993/94, 1993, 69—72.
65. Sibson, R. H., Faulting and fluid flow, Fluids in Tectonically Active Regimes of the Continental Crust, Mineralogical Association of Canada Short Course 18 (ed. Nesbitt, B. E.), 1990, 93—132.
66. Tavis, G. A., Woodall, R., Bartram, G. D., The geology of Kalgoorie gold field, Proceeding Symposium on Archean Rocks ——1970, Perth, Geological Society of Australia Special Publication 3 (ed. Glover, J. E.), 1971, 175—190.
67. McCuaig, T. C., Kerrich, R., P-T-t-deformation-fluid characteristics of lode gold deposits: evidence from alteration systematics, Ore Geology Review, 1998,12: 381.
68. Cox, S. F., Deformation of continents in the dynamics of fluid flow in mesothermal gold systems, Footway Fluid Flow and Mineralization, Geological Society London, 1999, Special Publication 155-123-140.
69. Hronsky, J. .M. A., Cassidy, K. F., Grigson, M. W., Deposit- and mine-scale structure, Gold Deposits of the Archaean Yilgarn Block, Western Australia: Nature, Genesis and Exploration Guides, Perth: Vanguard Press, 1990, 38—59.
70. Wood, P. C., Burrows, D. R., Thomas, A. V. et al., The Hollinger-Mclntyre Au-quartz vein system, Timmins, Ontario, Canada: geological characteristics, fluid properties and light stable isotope geochemistry, Gold '86 (ed. Macdonald A.J.), Konsult International Inc., 1986, 56—80.
71. Neumayer, P., Cabri, L. J., Groves, D. I. et al., The mineralogical distribution of gold and relative timing of gold mineralization in two Archean settings of high metamorphic grade in Australia, Canadian Mineralogist, 1993, 31: 711.
72. Andrews, A. J., Hugon, H., Durocher, M. et al., The anatomy of a gold bearing greenstone belt: Red Lake, Northwestern Ontario, Canada, Gold'86 (ed. MacDonald, A.J.), Consult International Inc., 1986, 3—22.
73. Knight, J. T., Groves, D. l., Ridley, J. R., District-scale structural and metamorphic controls on Archean lode-gold mineralization in the amphibolite facies Coolgardie Goldfield, Western Australia, Mineralium Deposita, 1993, 28: 436.
74. Kerrich, R., Allison, l., Flow mechanisms in rocks: microscopic and mesoscopic structures, and their relation to physical conditions of deformation in the crust, Geoscience Canada, 1978, 5: 110.
75. Sibson, R. H., Robert, F., Poulsen, H., High angle faults, fluid pressure cycling and mesothermal gold quartz deposits, Ge-

ology, 1988, 16: 551.
76. Robert, F., Boullier, A. M., Firdaous, K., Gold-quartz veins in metamorphic terranes and their bearing on the role of fluids in faulting, JGR, 1995, 100: 12861.
77. Smith, D. W., Craw, D., Koons, P. O., Tectonic hydrothermal gold mineralisation in the outboard zone of the Southern Alps, New Zealand. New Zealand, JGR, 1996, 39: 201.
78. Kerrich, R., Geochemistry of gold deposits in the Abitibi greenstone belt, Canadian Institute of Mining and Metallogeny Special Paper 27, 1983, 75.
79. Mueller, A. G. Groves, D. I., The classification of Western Australian greenstone-hosted gold deposits according to wall-rock-alteration mineral assemblages, Ore Geology Reviews, 1991, 6: 291.
80. Loucks, R., Mavrogenes, J. A., Gold solubility in supercritical hydrothermal brines measured in synthetic fluid inclusions, Science, 1999, 284: 2159.
81. Roedder, E., Fluid inclusion evidence bearing on the environments of gold deposition, Gold '82, Geol. Soc. Zimbabwe, Special Publication 1 (ed. Foster, R.P.), 1984, 129—163.
82. Kesler, S. E., Nature and composition of mineralizing solutions, Greenstone Gold and Crustal Evolution: NUNA Conference Volume (eds. Robert, F. P., Sheahan, A. Green, S.B.), 1990, 86—90.
83. Crawford, M. L., Fluid inclusions - what can we learn? Earth Science Reviews, 1992, 32: 137.
84. Burrows, D. R., Wood, P. C., Spooner, E. T. C., Carbon isotope evidence for a magmatic origin for Archean gold-quartz vein ore deposits, Nature, 1986, 321: 851.
85. Nesbitt, B. E., Gold deposits continuum: a genetic model for lode Au mineralization in the continental crust, Geology, 1988, 16: 1044.
86. Goldfarb, R. J., Snee, L. W., Miller, M. L. et al., Rapid watering of the crust deduced from ages of mesothermal gold deposits, Nature, 1991, 354: 296.
87. Jia, Y., Kerrich, R., Nitrogen isotope systematics of mesothermal lode gold deposits: Metamorphic, granitic, meteoric water, or mantle origin?, Geology, 1999, 27: 1051.
88. Honma, H., Itihara, Y., Distribution of ammonium in minerals of metamorphic and granite rocks, GCA, 1981, 45: 983.
89. Sucha, V., Elsass, F., Eberl, D. D. et al., Hydrothermal synthesis of ammonium illite, American Mineralogists, 1998, 83: 58.
90. Clayton, R. N., Isotopic variations in primitive meteorities, Philosophical Transactions of the Royal Society of London, 1981, 303: 339
91. Cartigny, P., Harris, J. W., Javoy, M., Eclogitic diamond formation at Jwaneng: no room for a recyled component, Science, 1998, 280: 1421.
92. Javoy, M., Pineau, F., The volatiles record of a “popping” rock from the Mid Atlantic Ridge at 14° N: chemical and isotopic composition of gas trapped in the vesicles, EPSL, 1991, 107: 598.
93. Javoy, M., Pineau, F., Demaiffe, D., Nitrogen and carbon isotopic compositin in the diamonds of Mbuji Mayi (Zaire), EPSL, 1984, 68: 399.
94. Boyd, S. R., Mattey, D. P., Pillinger, C. T. et al., Multiple growth events during diamond genesis: an integrated study of carbon and nitrogen isotopes and nitrogen aggregation state in coated stone, EPSL, 1987, 86: 341.
95. Boyd, S. R., Pillinger, C. T., Milledge, H. J. et al., C and N isotopic composition and the infrared absorption spectra of coated diamonds: evidence for the regional uniformity of CO_2-H_2O rich fluids in lithospheric mantle, EPSL, 1992, 109: 633.
96. Peters, K. E., Sweeney, R. E., Kaplan, I. R., Correlation of carbon and nitrogen stable ratios in sedimentary organic matter, Limnology and Oceanography, 1978, 23: 598.
97. Wlotzka, F., Nitrogen, Handbook of Geochemisrty II (ed. Wedepohl, K. H.), New York: Springer-Verlag, 1972, 7B-1-7O-3.
98. Hall, A., The ammonium content of Caledonoan granites, Journal of the Geological Society, London, 1987, 144: 671.
99. Boyd, S. R., Hall, A., Pillinger, C. T., The measurement of $\delta^{15}N$ in crustal rocks by static vacuum mass spectrometry: application to the origin of the ammonium in the Cornubian batholith, southwest England, GCA, 1993, 57: 1339.
100. Haendel, D., Mühle, K., Nitzsche, H. et al., Isotopic variations of the fixed nitrogen in metamorphic rocks, GCA, 1986, 50: 749.
101. Owens, N.J.P., Natural variations in ^{15}N in the marine environment, Adv. Mar. Bio. 24, 1987, 389—451.

102. Polat, A., Kerrich, R., Geodynamic controls on gold mineralization in greenstone belts of the Archean Superior Province, Abstracts with Program Geological Society of America, 1997, A-444.
103. England, P. C., Thompson, A. B., Pressure-temperature-time paths of regional metamorphism: I, Heat transfer during the evolution of regions of thickened continental crust, Journal of Petrology, 1984, 25: 894.
104. Redden, J. A., Peterman, Z. E., Zartman, R. E. et al., U-Th-Pb geochronology and preliminary interpretation of Precambrian tectonic events in the Black Hill, South Dakota, Geological Association of Canada Spectial Paper 37, 1990, 229—252.
105. Dahl, P. S., Holm, D. K., Gardner, E. T. et al., New constraints on the timing of Early Proterozoic tectonism in the Black Hill (South Dakota), with implications for docking of the Wyoming province with Laurentia, GSA Bulletin, 1999, 111: 1335.
106. Zhou, T., Lu, G., Tectonics, granitoids and mesozoic gold deposits in East Shandong, China, Ore Geology Reviews, 2000, 16: 71.
107. Bagby, W. C., Berger, B. R., Geologic characteristics of sediment-hosted, disseminated precious-metal deposits in the western United States, in Geology and Geochemistry of Epithermal Systems (eds. Berger, B.R., Bethke, P.M.), Reviews in Economic Geology, Society of Economic Geologists, 1985, 2: 169.
108. Sillitoe, R. H., Bonham, H. F., Sediment-hosted gold deposits——Distal products of magmatic-hydrothermal systems, Geology, 1990, 18: 157.
109. Phillips, G. N., Powell, R., Link between gold provinces, Economic Geology, 1993, 88: 1084.
110. Phillips, G. N., Thomson, D. F., Kuehn, C. A., Deep weathering of deposits in the Yilgarn and Carlin gold provinces: Regolith '98 Proceedings, CRC-LEME, Perth, 1998, 1—22.
111. Percival, T. J., Bagby, W. C., Radtke, A. S., Physical and chemical features of precious metal deposits hosted by sedimentary rocks in the western United States, Bulk Mineable Precious Metal Deposits of the Western United States (eds. Schafer, R.W., Cooper, J.J., Vikre, P.G.), Geological Society of Nevada, 1988, 11—34.
112. Christensen, O. D., Carlin trend geologic overview, Society of Economic Geologists Guidebook Series, 1993, 18: 12.
113. Roberts, R. J., Alignments of mining districts in north-central Nevada, U.S.G.S. Professional Paper 400-B, 1960, B17.
114. Shawe, D. R., Structurally controlled gold trends imply large gold resources in Nevada, Geology and Ore Deposits of the Great Basin (eds. Raines, G. L., Lisle, R. E., Schafe, R. W. et al.), Geological Society of Nevada, 1991, 199—212.
115. Grauch, V. J. S., Jachens, R. C., Blakely, R. J., Evidence for a basement feature related to the Cortez disseminated gold trend and implications for regional exploration in Nevada, Economic Geology, 1995, 90: 203.
116. Hausen, D. M., Kerr, P. F., Fine gold occurrence at Carlin, Nevada, Ore Deposits of the United States 1933—1967, The Graton-Sales Volume, American Institute of Mining, Metallurgical, and Petroleum Engineer, 1968, 908—940.
117. Radtke, A. S., Geology of the Carlin gold deposit, Nevada, U.S.G.S. Professional Paper 1267, 1985, 124.
118. Teal, L., Jackson, M., Geologic overview of the Carlin trend gold deposits and descriptions of recent deep discoveries, Society of Economic Geologists Guidebook Series (eds. Vikre, P., Thompson, T.B., Bettles, K. et al.), 1997, 28: 3.
119. Kuehn, C. A., Studies of Disseminated Gold Deposits near Carlin, Nevada——Evidence for a Deep Geologic Setting of Ore Formation (Ph.D. Thesis), Pennsylvania State University, 1989, 395.
120. Bakken, B. M., Gold Mineralization, Wall-Rock Alteration, And the Geochemical Evolution of the Hydrothermal System in the Main Orebody, Carlin Mine (Ph.D. Thesis), Stanford University, 1990, 236.
121. Hofstra, A. H., Leventhal, J. S., Northrop, H. R. et al., Genesis of sediment-hosted disseminated gold deposits by fluid mixing and sulfidization: Chemical-reaction-path modeling of ore-depositional processes documented in the Jerritt Canyon district, Nevada, Geology, 1991, 19: 36.
122. Lamb, J. B., Cline, J., Depths of formation of the Meikle and Betze/Post deposits, Society of Economic Geologists Guidebook Series (eds. Vikre, P., Thompson, T. B., Bettles, K. et al.), 1997, 28: 101.
123. Ilchik, R. P., Barton, M. D., An amagmatic model of Carlin-type gold deposits, Economic Geology, 1997, 92: 269.
124. Hofstra, A. H., Snee, L. W., Rye, R. O. et al., Age constraints on Jerritt Canyon and other Carlin-type gold deposits in the western United States——Relationship to mid-Tertiary extension and magmatism, Economic Geology, 1999, 94: 769.
125. Poulson, K. H., Carlin-type gold deposits and their potential occurrence in the Canadian Cordillera, Current Research 1996A, Geological Survey of Canada, 1996, 1—9.
126. Hart, C. J. R., Baker, T., Burke, M., New exploration concepts for country-rock-hosted, intrusion-related gold systems——Tintina gold belt in Yukon, The Tintina Gold Belt——Concepts, Exploration, and Discoveries: Special Volume 2,

2000, 145—172.
127. Li, Z., Peters, S. G., Comparative geology and geochemistry of sedimentary-rock-hosted (Carlin-type) gold deposits in the People's Republic of China and in Nevada, USA, U.S. Geological Survey Open-file Report 98-466, 1998, 160.
128. Mehrabi, B., Yardley, B. W. D., Cann, J. R., Sediment-hosted disseminated gold mineralisation at Zarshuran, NW Iran, Mineralium Deposita, 1999, 34: 673.
129. Asadi, H. H., Voncken, J. H. L., Hale, M., Invisible gold at Zarshuran, Iran, Economic Geology, 1999, 94: 1367.
130. Tooker, E. W., Geologic characteristics of sediment- and volcanic-hosted disseminated gold deposits—search for an occurrence model, U.S.G.S. Bulletin 1646, 1985, 150.
131. Emsbo, P., Hutchinson, R. W., Hofstra, A. H. et al., Syngenetic Au on the Carlin trend—Implications for Carlin-type deposits, Geology, 1999, 27: 59.
132. Murphy, J. B., Oppliger, G. L., Brimhall, G. H. et al., Plume-modified orogeny—An example from the western United States, Geology, 1998, 26: 731.
133. Oppliger, G. L., Murphy, J. B., Brimhall, G. H. et al., Is the ancestral Yellowstone hotspot responsible for Tertiary "Carlin" mineralization in the Great Basin of Nevada?, Geology, 1997, 25: 627.
134. Liu, D., Yunjin, T., Jianye, W. et al., Carlin-type gold deposits in China, Brazil Gold'91 (ed. Ladeira, E.A.), Rotterdam: Balkema, 1991, 89—93.
135. Zhang, F. X, Chen, Y. J., Li, C. et al., Geological and geochemical character and genesis of the Jinlongshan-Qiuling gold deposits in Qinling orogen: Metallogenic mechanism of the Qinling-pattern Carlin-type gold deposits, Science in China, 2000, 43(Suppl): 95 (this issue).
136. Metcalfe, I., Pre-Cretaceous evolution of SE Asian terranes, Tectonic Evolution of Southeast Asia (eds. Hall, R., Blundell, D. J.), Geological Society Special Publication 106, 1996, 97—122.
137. Yin, A., Nie, S., A Phanerozoic palinspastic reconstruction of China and its neighboring regions, The Tectonic Evolution of Asia (eds. Yin, A., Harrison, T.M.), Cambridge: Cambridge University Press, 1996, 442—485.
138. Daliran, F., Walther, J., Stuben, D., Sediment-hosted disseminated gold mineralization in the North Takab geothermal field, NW Iran, Mineral Deposits—Processes to Processing, Rotterdan: Balkema, 1999, 837—840.
139. Sengor, A. M. C., Natal'in, B, Paleotectonics of Asia——fagments of a synthesis, The Tectonic Evolution of Asia (eds. Yin, A., Harrison, T. M.), Cambridge: Cambridge University Press, 1996, 486—640.
140. Sillitoe, R. H., Gold-rich porphyry copper deposits; geological model and exploration implications, Mineral Deposit Modeling: Geological Association of Canada Special Paper 40, 1993, 465—478.
141. Berger, B. R., Eimon, W. C., Conceptual models of epithermal precious metal deposits, Ameriacan Institute of Mineralogy and Metallurgy, 1983, 191—205.
142. Sillitoe, R. H., Styles of high-sulphidation gold, silver and copper mineralisation in porphyry and epithermal environments, PACRIM '99 (ed. Australian Institute of Mining and Metallurgy), 1999, 29—44.
143. Abzalov, M.Z., Gold deposits of the Russian North East (The Northern Circum Pacific): Metallogenic overview, PACRIM '99 (ed. The Australasian Institute of Mining and Metallurgy), 1999, 701—714.
144. So, C. S., Zhang, D., Yun, S. T. et al., Alteration-mineralization zoning and fluid inclusions of the high sulfidation epithermal Cu-Au mineralization at Zijinshan, Fujian Province, China, Economic Geology, 1998, 93: 961.
145. Mitchell, A. H. G., Distribution and genesis of some epizonal Zn-Pb and Au provinces in the Carpathian-Balkan region, Transction of the Institute of Mining and Metallogy (B105), 1996, 127—138.
146. Foster, R. P., Gold mineralization in Europe, characteristics and tectonic setting, Minerals Industry International, 1997, 24—31.
147. Alderton, D. H. M., Thirlwall, M. F., Baker, J. A., Hydrothermal alteration associated with gold mineralization in the southern Apuseni Mountains, Romania; preliminary Sr isotopic data, Mineralium deposita, 1998, 33: 520.
148. Islamov, F., Kremenetsky, A., Minzer, E. et al., The Kochbulak-Kairagach ore filed, Au, Ag, and Cu deposits of Uzbekistan, Excursion B6 of the Joint SGA-IAGOD Symposium of International Field Conference of IGCP-373, 1999, 91—106.
149. Moralev, G. V., Shatagin, K. N., Rb-Sr study of Au-Ag Shkol'noe deposit (Kurama Mountains, north Tadjikistan): age of mineralization and time scale of hydrothermal processes, Mineralium Deposita, 1999, 34: 405.
150. Perkins, C., Walshe, J. L., Morrison, G., Metallogenic episodes of the Tasman fold belt system, eastern Australia, Economic Geology, 1995, 90: 1443.
151. Corbett, G. J., Leach, T. M., Southwest Pacific Rim gold-copper systems: Structure, alteration and mineralization, Society

of Economic Geologists Special Publication 6, 1998, 240.
152. White, N. C., Leake, M. J., McCaughey, S. N. et al., Epithermal gold deposits of the southwest Pacific, Journal of Geochemical Exploration, 1995, 54: 87.
153. Sillitoe, R. H., Giant and bonanza gold deposits in the epithermal environment: Assessment of potential genetic factors, Giant Ore Deposits, Society of Economic Geologists Special Publication 2, 1993, 125—156.
154. Sillitoe, R.H., Hannington, M.D., Thompson, J.F.H., High sulfidation deposits in the volcanogenic massive sulfide environment, Economic Geology, 1996, 91: 204.
155. Sillitoe, R. H., Characteristics and controls of the largest porphyry copper-gold and epithermal gold deposits in the circum-Pacific region, Australian Journal of Earth Sciences, 1997,44: 373.
156. Kesler, S. E., Russell, N., Seaward, M. et al., Geology and geochemistry of sulfide mineralization underlying the puebo Viejo gold-silver oxide deposit, Dominican Republic, Economic Geology, 1981, 76: 1096.
157. White, N. C., Poizat, V., Epithermal deposits, diverse styles, diverse origins?, Australian Institue of Mining and Metallurgy Publication Series 9, 1995, 623—628.
158. Goldfarb, R. J., Hart, C. J. R., Mortensen, J. K., Metallogeny of the northeastern Pacific rim? An example of the distribution of ore deposits along a growing continental margin, PACRIM'99 Symposium Volume (ed. Dow, J.), 1999, 273—286.
159. Lehmann, B., Heinhorst, J., Hein, U. et al., The Bereznjakovskoje gold trend, southern Urals, Russia, Mineralium Deposita, 1999, 34: 241.
160. Dube, B, Lauziere, K, Boisvert, E, Preliminary report on the geological setting of the acid-sulphate Hope Brook gold deposit, in SW Newfoundland, Report of Activities-Newfoundland (ed. Geological Survey Branch), 1995, 49—50.
161. Hayba, D. O., Bethke, P. M., Heald, P. et al., Geologic, mineralogic, and geochemical characteristics of volcanic-hosted epithermal precious-metal deposits, Geology and Geochemistry of Epithermal Systems (eds. Berger, B. R., Bethke, P. M.), Reviews in Economic Geology, 1985, 2: 129.
162. Heald, P., Foley, N. K., Hayba, D. O., Comparative anatomy of volcanic-hosted epithermal deposits: acid sulphate and adularia-sericite types, Economic Geology, 1987, 82: 1.
163. Hedenquist, J. W., Izawa, E., Arribas, A. et al., Epithermal Gold Deposits: Styles, Characteristics, and Exploration, Society of Resource Geology Special Publication 1, 1996, 1.
164. White, N. C., Hedenquist, J. W., Epithermal gold deposits: Styles, characteristics and exploration, Society of Economic Geologists, Newsletter, 1995, 23(1): 9.
165. Hedenquist, J. W., The ascent of magmatic fluid: Discharge versus mineralization, Magmas, Fluids, and Ore Deposits (ed. Thompson, J. F. H.), Mineralogical Association of Canada Short Course, 1995, 23: 263.
166. Kay, S. M., Mpodozis, C., Coira, B., Neogene magmatism, tectonism, and mineral deposits of the Central Andes (22° to 33° S Latitude), Geology and Ore Deposits of the Central Andes (ed. Skinner, B.J.), Society of Economic Geologists Special Publication 7, 1999, 27—59.
167. James, D. E., Sacks, S., Cenozoic formation of the Central Andes: A geophysical perspective, Geology and Ore Deposits of the Central Andes (ed. Skinner, B. J.), Society of Economic Geologists Special Publication 7, 1999, 1—25.
168. Burchfiel, B. C., Cowan, D. S., Davis, G. A., Tectonic overview of the Cordilleran orogen in the western United States, Geology of North America, 1992, G-3: 407.
169. Leier, P. V., Ivanov, V. V., Ratkin, V. V. et al., Epithermal gold-silver deposits of northeast Russia: the first ^{40}Ar-^{39}Ar age determinations of the ores, Doklady, 1997, 357: 1141.
170. Goryachev, N. A., Edwards, A. C., Gold metallogeny of North-East Asia, PACRIM '99, 1999, 287—302.
171. Rubin, C. M., Miller, E. L., Toro, J., Deformation of the northern circum-Pacific margin: variations in tectonic style and plate tectonic implications, Geology, 1995, 23: 897.
172. Pan, Y., Dong, P., The Lower Changjiang (Yangzi/Yangtze River) metallogenic belt, east central China: intrusion- and wall rock-hosted Cu-Fe-Au, Mo, Zn, Pb, Ag deposits, Ore Geology Reviews, 1999, 15: 177.
173. Li, X. H., Cretaceous magmatism and lithospheric extension in southeast China, Journal of Asian Earth Sciences, 2000, 18: 293.
174. Lattanzi, P., Epithermal precious metal deposits of Italy——an overview, Mineralium Deposita, 1999, 34: 630.
175. Neubauer, F., Cloetingh, S., Dinu, C. et al., Tectonics of the Alpine-Carpathian-Pannonian region: introduction, Tectonophysics, 1997, 272: 93.
176. Boorder, H. de, Spakman, W., White, S. H. et al., Late Cenozoic mineralization, orogenic collapse and slab detachment in

the European Alpine Belt, EPSL, 1998,164: 569.
177. Cooke, D. R., Bull, S.W., Large, R. R. et al., The importance of oxidized brines for the formation of Australian Proterozoic stratiform sediment-hosted Pb-Zn (SEDEX) deposits, Economic Geology, 2000, 95:1.
178. Solomon, M., Groves, D. I., The Geology and Origin of Australia's Mineral Deposits: Oxford Monogr, Geol. Geophy. 24, Oxford: Oxford University Press, 1994, 951.
179. Henley, R. W., Adams, D. P. M., Strike-slip fault reactivation as a control on epithermal vein-style gold mineralization, Geology, 1992, 20: 443.
180. Sillitoe, R. H., Major regional factors favouring large size, high hypogene grade, elevated gold content and supergene oxidation and enrichment of porphyry copper deposits, Conference Proceedings of Porphyry and Hydrothermal Copper & Gold Deposits: A Global Perspective (ed. Porter, T. M.), Glenside: Australian Mineral Foundation, 1998, 21—34.
181. Richards, J. P., kerrich, R., The Porgera gold mine, Papua New Guinea: magmatic hydrothermal to epithermal evolution of an alkalic-type precious metal deposit, Economic Geology, 1993, 88: 1017.
182. Lang, J. R., Lueck, B. A., Mortensen, J. K. et al, Triassic-Jurassic silica-undersaturated and silica-saturated alkalic intrusions in the Cordillera of British Columbia--Implications for arc magmatism, Geology, 1995, 23: 451.
183. Hu, S. X., Chen, Z. M., Fu, S. G. et al., Material sources and regional regularities of ore formation of porphyry copper and molybdenum deposits, Journal of Nanjing University (in Chinese with English abstract), 1984, (Special): 9.
184. Sheppard, S. M. F., Nielsen, R. L., Taylor, H. P., Oxygen and hydrogen isotope ratios of clay minerals from porphyry copper deposits, Economic Geology, 1969, 64: 755.
185. Beane, R. E., Titley, S. R., Porphyry copper deposits: part II, hydrothermal alteration and mineralization, Economic Geology Seventy-fifth Anniversary Volume (ed. Skinner, B. J.), 1981, 235—269.
186. Titley, S. R., Beane, R. E., Porphyry copper deposits; part I, geologic settings, petrology, and tectogenesis, Economic Geology Seventy-fifth Anniversary Volume (ed. Skinner, B. J.), 1981, 214—235.
187. Cox, D. P., Descriptive model of porphyry Cu-Au, Mineral Deposit Model, U. S. Geological Survey Bulletin 1693 (eds. Cox, D. P., Singer, D. A.), 1986, 110.
188. Dilles, J. H., Solomon, G. C., Taylor, H. P. et al., Oxygen and hydrogen isotope characteristics of hydrothermal alteration at the Ann-Mason porphyry copper deposit, Yerington, Nevada, Economic Geology, 1992, 87: 44.
189. Einaudi, M. T., Topics in porphyry copper-gold and related deposits, Short Course for Newmont Western Pacific Exploration Group, 1995, 31.
190. Freeport-McMoran Mining, Annual Report, Freeport-McMoran Copper-Gold Company, 1994, 1.
191. MacDonald, G. D., Arnold, L. C., Geological and geochemical zoning of the Grasberg igneous complex, Irian Jaya, Indonesia, Journal of Geochemical Exploration, 1994, 50: 143.
192. Tooker, E. W., Gold in the Bingham district, Utah, Gold in Porphyry Copper Systems, U. S. Geological Survey Bulletin 1857E, 1990, E1–E16.
193. Babcock, R. C., Jr., Ballantyne, G. H., Summary of the geology of the Bingham district, Utah, Porphyry Copper Deposits of the American Cordillera, Arizona Geological Society Digest 20, 1995, 316—335.
194. Clark, G. H., Panguna copper-gold deposit, in Geology of the Mineral Deposits of Australia and Papua New Guinea, Australian Institute of Mining and Metallurgy Monograph Series 14 (ed. Hughes, F. E.), 1990, 1807—1816.
195. Guilbert, J. M., Geology, alteration, mineralization, and genesis of the Bajo de la Alumbrera porphyry copper-gold deposit, Catamarca Province, Argentina, Porphyry Copper Deposits of the American Cordillera: Arizona Geological Society Digest 20, 1995, 646—656.
196. Muller, D., Forrestal, P., The shoshonite porphyry Cu-Au association at Bajo de la Alumbrera, Catamarca Provine, Argentina, Mineralogy and Petrology, 1998, 64: 47.
197. Mitchell, A. H. G., Leach, T. M., Epithermal Gold in the Philippines; Island Arc Metallogenesis: Geothermal Systems and Geology, London: Academic Press, 1991, 457.
198. Arribas, A., Jr., Hedenquist, J. W., Itaya, T. et al., Contemporaneous formation of adjacent porphyry and epithermal Cu-Au deposits over 300 Ma in northern Luzon, Philippines, Geology, 1995, 23: 337.
199. Meldrum, S. J., Aquino, R. S., Gonzales, R. I. et al., The Batu Hijau porphyry copper-gold deposit, Sumbawa Island, Indonesia, Journal of Geochemical Exploration, 1994, 50: 203.
200. Clode, C., Proffett, J., Mitchell, P. et al., Relationships of intrusion, wall-rock alteration and mineralisation in the Batu Hijau copper-gold porphyry deposit, Proceedings of the 1999 Pacrim Congress, Publication Series No 4/99, 1999, 485—498.

201. Rush, P. M., Seegers, H. J., Ok Tedi copper-gold deposits, Geology of the Mineral Deposits of Australia and Papua New Guinea: Australian Institute of Mining and Metallurgy, Monograph Series 14 (ed. Hughes, F. E.), 1990, 1747—1754.
202. Meyer, C., Hemley, J. J., Wall rock alteration, Geochemistry of Hydrothermal Ore Deposits (ed. Barnes, H. L.), New York: Rinehart and Winston, 1967, 166—235.
203. Lowell, J. D., Guilbert, J. M., Lateral and vertical alteration-mineralization zoning in porphyry ore deposits, Economic Geology, 1970, 65: 373.
204. Sillitoe, R. H., Gold-rich porphyry copper deposits of the Circum-Pacific region; an updated overview, Proceedings of the 1990 Pacific Rim Congress, Parkville, Australia (eds. Foots, J., Brennan, T.), 1990, 119—126.
205. Solomon, M., Subduction, arc reversal, and the origin of porphyry copper-gold deposits in island arcs, Geology, 1990, 18: 630.
206. Muller, D., Groves, D. I., Direct and indirect associations between potassic igneous rocks, shoshonites and gold-copper deposits, Ore Geology Reviews, 1993, 8: 383.
207. Muller, D., Groves, D. I., Potassic Igneous Rocks and Associated Gold-Copper Mineralization, Berlin: Springer, 2000, 252.
208. Burnham, C. W., Hydrothermal fluid at the magmatic stage, Geochemistry of Hydrothermal Ore Deposits (ed. Barnes, H. L.), New York: Rinehart and Winston, 1967, 34—76.
209. Cline, J. S., Genesis of porphyry copper deposits; the behavior of water, chloride, and copper in crystallizing melts, Porphyry Copper Deposits of the American Cordillera: Arizona Geological Society Digest 20, 1995, 69—82.
210. Sillitoe, R. H., Thompson, J. F. H., Intrusion-related vein gold deposits; types, tectono-magmatic settings and difficulties of distinction from orogenic gold deposits, Resource Geology, 1998, 48: 237.
211. Hu, S. X., Wang, H. N., Wang, D. Z. et al., Geology and Geochemistry of Gold Deposits in East China (in Chinese), Beijing: Science Press, 1998, 343.
212. Baker, R. C., Guilbert, J. M., Regional structural control of porphyry copper deposits in northern Chile, Abstracts with Programs of 1987 Annual Meeting and Exposition of Geological Society of America—19, Geological Society of America, 1987, 578.
213. Sasso, A. M., Clark, A. H., The Farallon Negro Group, Northwest Argentina: Magmatic, hydrothermal and tectonic implications for Cu-Au metallogeny in the Andean back-arc, Society of Economic Geologists Newsletter No 34, 1998, 8—18.
214. Skewes, M. A., Stern, C. R., Genesis of the giant late Miocene to Pliocene copper deposits of central Chile in the context of Andean magmatic and tectonic evolution, International Geology Review, 1995, 37: 893.
215. Kirkham, R. V., Tectonic and structural features of arc deposits, Metallogeny of Volcanic Arcs, British Columbia Geological Survey, 1998, B1—45.
216. Rak, P., The Relationship Between Gold Deposit Distribution and Major Tectonic Events in Southeast Asia (B.Sc. Honours Thesis), The University of Western Australia, 1999, 98.
217. Hamilton, W. B., Tectonics of the Indonesian region, U. S. Geological Survey Professional Paper 1078, 1979, 345.
218. Pilger, R. H., Jr., Plate reconstructions, aseismic ridges, and low-angle subduction beneath the Andes, Geological Society of America Bulletin, 1981, 92: 1448.
219. Johnson, R. W., Mackenzie, D. E., Smith, I. E., Volcanic rock associations at convergent plate boundaries, reappraisal of the concept using case histories from Papua New Guinea, Geological Society of America Bulletin, 1978, 89: 96.
220. McDowell, F. W., McMahon, T. P., Warren, P. Q. et al., Pliocene Cu-Au-bearing igneous intrusions of the Gunung Bijih (Ertsberg) District, Irian Java, Indonesia: K-Ar geochronology, Journal of Geology, 1996, 104: 340.
221. Dickinson, W. R., Snyder, W. S., Plate tectonics of the Laramide Orogeny, Laramide Folding Associated with Basement Block Faulting in the Western United States (ed. Matthews, V.), Geological Society of America Memoir 151, 1978, 355—366.
222. Bird, P., Laramide crustal thickening event in the Rocky Mountain foreland and Great Plains, Tectonics, 1984, 3: 741.
223. Yang, T. F., Lee, T., Chen, C. H. et al., A double island arc between Taiwan and Luzon; consequence of ridge subduction, Tectonophysics, 1996, 258: 85.
224. van Leeuwen, T. M., 25 years of mineral exploration and discovery in Indonesia, Journal of Geochemical Exploration, 1994, 50: 13.
225. DeMets, C., Gordon, R. G., Argus, D. F. et al., Effect of recent revisions to the geomagnetic reversal time scale on estimates of current plate motions, Geophysical Research Letters, 1994, 21: 2191.

226. Hall, R., Reconstructing Cenozoic SE Asia, Tectonic Evolution of Southeast Asia: Geological Society Special Publication 106 (eds. Hall, R., Blundell, D. J.), 1996, 153—184.
227. Fletcher, I. R., Garwin, S. L., McNaughton, N. J., SHRIMP U-Pb dating of Pliocene zircons, Abstracts and Proceedings of Beyond 2000: New Frontiers in Isotope Geoscience, Lorne, 2000, 2000, 73—74.
228. Richardson, A. N., Blundell, D. J., Continental collision in the Banda Arc, Tectonic Evolution of Southeast Asia: Geological Society Special Publication 106 (eds. Hall, R., Blundell, D. J.), 1996, 47—60.
229. McCaffrey, R., Active tectonics of the eastern Sunda and Banda arcs, JGR- B, 1988, 93: 163.
230. McCaffrey, R., Slip partitioning at convergent plate boundaries of SE Asia, Tectonic Evolution of Southeast Asia: Geological Society Special Publication 106 (eds. Hall, R., Blundell, D. J.), 1996, 3—18.
231. Bonatti, E., Harrison, C. G. A., Fisher, D. E. et al., Easter volcanic chain (Southeast Pacific): a mantle hot line, JGR, 1977, 82: 2457.
232. Armstrong, R. L., Hollister, V. F., Harakel, J. E., K-Ar dates for mineralization in the White Cloud-Cannivan porphyry molybdenum belt of Idaho and Montana, Economic Geology, 1978,73: 94.
233. Tooker, E. W., Gold in the Butte District, Montana, Gold in Porphyry Copper Systems. U. S. Geological Survey Bulletin 1857E, 1990, E17–E27.
234. Meyer, C., Ore deposits as guides to geologic history of the Earth, Annual Reviews Earth and Planetary Science, 1988, 16: 147.
235. Hitzman, M. W., Oreskes, N. Einaudi, M. T., Geological characteristics and tectonic setting of Proterozoic iron oxide (Cu-U-Au-REE) deposits, Precambrian Research, 1992, 58: 241.
236. Davidson, G. J. Large, R. D., Proterozoic copper-gold deposits, AGSO Journal of Australian Geology and Geophysics, 1998, 17: 105.
237. Williams, P. J., Metalliferous Economic Geology of the Mt Isa Eastern Succession, Queensland, Australian Journal of Earth Sciences, 1998, 45: 329.
238. Oreskes, N., Einaudi, M. T., Origin of rare earth element-enriched hematite breccias at the Olympic Dam Cu-U-Au-Ag deposit, Roxby Downs, South Australia, Economic Geology, 1990, 85: 1.
239. Huhn, S. R. B. Nasceimento, J. A. S., Sao os depositas cupriferos de Carajas do Tipo Cu-Au-U-ETR, Contribuicoes a Geologia da Amazonia, 1998, 143—160.
240. Lindemayer, Z. G., O deposito de Cu (AU-Mo) do Salobo, Serra Dos Carajas, Revisitado, Workshop Depositus Minerair Brasilieiros de Metair-Base, 1998, 29—37.
241. Ryan, P. J., Lawrence, A. L., Jenkins, R. A. et al., The Candelaria copper-gold deposit, Chile, Porphyry Copper Deposits of the American Cordillera, Arizona Geological Society Digest 20 (eds. Wahl-Pierce, F., Bolm, J. G.), 1995, 625—645.
242. Dilles, J. H. Einaudi, M. T., Wall-rock alteration and hydrothermal flow paths about the Ann-Mason porphyry copper deposit, Nevada – a 6km vertical reconstruction, Economic Geology, 1992, 85: 1963.
243. Reeve, J. S., Cross, K. C., Smith, R. N. et al., The Olympic Dam copper-uranium-gold-silver deposit, South Australia, Geology of Mineral Deposits of Australia and Papua New Guinea: Australasian Institute Mining and Metallurgy Monograph 14 (ed. Hughes, F.), 1990, 1009—1035.
244. Gow, P. A., Wall, V. J., Oliver, N. H. S. et al., Proterozoic iron-oxide (Cu-U-Au-REE) deposits: further evidence of hydrothermal origins, Geology, 1994, 22: 633.
245. Mountain, B. W., Woods, S. A., Chemical controls on the solubility, transport and deposition of platinum and palladium in hydrothermal solutions: a thermodynamic approach, Economic Geology, 1989, 83: 492.
246. Philpotts, A. R., Origin of certain iron-titanium oxide and apatite rocks, Economic Geology, 1967, 62: 303.
247. Wyborn, L., Younger ca 1500 Ma granites of the Williams and Naraku Batholiths, Cloncurry District, eastern Mt Isa Inlier: geochemistry, origin, metallogenic significance and exploration indicators, Australian Journal of Earth Sciences, 1998, 45: 397.
248. Barton, M. D. Johnson, D. A., Evaporitic-source model for igneous-related Fe-oxide-(REE-Cu-Au-U) mineralization, Geology, 1996, 24: 259.
249. Johnson, J. P. Cross, K. C., U-Pb geochronological constraints on the genesis of the Olympic Dam Cu-U-Au-Ag deposit, South Australia, Economic Geology, 1995, 90: 046.
250. Campbell, I. H., Compston, D. M., Richards, J. P. et al., Review of the application of isotopic studies to the genesis of Cu-Au mineralization at Olympic Dam and Au mineralization at Porgera, Tennant Creek district and Yilgarn Craton, Aus-

tralian Journal of Earth Sciences, 1998, 45: 201.
251. Vearncombe, S., Barley, M. E., Groves, D. I. et al., 3.26 Ga black smoker-type mineralization in the Strelley Belt, Pilbara Craton, Western Australia, Journal of the Geological Society of London, 1995, 152: 587.
252. Franklin, J. M., Volcanic-associated massive sulfide deposits, Mineral Deposit Modeling, Geological Association of Canada Special Paper 40, 1993, 315—334.
253. Franklin, J. M., Lydon, J. W., Sangster, D. F., Volcanic-associated massive sulfide deposits, Economic Geology 75th Anniversary Volume, 1981, 485—627.
254. Lydon, J. W., Volcanogenic massive sulfide deposits: part 2, genetic models, Geoscience Canada, 1988, 15: 43.
255. Large, R. R., Huston, D. L., McGoldrick, P. J. et al., Gold distribution and genesis in Australian volcanogenic massive sulfide deposits and significance for gold transport models, Economic Geology Monograph 6, 1989, 520—536.
256. Hannington, M. D., Scott, S. D., Sulfidation equilibria as guides to gold mineralization in volcanogenic massive sulfides: Evidence from sulfide mineralogy and the composition of sphalerite, Economic Geology, 1989, 84: 1978.
257. Tourigny, G., Douget, D., Bourget, A., Geology of the Bousquet 2 mine: An example of a deformed, gold-bearing polymetallic sulfide deposit, Economic Geology, 1993, 88: 1578.
258. Gibson, H. L., Watkinson, D. H., Comba, C. D. A., Silicification: Hydrothermal alteration in an Archean geothermal system within the Amulet rhyolite formation, Noranda, Quebec, Economic Geology, 1983, 78: 954.
259. Hodgson, C. J., Lydon, J. W., The geological setting of volcanogenic massive sulfide deposits and active hydrothermal systems: Some implications for exploration, Canadian Institute of Mining and Metallurgy Bulletin, 1977, 70: 95.
260. Hannington, M. D., Poulsen, K. H., Thompson, J. F. H. et al. Volcanogenic gold in the massive sulfide environment, in Volcanic-Associated Massive Sulfide Deposits: Processes and Examples in Modern and Ancient Settings (eds. Bbarrie, C. T., Hanningto, M. D.), Reviews in Economic Geology, 1999, 8: 319.
261. Wyman, D. A., Kerrich, R., Fryer, B. J., Gold mineralization overprinting iron formation at the Agnico-Eagle deposit, Quebec, Canada: mineralogical, microstructural and geochemical evidence, Gold'86, An International Symposium on the Geology of Gold Deposits, 1986, 108—123.
262. Hedenquist, J. W., Mineralization associated with volcanic-related hydrothermal systems in the circum-Pacific basin, 4th Forth Circum-Pacific Energy and Mineral Resources Conference, Singapore, 1986 (ed. Horn, M. K.), American Association of Petroleum Geologists, 1987, 513—524.
263. Arribas, A., Jr., Characteristics of high-sulfidation epithermal deposits and their relation to magmatic fluid, Mineralogical Association of Canada Short Course Series, 1995, 23: 419.
264. Goodfellow, W. D., Lydon, J. W., Turner, R. J. W., Geology and genesis of stratiform sediment-hosted (SEDEX) zinc-lead-silver sulfide deposits, Mineral Deposit Modeling, Geological Association of Canada Special Paper 40, 1993, 201—254.
265. Roth, T., Thompson, J. F. H., Barrett, J., The precious metal-rich Eskay Creek deposits, Northwestern British Columbia, Reviews in Economic Geology, 1998, 8: 367.
266. Sherlock, R. L., Roth, T., Spooner, E. T. C. et al., Origin of the Eskay Creek precious metal-rich volcanogenic massive sulfide deposit: Fluid inclusion and stable isotope evidence, Economic Geology, 1999, .94: 803.
267. Ludden, J. N., Peloquin, S. A., A geodynamic model for the evolution of the Abitibi belt-implications for the origins of volcanic massive sulfide (VMS) deposits, Trace Element Geochemistry of Volcanic Rocks: Applications for Massive Sulfide Exploration (ed. Wyman D. A.), GAC Short Course Notes, 1996,12: 205.
268. Wyman, D. A., Kerrich, R., Groves, D. I., Lode gold deposits and Archean mantle plume-island arc interaction, Abitibi subprovince, Canada, Journal of Geology, 1999, 107: 715.
269. Stern, R. A., Syme, E. C., Lucas, S. B., Geochemistry of 1.9 Ga MORB- and OIB-like basalts from the Amisk collage, Flin Flon Belt, Canada: Evidence for an intra-oceanic origin, GCA, 1995, 59: 3131.
270. Syme, E. C., Bailes, A. H., Stern, R. A. et al., Geochemical characteristics of 1.9 Ga tectonostratigraphic assemblages and tectonic setting of massive sulfide deposits in the Paleoproterozoic Flin Flon Belt, Canada, Trace Element Geochemistry of Volcanic Rocks: Applications for Massive Sulfide Exploration (ed. Wyman D. A.), GAC Short Course Notes, 1996, 12: 279.
271. Allen, R. L., Weihed, P., Svenson, S. A., Setting of Zn-Cu-Au-Ag sulfide deposits in the evolution and facies architecture of a 1.9 Ga marine volcanic arc, Skellefte district, Sweden, Economic Geology, 1997, 91: 1022.
272. Lentz, D. R., Petrology, geochemistry, and oxygen isotope interpretation of felsic volcanic and related rocks hosting the

Brunswick 6 and 12 massive sulfide deposits (Brunswick Belt), Bathurst mining camp, New Brunswick, Canada, Economic Geology, 1999, 94: 57.

273. Boulter, C. A., Comparison of Rio Tinto, Spain, and Guaymas basin, Gulf of California: An explanation of a supergiant massive sulfide deposits in an ancient sill-sediment complex, Geology, 1993, 21: 801.
274. Moores, E. M., Twiss, R .J., Tectonics, New York: Freeman, W.H., and Company, 1995, 425.
275. Cloos, M., Lithosphere buoyancy and collisional orogenesis: subduction of oceanic plateau, continental margins, island arcs, spreading ridges, and seamounts, Geological Society of America Bulletin, 1993, 105: 715.
276. Abbott, D. H., Plumes and hotspots as sources of greenstone belts, Lithos, 1996, 37: 113.
277. Hofmann, A. W., Mantle geochemistry: the message from oceanic volcanism, Nature, 1997, 385: 219.
278. Polat, A., Kerrich, R., Wyman, D. A., Geochemical diversity in oceanic komatiites and basalts from the late Archean Wawa greenstone belts, Superior Province, Canada: trace element and Nd isotope evidence for a heterogeneous mantle, Precambrian Research, 1999, 94: 139.
279. Polat, A., Kerrich, R., Formation of an Archean tectonics melange in the Schreiber-Hemlo greenstone belt, Superior Province, Canada: Implications for Archean subduction-accretion process, Tectonics, 1999, 18: 733.
280. Taylor, S. R., McLennan, S. M., The Continental Crust: its Composition and Evolution, Blackwell, Oxford, 312.
281. Rudnick, R. L., 1995, Making continental crust, Nature, 1985, 378, 571—578.
282. Isley, A. E., Abbott, D. H., Plume-related mafic volcanism and the deposition of banded iron formation, JGR, 1999, 104: 461.
283. Fyfe, W. S., The evolution of Earth's crust: modern plate tectonics to ancient hot spot tectonics?, Chemical Geology, 1978, 23: 89.
284. Armstrong, R. L., Radiogenic isotopes: the case study for crustal recycling on a near steady state non-continental growth Earth, Philosophical Transactions of the Royal Society of London, 1981, 301: 472.
285. Von Huene, R., Scholl, D. W., Observations at convergent margins concerning sediment subduction, subduction erosion, and the growth of continental crust, Reviews of Geophysics, 1991, 29: 279.
286. White, W. M., Duncan, R. A., Geochemistry and geochronology of the Society island: new evidence for deep mantle recycling, earth processes, Reading the Isotopic Code, Geophysical Monograph 95, 1996, 1.
287. Kerrich, R., Wyman, D., Hollings, P. et al., Variability of Nb/U and Th/La in 3.0 to 2.7 Ga Superior Province ocean plateau basalts: implications for the timing of continental growth and lithosphere recycling, EPSL, 1999, 168: 101.
288. Dalziel, I. W. D., Lawyer, L. A., Murphy, J. B., Plumes, orogenesis, and supercontinental fragmentation, EPSL, 2000, 178: 1.
289. Halliday, A., Lee, D. C., Tungsten isotopes and the early development of the Earth and Moon, GCA, 1999, 63: 4157.
290. Taylor, S. R., The origin of the earth, Understanding the Earth (eds. Brown, G., Hawkesworth, C., Wilson, C.), London: Cambridge University Press, 1992, 25—43.
291. Qiu, Y., Groves, D. I., Late Archean collision and delamination in the southwest Yilgarn craton: The driving force for Archean orogenic lode gold mineralization?, Economic Geology, 1999, 94: 115.
292. Barnes, H. I., Solubilities of ore minerals, Geochemistry of Hydrothermal Ore Deposits (ed. Barnes, H. L.), New York: Wiley, 1979, 404—460.
293. Craw, D., Koons, P. O., Tectonically-induced hydrothermal activity and gold mineralization adjacent to major fault zones, Economic Geology Monograph 6, 1989, 463—470.
294. Chen, Y. J., Guo, G. J., Li, X., Metallogenic geodynamic background of gold deposits in Granite-greenstone terrains of North China craton, Science in China, Ser. D, 1998,41(2): 113.
295. Tarney, J., Pickering, K. T., Dewey, J.F. (Eds.), The Behaviour and Influence of Fluids in Subduction Zones, London: The Royal Society, 1991, 392.
296. Wright, I. C., Ronde, C. E. J., Faure, K. et al., Discovery of hydrothermal sulfide mineralization from southern Kermadec arc volcanoes (SW Pacific), EPSL, 1998, 164: 335.
297. Rona, P. A., Scott, S. D., A special issue on sea-floor hydrothermal mineralization: New perspectives, Preface, Economic Geology, 1993, 88: 1935.
298. Binns, R. A., Scott, S. D., Bogdanov, Y. A. et al., Hydrothermal oxide and gold-rich sulfate deposits of Franklin seamount, Western Woodlark basin, Papua New Guinea, Economic Geology, 1993, 88: 2122
299. Fouquet, Y., von Stackelberg, U., Charlou, J. L. et al., Metallogenesis in back-arc environments: the Lau basin example,

Economic Geology, 1993, 88: 2154.
300. Herzig, P., Hannington, M. D., Fouquet, Y. et al., Gold-rich polymetallic sulfide from the Lau back arc and implications for the geochemistry of gold in sea-floor hydrothermal systems of the southwest Pacific, Economic Geology, 1993, 88: 2182.
301. Binns, R. A., Scott, S. D., Actively forming polymetallic sulfide deposits associated with felsic volcanic rocks in the eastern Manus back-arc basin, Papua New Guiena, Economic Geology, 1993, 88: 2226.
302. Hallbach, P, Pracejus, B, Marten, A, Geology and mineralogy of massive ore from the central Okinawa trough, Japan, Economic Geology, 1993, 88: 2210.
303. Taylor, B., Preface, Backarc Basin (ed. Taylor, B.), New York: Plenum Press, 1995, ix–xi.
304. Pearce, J. A., Peate, D. W., Tectonic implications of the composition of volcanic arc magmas, Annual Review Earth Planetary Science, Special Publication, 1995, 76: 373.
305. McInnes, B. I. A., McBride, J. S., Evans, N. J. et al., Osmium isotope constraints on ore metal recycling in subduction zones, Science, 1999, 286: 512.
306. Mathur, R., Ruiz, J., Munizaga, F., Relationship between copper tonnage of Chilean base-metal porphyry deposits and Os isotope ratios, Geology, 2000, 28: 555.
307. Hoffman, P. F., Precambrian geology and tectonic history of North America, The Geology of North America (eds. Bally, A. W., Palmer, A. R.), 1989, 447—512.
308. Windley, B. F., The Evolving Continents, New York: John Wiley, 1995, 526.
309. Menzies, M. A., Rogers, N., Tindle, A. et al., Metasomatic and enrichment processes in lithosphere peridotites, an effect of asthenosphere-lithosphere interaction, Mantle Metasomatism (eds. Menzies, M.A., Hawkesworth, C. J.), London: Harcourt Brace Jovanovich, 1978, 313—364.